Villanova University
The Graduate School
Department of Civil and Environmental Engineering

A SIDE-BY-SIDE WATER QUALITY COMPARISON OF PERVIOUS CONCRETE AND POROUS ASPHALT, AND AN INVESTIGATION INTO THE EFFECTS OF UNDERGROUND INFILTRATION BASINS ON STORMWATER TEMPERATURE.

A Thesis in
Water Recourses and Environmental Engineering
By
James D. Barbis

Submitted in partial fulfillment
Of the requirements
For the degree of
Masters of Science
December 2009

A SIDE-BY-SIDE WATER QUALITY COMPARISON OF PERVIOUS CONCRETE AND POROUS ASPHALT, AND AN INVESTIGATION INTO THE EFFECTS OF UNDERGROUND INFILTRATION BASINS ON STORMWATER TEMPERATURE.

By

James D. Barbis

December 2009

_____	_____
Andrea Welker, Ph.D, P.E. Associate Professor of Civil and Environmental Engineering	Date
_____	_____
Robert Traver, Ph.D, P.E. Professor of Civil and Environmental Engineering	Date
_____	_____
Ronald A. Chadderton, Ph.D, P.E. Chairman, Department of Civil and Environmental Engineering	Date
_____	_____
Gary A. Gabriele, Ph.D Dean, College of Engineering	Date

Acknowledgements

Thank to my family, Elisa, John, and Tim, for always teaching me the value of hard work, and have always pointing me in the right direction. Stacy thank you for your love and support. I can always count on you being there through the difficult times.

I would like to extend my gratitude to the EPA, Prince George's County, MD, and the National Ready Mix Concrete Association for providing funding that supported this valuable research.

I would also like to thank everyone in the Villanova University Civil and Environmental Engineering Department for all of their assistance through my graduate experience. Especially, Dr. Andrea Welker, Dr. Robert Traver, Dr. Bridget Wadzuk, Dr. Metin Duran, and Dr. John Komlos your experience and guidance have been invaluable over the years. I need to recognize Linda DeAngelis, Mary Ellen Dukart, George Pappas, and John Stoffey because without their knowledge and assistance this research would not be possible.

A Special thank you to Clay Emerson, Matthew Machusik, Meghan Feller, Jaqulyn Marge, Gerrad Jones, Kristen Mogavero, and Pattrick Jeffers for all of their assistance throughout graduate school. Thanks for all the help with the lab testing, and crawling under cars to remove frozen first flush samplers.

Abstract

This thesis will present the findings of a three-part study of porous pavements. The study was completed on the porous asphalt / pervious concrete study site on the Villanova University's campus.

The first part of the study compares the performance of pervious concrete and porous asphalt to control stormwater quality. Eleven different stormwater parameters, pH, Conductivity, Total Suspended Solids, Chlorides, Total Nitrogen, Total Phosphorus, Total Dissolved Copper, Total Dissolved Lead, Total Dissolved Cadmium, Total Dissolved Chromium, and Total Dissolved Zinc were analyzed, and the corresponding locations from the pervious concrete and porous asphalt were compared using the Mann-Whitney U test.

The second part of the study reports the findings of a bench top study designed to test the amount of Polyatomic Aromatic Hydrocarbons (PAHs) that may leach out of either porous asphalt or pervious concrete. For this part of the study, samples of each pavement type were left submerged in reagent grade water for 100 days. After 100 days, the PAHs were extracted using a liquid-liquid procedure and analyzed using a Gas Chromatograph Mass spectrometer.

Finally, the results of a study looking at the effects of the infiltration bed beneath the porous pavement system has on the stormwater temperature will be presented. The hypothesis being that the stormwater releases the energy it receives from the air and traditional asphalt surface to the stone infiltration bed. For this study temperature observations from the air, the stormwater surface runoff, and the porous pavement surface were compared to the water temperature once it had reached the bottom of the

infiltration bed. Next, The Bioretention Thermal Model, created by Matthew Jones as part of his PHD while attending North Carolina State University, was used to model and mathematically confirm and validate the hypothesis.

Table of Contents:

Table of Tables

Table of Figures

Table of Equations

Chapter 1 Introduction

1.1 Background

Over the past decades there has been an increase in urbanization and in the amount of impervious surfaces covering the land. An impervious surface is any material that prevents precipitation from infiltrating into the soil, which includes pavements and rooftops. To manage the increased rainfall leaving these impervious areas, stormwater systems were installed which were designed to convey the precipitation excess directly into local stream.

These stormwater conveyance systems caused many adverse environmental and hydrologic changes. The stormwater carried by these systems contained many harmful pollutants that were deposited on to the impervious surfaces from the atmosphere, vehicles, human activities, and from animal waste. The stormwater systems carried the extra runoff volumes and increased flow rates directly to the streams, which led to channel widening and an increase in sediment downstream. The health of the aquatic ecosystem is adversely effected when these large flow rates are combined with the increase in pollutant loads (Center For Watershed Protection 2003).

To prevent the degradation of the aquatic environment, engineering practices that mimic the natural hydrologic cycle are now being implemented. When properly applied these Stormwater Best Management Practices (BMPs) use evaporation, transpiration, infiltration and filtration to prevent pollutants and sediments from entering the stream environment (PADEP 2007). This thesis will focus on a particular BMP located on Villanova University's campus, porous pavement.

1.2 Porous Pavements:

In the Pennsylvania Stormwater BMP Manual (2007) porous pavements are described as "a pervious surface course underlain by a stone bed of uniformly graded and clean-washed coarse aggregate, 1-1/2 to 2-1/2 inches in size, with a void space of at least 40%."

Figure 1.1 Representation of a properly designed Porous Asphalt system (PADEP 2007).

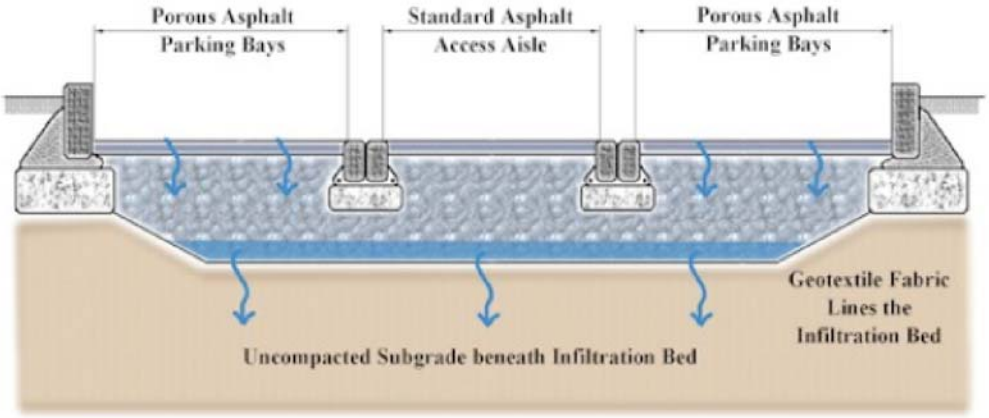

There are several different types of porous pavements; two commonly installed surface types are porous asphalt, and pervious concrete. Porous asphalt and pervious concrete are similar to their impervious counterparts. The main difference between a porous and traditional surface is that the aggregate is carefully screened and all of the fines are removed. This allows stormwater to drain through the pavements surface directly into the underling stone bed (PADEP 2007).

1.2.1 Porous Asphalt Properties

Porous asphalt has been used as a stormwater control method since 1972 when the Franklin Institute in Philadelphia Pennsylvania first developed it (Ferguson 2005). Since then the surface mix has been well studied and now is in use across the world. Porous

asphalt is similar to traditional asphalt except that the size range of the aggregate is much narrower and larger. Typically the binder used is similar to that used in traditional asphalt in most cases. The porosity of porous asphalt generally ranges between 16-25%. The pore spaces result in infiltration rates of up to 35 m/hr (1400 in/hr) which is much greater than rainfall rates, and makes the pavement and excellent stormwater control device (Schaus 2007).

1.2.2 Pervious Concrete Properties

Pervious concrete was first used as a stormwater control device in the 1970's in Florida. The mix is very similar to traditional concrete except that the fine aggregate particles are removed. The large aggregate produces void spaces in the surface, and the porosity can be as high as 20%. The large void space allows for water to infiltrate through the surface at a rate of 7-20 m/hr (288-770 in/hr), which is much higher then any storm intensity (Tennis et al. 2004).

1.2.3 Porous Pavement applications

Both porous asphalt and pervious concrete generally do not meet the strength and durability requirements for use as roadways. Porous asphalt has a compression strength of up to 14 MPa, (2000 psi) and a tensile strength of up to 0.4 MPa (60 psi) (Schaus 2007). Pervious concrete has a compression strength of up to 20.5 MPa (3000 psi) and tensile strength of up to 3.5 MPa (500 psi) (Tennis et al. 2004). The strength depends on the size of the aggregate used in the mix. If smaller aggregate is used, the strength is increased for both pavements types, but the infiltration rate is decreased.

Figure 1.2: Relationships between compressive and tensile strength versus void ratio for Pervious Concrete (Delatte et al. 2007).

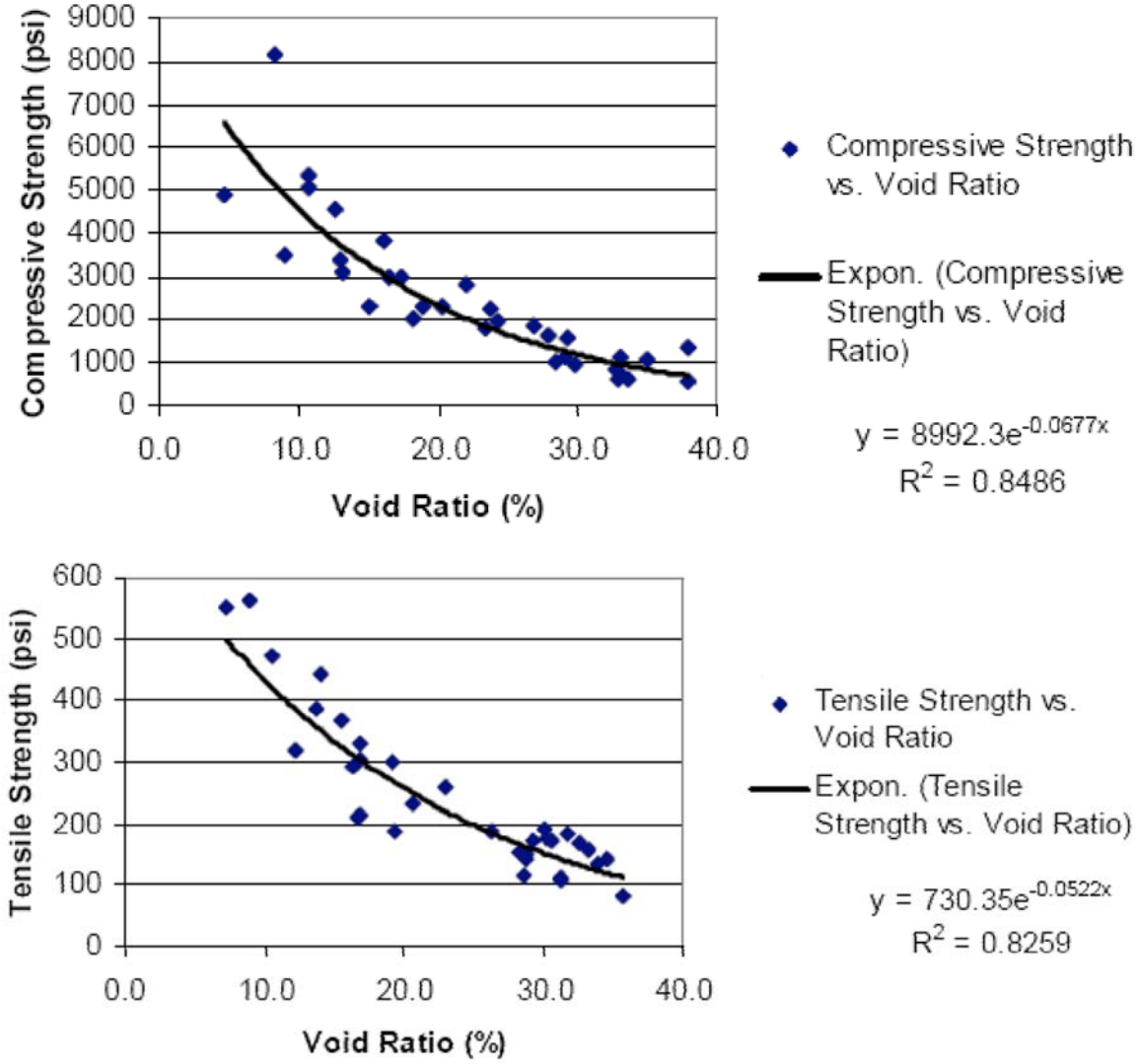

Although porous pavements are not commonly used for roadways, there is one report of porous asphalt being used for a roadway in Chandler Arizona. It was built in 1986 and is still in use, but has required significant repairs (National Asphalt Pavement Association 2007). Both pavement types have been used as a top layer on traditional roadways to reduce noise, moisture on the roadway, and the risk of hydroplaning. Because of the strength and maintenance concerns, porous asphalt and pervious concrete are generally used in situations where the strength of the pavement is less of a concern,

such as parking lots, walking and biking paths, basketball and tennis courts (PADEP 2007).

Unclogged porous pavements are not as vulnerable to the freeze thaw effect as compared to their traditional counterparts because of the increased pore space in the surface and the fact the stormwater collects in the stone bed well below the pavements surface. Because of the lack of freeze-thaw, a properly maintained porous pavement system can be an effective method of stormwater volume and quality control for many years (PADEP 2007). Recent investigations of failed pervious concrete sites in Denver, Colorado found that in situations when the pervious concrete infiltration capabilities have been degraded, generally through clogging of the pore spaces, detrimental freeze thaw effects are observed (Thompson Materials Engineers 2008).

1.3 Watershed and site description

The porous pavement comparison (PAPC) site is located behind Mendel Hall on Villanova University's campus in southeastern Pennsylvania. The runoff from this parking lot is conveyed through traditional stormwater piping into a constructed stormwater wetland on the Villanova University campus and to the headwaters of Mill Creek. Figure 1.3 shows an aerial photograph of the section of the Villanova University's campus containing the PAPC site, constructed stormwater wetlands, and the headwaters of Mill Creek.

The site is a retrofit of a traditional parking lot that is used year round by faculty. A 20 space section of the parking lot was converted to porous pavements, with half of the spaces being porous asphalt and the other half being pervious concrete. Figure 1.4 is an aerial photograph of the PAPC site and its contributing drainage area.

Beneath each surface is a stone infiltration bed, which ranges in depth from 0.5 m (1.5 ft) to 1.5m (5 ft). The infiltration bed consists of clean, washed AASHTO #2 stone (approximately 102 millimeters, or 4 inches in diameter) lined with a non-woven geotextile. The size of the infiltration beds allow for 51 millimeters (2.0 inches) of rain to fall on the 0.07 hectare (0.18 acre) drainage area to be stored and infiltrated. A jersey barrier covered with a geomembrane to prevent cross contamination separates the two pavements.

Figure 1.3: Mill Creek watershed, Porous pavement comparison site (A), Constructed stormwater wetlands (B), Mill Creek head waters (C).

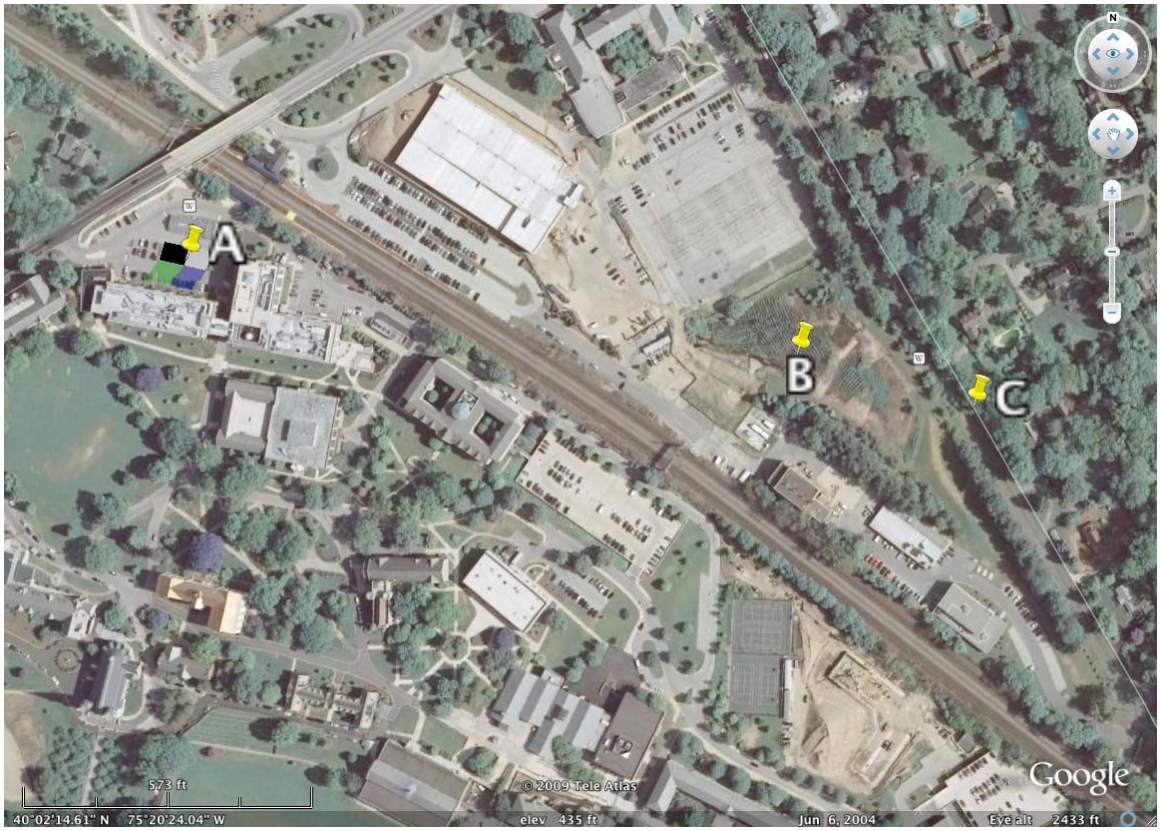

Figure 1.4: Porous pavement comparison site (A), pervious concrete (grey), approximate pervious concrete watershed (blue), porous asphalt (black), approximate porous asphalt watershed (green)

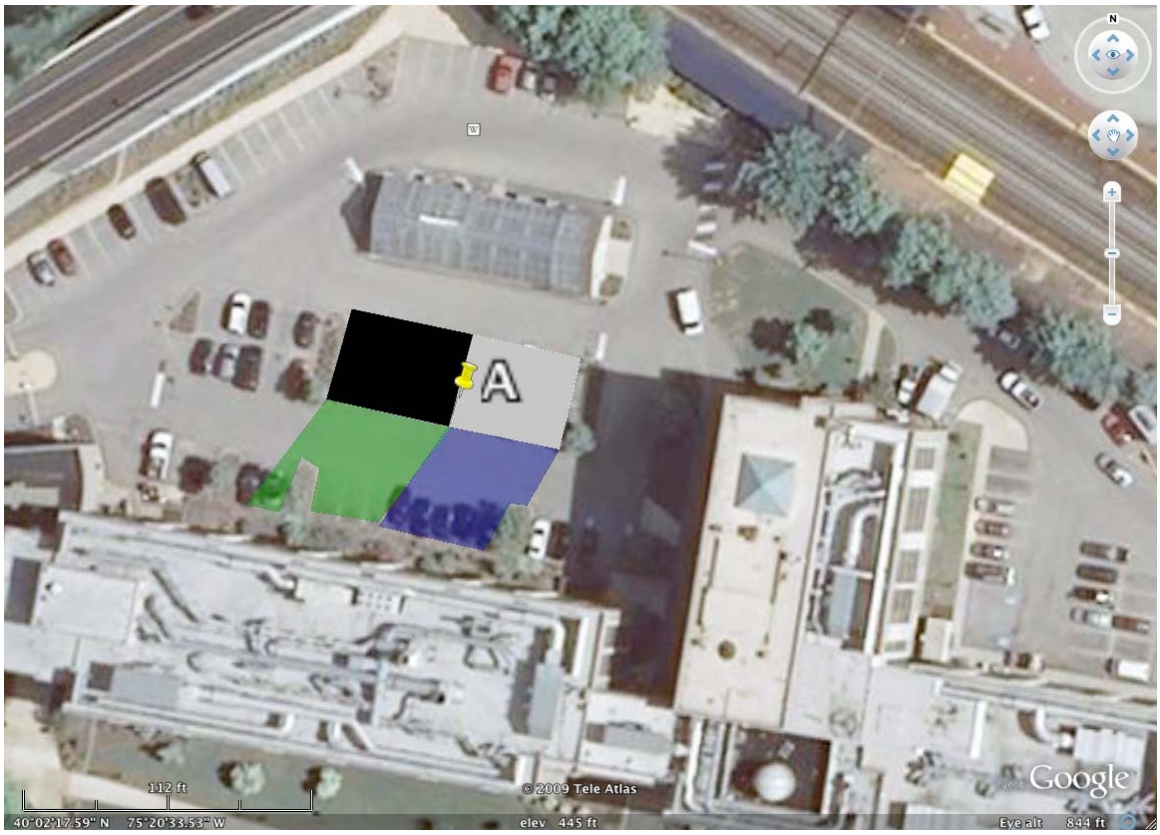

1.4 Site construction

1.4.1 Demolition and excavation

The construction of the site began in September 2007 by Scott Contractors with the demolition of the traditional asphalt parking lot and the excavation of the soil to create the infiltration beds. The demolition of a 30.5 m by 9.1 m (100 ft X 30 ft) section of traditional asphalt was removed exposing the underlying soil. Because of the steep slope of the site and a desire to keep the bottom of the bed level, the resulting infiltration bed depths range from 0.6 m to 1.5 m (2 ft to 5 ft). A Gradall excavator was used in excavation, but was kept out of the bed as much as possible to avoid compaction of the subsoil. During excavation it was found during the course of the site's life as a parking

lot, a significant amount of compaction of the soil had already taken place, and a smaller backhoe was allowed to enter the bed for final grading and the excavation of a trench for outflow piping.

Figure 1.5: Excavation of infiltration beds

Once the bed was excavated, outlet boxes were installed level with the bottom of the bed on each side. These boxes were constructed out of concrete except for the side facing the infiltration bed where a steel screen was placed to allow water in the storage bed to enter the outlet box. In the middle of the outlet box a solid steel plate that is 0.6m (2 ft) high was installed. This plate allows water to be stored in the bed, and overflow once the water level reaches above 0.6 m. It overflows through a V notch weir and is conveyed through piping into the original storm drainage system.

While the soil in the bottom of the bed was exposed, a single head infiltrometer test was performed. The results showed little to no infiltration in the four tests performed in the infiltration bed. These results were expected because of the compaction level of the soil. Soil samples were collected for analysis in the lab. Figure 1.7 shows the soil

gradiation curve and Atterberg limits of the porous pavement comparison subsoil (Jeffers 2009).

Figure 1.6: Outlet box with screen

Figure 1.7:Soil gradiation curve and Atterberg limits, PC3 & PC4-pervious concrete side, PA3-Porous asphalt side (Jeffers 2009)

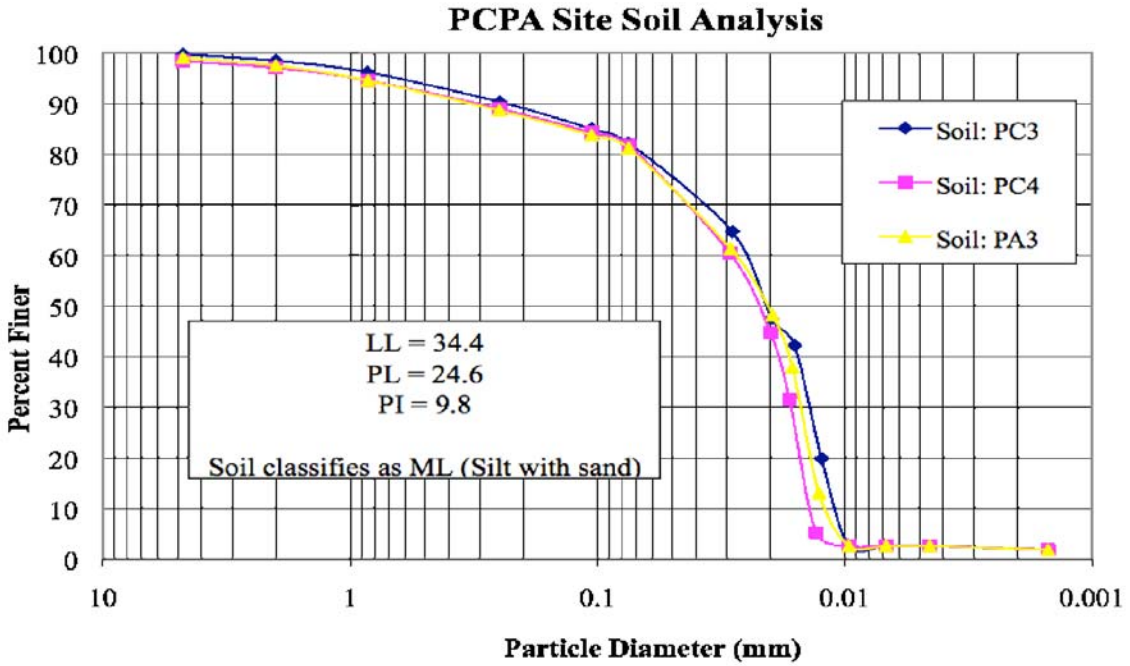

As Mentioned earlier to separate the beds, a jersey barrier was placed on the bottom of the infiltration bed directly in the middle creating two separate beds. The bed instrumentation was then run through conduit into the outlet box on the concrete side. Chapter 3 has a full description of the instrumentation installed on the site. Next, the non-woven geotextile was placed on the bottom and sides of the bed to prevent any soil from migrating into the bed, and an impermeable membrane was draped over the jersey barrier to further separate the beds and prevent cross contamination.

Figure 1.8: Excavated infiltration bed with the jersey barrier (middle) covered by the impermeable membrane (grey) and the non-woven geotextile (black)

The bed was then filled with clean, washed AASHTO #2 stone (approximately 102 millimeters, or 4 inches in diameter).

Figure 1.9: Completed infiltration bed filled with clean, washed #2 stone.

1.4.2 Porous asphalt installation

The porous asphalt mix was designed by Cahill Associates, and was the same mix that was being installed at a local middle school parking lot. The mix contains a narrow gradation of stone aggregate, an asphalt binder, and fibers. The gradation of the aggregate can be seen in Figure 3-4. The binder is a PG 64-22 binder, meaning that it is suitable for daily average high temperatures of 64˚C and daily average low temperatures of -22˚C. This binder makes up 5.8 % of the total mix. Finally, the mix consists of 0.20 % of fibers to make the mix stiffer and to prevent draindown of the asphalt binder.

Figure 1.10: Asphalt mix gradation (Jeffers 2009)

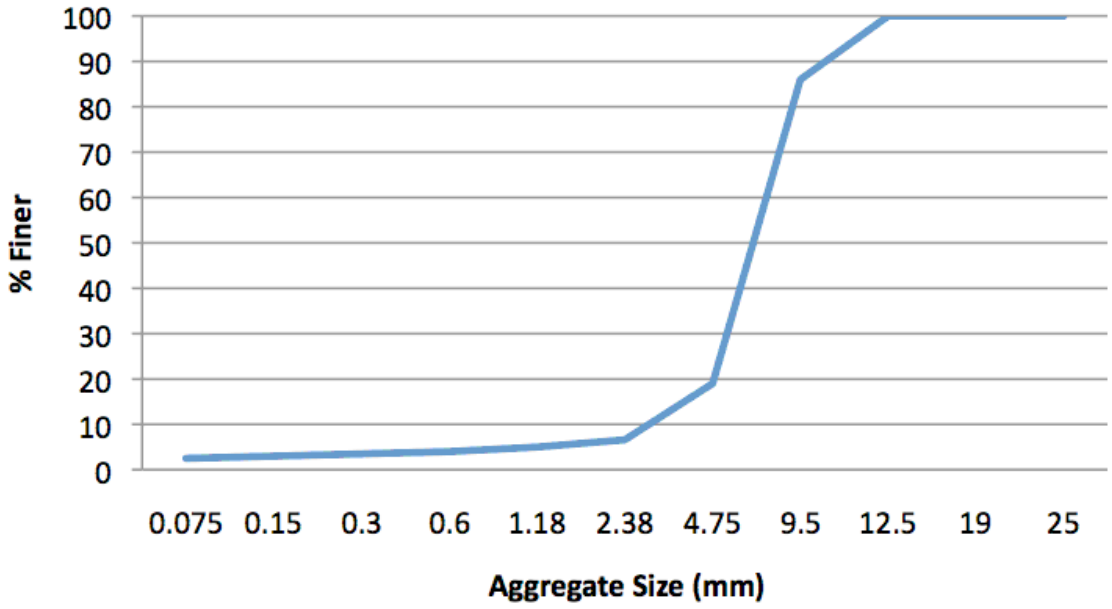

The installation of the asphalt occurred in one day and took approximately three hours to complete. Prior to installation, two first flush samplers were placed at the up slope end adjacent to the traditional pavement to collect first flush runoff samples.

Figure 1.11:Installation of a first flush sampler on the porous asphalt pavement side.

A team of five used standard equipment and procedures in the installation of the asphalt, such as an asphalt paver, which can hold large quantities of the hot asphalt. This paver spreads a level strip of asphalt that is approximately 2.4 m (8 feet) in length. The depth of the asphalt was 63.5 mm (2.5 inches). For the tight areas and the edges where the paver could not be used the asphalt was placed by hand. Part of the standard installation procedure is using diesel fuel as a lubricant on the equipment to prevent the hot asphalt from sticking to the rakes and other pieces of equipment, and allowing for the even distribution of asphalt throughout the site. Consequently, the spraying of diesel fuel over the site was done quite frequently over the course of the installation. After the asphalt was laid, a mechanical roller was used to compact the asphalt surface. The result of this compaction left some small areas where there is no visible pore space. These areas are small and sporadically spaced, and do not affect the overall performance of the asphalt surface.

Figure 1.12: Installation of porous asphalt surface

1.4.3 Pervious concrete installation

The pervious concrete mixture was designed by Phil Kresge of the NRMCA. The mix design for the research project consists of stone aggregate, Portland cement, water, and several modifiers. 78.8% of the mixture consists of #8 stone aggregate, 16.9% of the mixture is Portland cement, and water makes up 4.2% of the pervious concrete. A high range water reducer (0.06%), viscosity modifier admixture (0.05%), and set retarding mixture (0.03%) were also added to the mix to improve workability of the concrete.

The pervious concrete installation was performed by Engelmann Construction over two 4-hour days, with a 4.6 m by 15.2 m (15 ft by 50 ft) area being poured each day. Two first flush samplers were placed flush with the south edge adjacent to the original pavement to collect first flush runoff samples. The process began with setting up forms and spraying them with a diesel fuel lubricant. While the forms were being set up, the stone bed was wetted thoroughly so that the concrete would not dry too quickly and crack after being laid. Once the gravel was soaked, the concrete was poured from a mixer to cover an approximately 4.6 m by 2.1 m (15 ft by 7 ft) area at a depth of 152 mm (6 in). A three person crew spread the concrete to approximately level using hand shovels and rakes. Next, another three person crew ran a 4.9 m (16 ft) long roller screed, lubricated with diesel fuel, over the poured area to level the concrete. Finally, a tarp was pulled over the finished area to prevent quick drying. This tarp must be placed over the finished area within 15 minutes of the concrete mix leaving the mixer to ensure successful results. This process was then repeated until the entire 4.6 m by 15.2 m (15 ft by 50 feet) area was poured and leveled. Two evenly spaced control joints were grooved in the fresh

concrete across the 15.2 m (50 ft) dimension to allow for expansion of the concrete.

Figure 1.11 shows the installation of the pervious concrete.

Figure 1.13: Installation of pervious concrete

Figure 1.14: Completed porous pavement comparison site. Porous asphalt (black) and pervious concrete (grey)

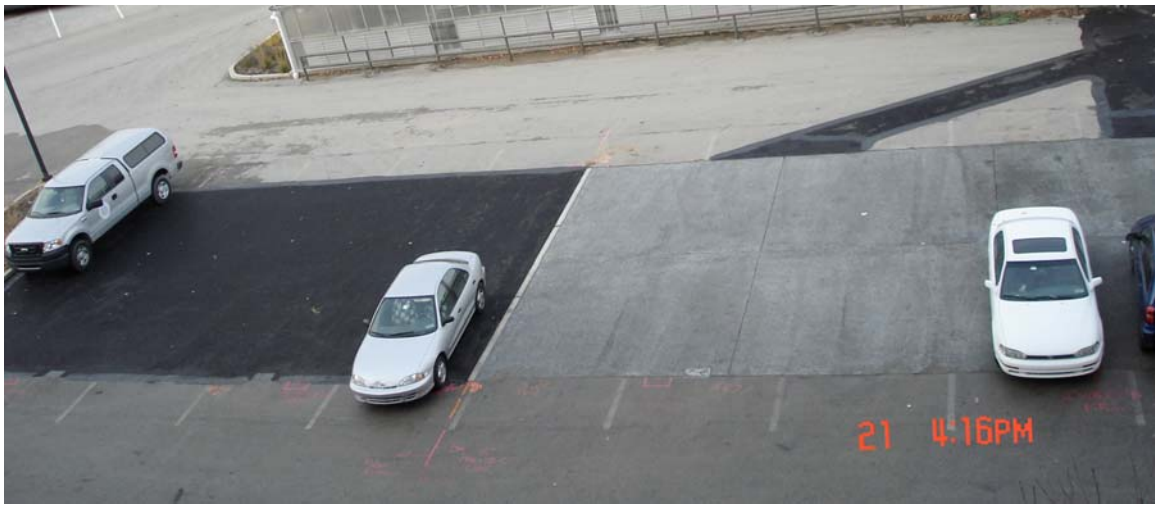

1.4.4 Site Challenges

Not long after the completion of the site it became obvious that the site was not storing as much volume as expected. Several attempts were made to solve the leakage

problems of the site. It was observed that water was getting behind the metal plate in the outlet box, and emptying through the overflow piping and on both sides.

The first attempt to fix this problem was to try and further seal the space around the metal plate with hydraulic concrete. Although we did see a decrease in the rate at which the storage basin was draining, the site was still emptying at a rate much greater then an appropriate, and we concluded that there were still leaks.

Next, a pipe camera was used in the outlet pipe to try and identify any leaks. When we filled the bed with water from a hose, the camera showed water entering the pipe approximately 18 m (60 ft) from the outlet of the overflow pipe. This site was directly underneath the Jersey Barrier. It was hypothesized that when the Jersey Barrier was installed it cracked the outlet pipe and caused the leakage. To attempt to fix the leak in the pipe, a small section of the pervious asphalt and pervious concrete was removed and the underlying stone was excavated until the outlet pipe was visible. At that time it was determined that there was no crack but the joint was the cause of the leak, and the outlet pipe was essentially acting as an underdrain.

Because there were approximately three joints under the porous asphalt side and two under the pervious concrete it explained why the porous asphalt side showed considerably faster drainage. We concluded that the best option was to grout and seal the entire length of outlet pipes. This was done in November 2008, approximately one year after construction was completed.

After the grouting, there was no longer leakage from the site, but in the attempt to fix the outlet pipe a leak was created in the jersey barrier and all of the water traveled from the asphalt side and was stored on the concrete side. It is believed that there was

not a leak before the surface was excavated. Because of this, the data used to compare the surface is from November 2007 until October of 2008.

1.5 Project Overview

The use of porous pavement as a stormwater BMP is becoming more popular and widespread, and the research is showing that porous pavements are effective at reducing peak flows, runoff volumes and improving runoff quality (Boving et al. 2008; Bratteboro and Booth 2003; Jackson 2003; Kwiatkowski et al. 2007; PADEP 2007; University of Rhode Island Corporative Extension 2006). What are not as well known are the subtle differences between pavement types, and if one type is better suited for use in some applications than others. This research is designed to study porous asphalt and pervious concrete, and compare their effectiveness in improving the stormwater runoff quality. Stormwater samples were collected from first flush samplers on the surface to monitor the water quality entering the infiltration bed, and porewater samples were collected from depth of 15 cm (6in), 30 cm (12in), and 45 cm (18in) below the infiltration bed. Chapter 5 will discuss the results of a bench top hydrocarbon test done on samples from both surfaces. Temperature was also monitored at the surface and in the infiltration bed; Chapter 6 discusses the effects of pervious pavement and its effect on stormwater temperature.

Chapter 2 Literature Review

2.1 Increase in impervious cover and its effect on watershed degradation

Impervious cover is any surface that prevents water from infiltrating into the soil. Over the past decade the amount of impervious cover has increased dramatically. (Stankowski 1972) found that an areas population density is directly related to the amount of impervious cover

Impervious areas are a critical contributor to the hydrologic changes that degrade waterways. It generates pollutants and prevents natural pollutant processing by soil microorganisms. Impervious areas also serve as a conveyance system transporting pollutants into the waterways. The increased volume leads to the erosion of the stream bank, and large sediment loads downstream (Arnold and Gibons 1996)

By preventing stormwater infiltration, the hydrologic cycle is disrupted. The Center for Watershed Protection (2003) performed a comprehensive literature review analyzing the effects of impervious area and its effect on aquatic environments on number of different factors. These results summarized in Table 2.1.

Table 2.1: The impacts of impervious cover in a watershed on the hydrologic, physical and biological systems (Center For Watershed Protection 2003)

Impervious Cover Effect	Relationship to Aquatic Habitat Health	Conclusions
Hydrologic	Inverse	Increased volume stormwater runoff Increase in bank full flow frequency Direct effect on the physical and habitat characteristics
Physical	Inverse	Channel enlargement due to increased volumes Reduction in stream sinuosity Reduction in large woody debris, and simplification of stream habitats Increase in water temperature Stream habitat diminishes at 10% of watershed impervious cover Severe degradation occurs at 20% of watershed impervious cover
Biological Impacts	Inverse	Aquatic insect and freshwater fish diversity decreased when watershed level approached 10 to 15% of impervious cover

The upcoming sections will focus on the literature analyzing the water quality of stormwater, and the literature on pervious concrete and porous asphalt.

2.2 Sources of pollutants from traditional stormwater parking lots and highway runoff

2.2.1 Highway and parking lot runoff sources and characterization

Impervious surfaces, which include roadways and parking lots, have been found to have adverse effects on the water quality of the rivers and streams. There have been multiple studies to determine the sources and characterize the pollutants in the stormwater runoff.

The sources of roadway and parking lot pollutants come from the pavements themselves, vehicles, litter and spills on to the roadway surface. Vehicles provide a large percentage of the pollutants through tire wear, fuel losses, lubrication losses, and exhaust emissions. The land environment surrounding the pavements will also convey pollutants

to the pavements. These pollutants come in the form of nutrients, pesticides, and deposits from the atmosphere (Barrett et al. 1995).

Barnes et al. (2001) described six categories of nonpoint source pollution. Those categories and their sources are located in table 2.2.

Table 2.2: Categories, parameters and Potential sources of nonpoint source pollution (Barnes et al. 2001)

Category	Parameters	Potential Sources
Bacteria	Total and fecal coliform, fecal streptococci, other pathogens	Animals, birds, soil bacteria, humans
Nutrients	Nitrogen and phosphorus	Animal waste, lawn fertilizers, decomposing organic matter, urban street refuse, atmospheric deposition
Biodegradable Chemicals	BOD wastes, COD wastes, TOC	Leaves, grass clippings, animals, street litter, oil and grease
Organic Chemicals	Pesticides, PCBs	Pest and weed control, packaging, leaking transformers, hydraulic and lubricating fluids
Inorganic Chemicals	Suspended solids, dissolved solids, toxic metals, chlorides	Erosion from lawns, stream banks and channels, and construction sites. Dust and dirt from streets, atmospheric deposition, industrial pollution, illegal dumping during storms, traffic, and deicing salts
Physical and Aesthetic	Thermal, discoloration, odors	In the summer from streets, parking lots, sidewalks, and rooftops runoff. In all seasons from industrial sites, animal wastes, organic matter, and hydrocarbons

The EPA studied urban runoff from locations across the nation, and found that metals such as copper, lead and zinc were detected in more than 90% of the stormwater samples. Organic chemicals were found in more than 10% of the samples (U.S. EPA 1983).

(Irish et al. 1995) concluded that urban runoff should be categorized by the runoff controls that could reduce its effects. The three categories are:

- Pollutants that are influenced by dry period conditions and therefore may be mitigated by dry period activities.

- Constituents that are influenced by storm conditions and may be mitigated by runoff controls.
- Constituents that can be mitigated through combinations of structural runoff controls as well as dry period activities.

2.2.2 Polycyclic Aromatic Hydrocarbons in asphalt sealants and parking lots

The city of Austin Texas looked at the pollutant levels of Polycyclic Aromatic Hydrocarbons (PAHs) that were coming from asphalt pavement sealers. They studied the level of PAHs in commercially available sealants. Three categories of sealants were studied, retail, commercial and municipal. Retail sealants are a product that would be used to resurface or repair ones driveway and can be purchased at local hardware stores. Commercial products are purchased from a commercial distributor, and would be used for the resurfacing of commercial and residential parking lots. Municipal sealants are used for the repair of city streets. After analyzing each of these products the authors made the following conclusions (McClintock et al. 2005):

- The total PAH concentration of coal-tar based sealants products is much greater than that found in asphalt-based sealants.
- When all of the sealant products were included, a strong exponential relationship exists between the coal tar percentage and total PAHs.
- The commercial products were higher in PAHs and in coal-tar percentage than the retail products.
- The asphalt materials and scrapings from unsealed asphalt surfaces had lower PAHs than any of the sealants or scrapings. Total PAHs for these materials were significantly lower than scrapings from either asphalt-based or coal-tar based sealed lots

McClintock et al (2005) made the following conclusions from the studying the particulates leaving parking lots:

- Sealant PAHs available for export to local streams via sediment (attached to particulates from sealed parking lots) are significantly higher than those leaving unsealed lots, where vehicular and air deposition are the main source of PAHs.
- Within the asphalt-based sealants, the lots with more vehicular traffic were generally higher than the test lots (concrete and unsealed asphalt lots) indicating the additional vehicles were a source of PAHs.
- The general signature of the primary 16 PAHs was very similar between the test and in-use lots, indicating that the sealant signature may be similar to or overwhelmed by any unique vehicular source signature.

From this research it was determined that there is movement of PAHs from sealed parking lots into the aquatic environment in Austin, Texas. The report called for the limiting of the input of coal-based sealants from the environment.

Chapter 5 provides more information regarding PAH levels in asphalt along with an analysis to determine if PAHs leach out of porous pavements.

2.3 Infiltration Best Management Practices and stormwater runoff water quality affects.

Porous pavements used in conjunction with an infiltration is an accepted best management practice (PADEP 2007). The next section will look at the literature focusing on water quality improvements found when porous pavements are used as a stormwater BMP practice.

The Pennsylvania Best Management Practice Manual (2007) describes a porous pavement system as a pervious surface course underlain by a stone bed of uniformly graded and clean-washed coarse aggregate, 38.1 mm to 63.5 mm in size, with a void space of at least 40% (PADEP 2007).

Kwiatkowski et al. (2007) studied a pervious concrete infiltration basin on the campus of Villanova University. The watershed consisted of a pedestrian area and

rooftops. Overall the site was 60% impervious surface. The findings showed that the surface and limestone infiltration bed neutralized acidic rainwater entering the site. The nutrient levels of the samples taken from the porous pavement system were much lower then those in the surrounding soil water. This showed that the infiltration system was not a source of nutrient contamination.

The chloride level was seasonal at the pervious concrete site, with levels being very high in the winter due to deicing practices on and around the watershed. Chloride contamination is a concern with any infiltration system because chlorides are conservative. In other words it is not sorbed onto the rock during infiltration (Kwiatkowski et al. 2007).

Finally, the level of copper was monitored at the pervious concrete site, and detectable levels were found entering the infiltration bed from the surrounding copper downspouts. The copper concentrations were effectively removed through the infiltration process. The concentration was reduced significantly in the first 0.3 m (1 ft) of soil (Kwiatkowski et al. 2007).

One concern is the effect that infiltrating stormwater will have on the underlying soil and groundwater. One study that looked at the relationship between PAHs and infiltration basins found that in a subsurface infiltration system, which received roadway stormwater runoff for several decades, found that there was an inverse relationship between the amount of contaminants entering the groundwater and soil depth (Mikkelsen et al. 1997).

Mikkelsen et al. (1997) also found that there is a potential for highly absorbable contaminants present in urban stormwater runoff to accumulate in the soil surface at

environmentally harmful levels. Finally, they found that infiltrated stormwater did not pose a high risk of contamination to the underlying groundwater.

Barraud et al. (1999) compared a new infiltration basin to one that had been in operation for 30 years and found that the concentration of hydrocarbons was highest in the top few centimeters of soil, and rapidly declined with soil depth. Over a long-term period, heavy metals and oils can contaminate the soil over a radius of at least one meter around the infiltration basin. The pollutants can spread over time even though the concentrations remain low. Table 3 compares the metal and hydrocarbon concentrations in the first 10 cm of the soil in a new infiltration soakway and one that is 30 years old in Valence, France.

Table 2.3: Comparison the metal and hydrocarbon concentrations in the first ten centimeters of soil in a new infiltration soakway and one that is 30 years old in Valence France (Barraud et al. 1999)

New soakway						
Element	**Concentration in sand-cores (mg/kg)**			**Trapped mass (g)**	**Input mass (g)**	**Retention (%)**
	0-5 cm	**5-10 cm**	**mean**			
Zn	857	917	887	70	80-130	54-88
Pb	197	212	204.5	16	10-16.3	98-?
Cd	2.2	2.5	2.35	0.18	<	?
PAH	0.29	0.1	0.19	0.02	<	?
Mineral oil	1290	1600	1445	113	10	?
30 year old soakway						
Element	**Concentration in sand-cores (mg/kg)**			**Trapped mass (g)**	**Input mass (g)**	**Retention (%)**
	1-10 cm					
Zn	143			118	380	31
Pb	82			67	46	?
Cd	0.9			0.7	2.37	29.5
PAH	0			0	0	<
Mineral oil	886			710	55	?
<: not calculable (below detection threshold)						
?: not calculable						

Welker et al. (2006) analyzed the copper concentrations in two seepage pit sites, Monastery and Tolentine, on the Villanova University campus. These seepage pits have

received stormwater from the surrounding rooftops for approximately a century. Soil samples were analyzed at 15 cm (6in) increments over a depth of 200 cm (6.5 ft). These samples were then compared to a reference sample taken outside of the pit (null) to determine the effect of the stormwater on the soil quality.

Of the three samples the null samples contained the lowest concentrations of copper with highest concentration of 2.62 ppm being found in the first 20 cm of soil. The Monastery pit had the highest concentration out of all of the samples with a peak average concentration of 728 ppm. This peak concentration was located 46 cm (1.5 ft) below the surface. The peak concentration for the Tolentine Seepage Pit was also at 46 cm (1.5 ft) cm below the surface. The Tolentine peak was 420 ppm. Figure 1 shows the copper concentrations at the 15 cm (6 in) increments for the three samples (Welker et al. 2006).

Welker et al. concluded that copper build up can be a long term issue, but after over 100 years of use the copper concentrations were still well below PADEP standards for clean fill. He also found that copper can possibly travel into the soil over long periods of time, which indicated by a second copper peak at 183cm (72 in) below the surface.

Figure 2.1: Soil copper concentration (ppm) from two-century-old seepage pits compared with a control null site (Welker et al. 2006).

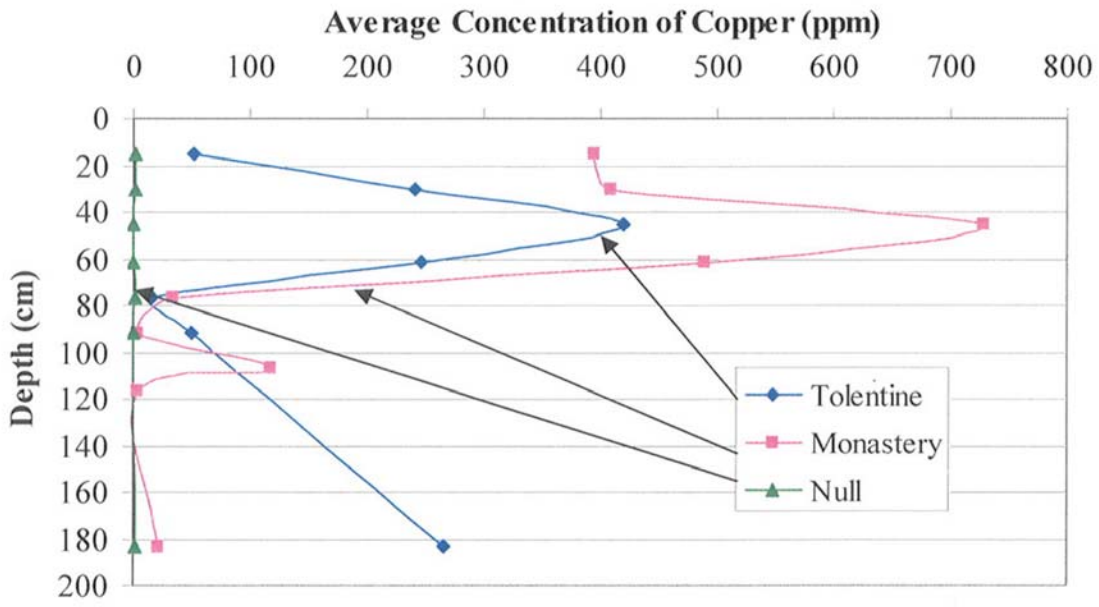

Newman et al. looked at porous pavement systems for total hydrocarbon and grease concentrations, and found that after four years the system retained 99% of the oil, and if the system is properly constructed, the porous pavement surface may be able to trap and degrade any oil accidentally released onto parking lot surfaces (Newman et al. 2002).

Pratt et al. studied the microbial populations in a simulated porous pavement system, and the investigated their survival rates when introduced to chronic, low level hydrocarbons contamination. They found that pervious concrete pavement systems, which included an infiltration basin, can effectively degrade hydrocarbons with nutrients being the limiting factor in the biodegradation of the PAH molecules. A total of 257 g of oil was added within the study period, with 6.3 g recovered in the effluent; a removal percentage of 97.6%. This high removal percentage is due to the entire system working

at removing the oil. The system includes retention in the surface and base layer along with the microbial degradation (Pratt et al 1999) .

A newly constructed 800 space porous asphalt parking lot in Rhode Island was studied for ground water contamination. The study looked at the concentrations of chlorides, metals (zinc and copper), nutrients, and PAH concentrations in two sampling ports located just above the geotextile lining the infiltration bed and 0.6 m below the geotextile in the native soil (Boving et al. 2008).

The chloride levels were high in the winter despite applying no deicing materials directly on the surface. They concluded that the cars using the parking lot carried the deicing material on to the pavements from outside roads. The chloride concentration decreased to below the detection limit by early summer. The nutrients levels that were detected were highest in the spring and fall, and fell below the drinking water limits. The zinc and copper concentration remained below the recommended limits of 5 ppm for zinc and 1.3 ppm for copper. The highest concentrations were found after times when the parking lot was full. The levels were also highest in the late winter and early spring when the corrosion of the vehicles parking in the lot is the highest. The PAH concentration varied from below the detection limit of .3 ppb to 4.9 ppb, depending on the amount of use above the sampling port with higher use area having higher concentrations. Overall, the porous pavment effectively removes or retards PAH (Boving et al. 2008).

The increase in impervious area in recent decades has had negative effects on stream flow, water quality, and stream bank stability. Stormwater BMPs when designed properly provide volume reduction, and pollutant removal through infiltration. Heavy metals and hydrocarbons are trapped in the first meter of the soil, and the risk of these

pollutants entering the groundwater is low. Microorganisms have been found at the base of porous pavement systems, which provide evidence of an ecosystem and opportunity for the degradation of some hydrocarbons.

Chapter 3 Methods

The methods section provides the background for the instrumentation and procedures used in this report. This chapter focuses on the water quality methods used to determine the effectiveness of the porous pavements at removing stormwater pollutants.

3.1 Quality control

To ensure consistent collection and analysis of all of the stormwater samples from the Porous Pavement Comparison Site (PAPC), a Quality Management plan (QMP) was set up. This plan set the criteria for determining minimum precipitation intensity, instrumentation calibration frequency, and the procedures for sample collection and analysis. The QMP was adapted to the PAPC site from the Quality Management Plans for the other infiltration BMP sites in the Villanova University Stormwater BMP Park (Villanova Urban Stormwater Partnership 2008).

For the QMP, a six letter systematic labeling system was created for all of the water quality sampling locations. The labeling system identifies the project site, surface type, sample description or depth, and the location of the sample relative to the particular surface. Table 3.1 shows the labeling system.

Table 3.1:Labeling system for the PAPC water quality samples.

Site	Description
PP	Porous pavement comparison site
surface type	**Description**
A	Pervious Concrete surface
C	Porous Asphalt Surface
Sample Type / Soil Depth	**Description**
FF	First flush
GS	Grab sample
6	Soil water sample 6 inches deep
12	Soil water sample 12 inches deep
18	Soil water sample 18 inches deep
Nest Number	**Description**
1	Samples on the east side (closest to the concrete outlet side) of the suface
2	Samples on the west side (closest to the asphalt outlet side) of the suface

3.2 Instrumentation

3.2.1 Rain Gauge

A tipping bucket rain gauge, which is owned by the Villanova University's Astronomy Department Weather Center, measures the amount of rainfall every ten minutes, and can be accessed through the website: http://www.wunderground.com/weatherstation/WXDailyHistory.asp?ID=KPAVILLA1. The location of the rain gauge is on the roof of Mendel Hall, a classroom building adjacent to the PAPC site. To ensure that the rainfall measurements are accurate the rain gauge is calibrated every three months. Figure 3.1 shows the location of the rain gauge in comparison to the PAPC site.

Figure 3.1: Location of rain gauge in comparison to porous pavement comparison site.

3.2.2 First Flush Samplers

To collect and analyze the constituents entering the porous pavements from the surrounding impervious surfaces four GKY first flush samplers were installed on the uphill edge (south edge) of the pavements, two on each pavement. The GKY First Flush Sampler is a polycarbonate housing with a grated lid. A 5 liter sample container fits inside the housing. The lid of the first flush sampler sits flush with the pavement's surface, and is designed with buoyant flap valves that allow stormwater to enter until the sample container is full, and then close (GKY and Associates inc. 2000). Figure 3.2 shows the installation of a First Flush Sampler on the pervious asphalt side.

3.2.3 Concrete access boxes and pressure/temperature sensors

To access and analyze the water in the infiltration bed, a concrete access box was placed adjacent to the stone infiltration bed on the east and west side, and set flush with the base of the bed. The side of the access box facing the infiltration beds is open and a steel screen is attached, which allows the water in the bed to enter the concrete box while at the same time holding back the stone in the infiltration bed. This allowed for the collection of grab samples from the infiltration bed. Figure 3.3 shows the concrete access box and the screen separating the stone bed.

Figure 3.2: Access box with screen facing infiltration bed, and tubing from pore water samplers.

At the bottom of each concrete box an Instrumentation Northwest (INW) PT2X Submersible Pressure/ Temperature Smart Sensors was installed. These sensors are self-data logging and measure both the depth of water in the infiltration bed and the temperature. The data was collected at 5 min increments and downloaded every two weeks using the Aqua4plus computer software provided with the transducer. The sensors

were calibrated once every three months. Figure 3.4 shows the INW PT2X pressure/ temperature sensor.

Figure 3.3: Picture of the INW PT2X Pressure/Temperature Smart Sensor.

3.2.4 Soil water samplers

In the subsoil below each of the infiltration beds six UMS SPE20 pore water samplers with 6.35 mm (.25in) diameter tubing running through conduit into the concrete access box. Pore water samplers (suction cups) are designed to extract soil water from saturated and non-saturated soils. To extract a soil water solution, a negative pressure has to be applied. The SPE20 sampler can be used for determination of substances for which ceramic cups are not suitable, like hydrocarbons or heavy metals (UMS GmbH 2005).

The samplers were set using a hand agar at depths of 15 cm (6 in), 30 cm (12 in), and 46 cm (18 in) in the soil, two sets of samplers were placed at each depth. The first set was set at 3 m (10 ft) and 6 m (20 ft) from the east (concrete) side of the concrete bed. The nests under the Porous Asphalt surface are located at 18 m (60 ft) and 21 m (70 ft) from the concrete access box. Filling/venting caps were attached to each soil water pore

sampler tubes in the concrete access box.

When the appropriate bottle is screwed into this cap it allows for a vacuum to be applied to the whole system, which is required for obtaining the soil water sample. In contrast to the soil matrix, the pores of the cup and all tubes are completely filled with water. If the vacuum pressure is too large, the soil surrounding the cup might be drained, which essentially reduces the cup's capability to conduct water. Therefore, the negative pressure should be kept to a minimum. In general it is sufficient to apply a vacuum pressure, which is only 5 kPa (0.725 psi) higher than the soil water tension (UMS GmbH 2005).

Figure 3.5 shows a representation of the approximate position of each piece of instrumentation used in the collection of samples for water quality analysis (not to scale).

Figure 3.4:Site instrumentation: Porous Asphalt (black), Pervious Concrete (grey), GKY first flush sampler (light blue), Access box (red), soil pore water samplers; 6 in deep (light green), 12 in deep (dark green), 18 in deep (white), Instrumentation Northwest PT2X Submersible Pressure/ Temperature Smart Sensors (blue).

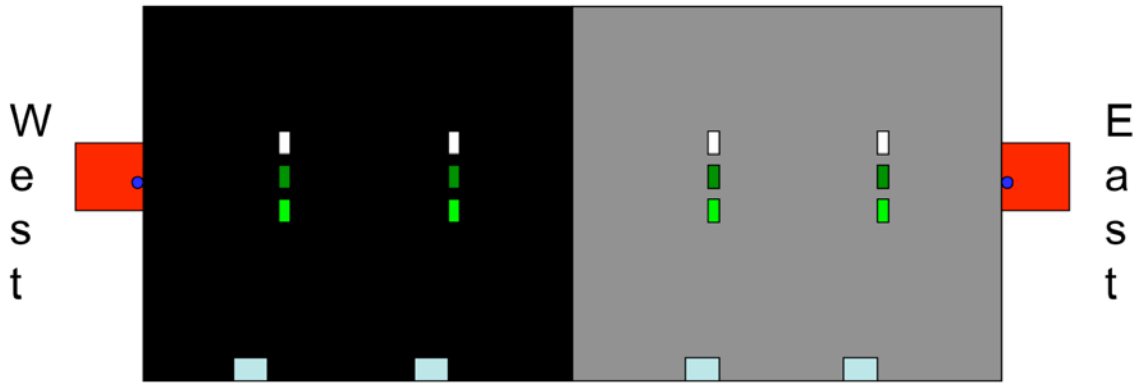

3.2.5 Rain event designation and instrumentation set up

The goal of this study was to test all rain events when 6.35 mm (.25 in) of rain fell in an 8-hour period. The first flush samplers were prepared prior to any precipitation by placing a clean, acid washed, first flush insert in to the sampler. The soil pore water samplers are set up after a minimum of 4.1 mm (0.15) inches of precipitation has fallen.

To set up the soil pore water samplers, a 500 ml Nalge-Nunc heavy-duty vacuum bottles are attached to the filling/ venting caps. Using a hand vacuum pump, a vacuum of 70-82 KPa (10-12 psi) is applied to each bottle. The bottles are then left for 24-36 hrs, and collected when a sufficient amount of sample had been obtained.

3.2.6 Stormwater samples collection and handling

The first flush, soil water and grab samples are collected 24 to 36 hrs after the beginning of the rainfall event. The first flush inserts are removed, labeled, and capped using first flush insert lids. The bottles containing the soil water are removed, labeled and capped. If there is ponded water in the infiltration bed, a grab sample is collected using a 500 ml plastic Teflon bottle. Once all of the samples have been collected and labeled appropriately the samples are taken to the Water Resources Teaching and Research Laboratory at Villanova University for analysis.

3.3 Water Quality Analysis

For each stormwater sample that entered the laboratory, approximately 50 ml were allocated for nutrient, chlorides, pH and conductivity testing. 320 ml were allocated for suspended metals, dissolved metals, total dissolved, and total suspended solids testing. 20 ml of the 320 ml was separated for dissolved metals testing.

The dissolved metals samples were preserved for up to six months by adding a 2% nitric acid matrix and kept refrigerated. The 50 ml sample also serves as a reserve sample in case tests for nutrients or chlorides need to be rerun. The next sections will describe the background and procedure for each of the tests mentioned above.

3.3.1 pH and Conductivity

The Hach Company Sension156 Multiparameter meter was used to measure pH

and conductivity. The Sension Model 51935-00 Gel-filled pH Electrode is a combined pH and temperature probe. The range of the electrode is 0 to 14 pH units. To prevent contamination of samples and to ensure accurate readings, the electrode was rinsed with deionized water and blotted dry between sample measurements (Kwiatkowski 2004).

The Model 51935-00 is a combined conductivity and temperature probe. The range of the conductivity probe is 0.01 mS to 200 mS. The resolution of the multiparameter meter varies depending on the range of the sample being tested. Between 0.00 and 19.99 mS/cm, the resolution is 0.01 mS/cm. For conductivities between 20.0 and 199.9 mS/cm, the resolution is 0.1 mS/cm and 1 mS/cm between 200 and 1,999 mS/cm. The accuracy while in conductivity mode is ± 0.5% of the range. Between sample testing, the probe was rinsed with deionized water and blotted dry to ensure accurate readings (Kwiatkowski 2004).

3.3.2 Total Nitrogen and Total Phosphorus

The Total Nitrogen and Total Phosphorus tests are conducted using the Hach DR/4000 Spectrophotometer. The spectrophotometer is designed to measure the concentration of a sample based on the amount of light absorbed at a specific wavelength. The absorbance can be related to various chemical parameters through the use of experimental procedures (Dukart 2008b).

The Total Nitrogen and Total Phosphorus spectrophotometer analyses are performed in manufacturer prepared digestion vials. Care is taken not to touch the glass vials. The glass vials are also wiped with a soft cloth prior to analysis in the spectrophotometer. Vials are emptied immediately following the analysis into specified

hazardous waste containers. The vials are not reusable and are disposed of as per the product's Material Safety Data Sheet (MSDS) (Dukart 2008b)

The Total Nitrogen and Total Phosphorous tests require the samples to undergo a digestion period at specific temperatures. The Hach COD Reactor Model 45600 is used to incubate the samples for the required times. The COD Reactor holds up to 25 16x100 mm vials and is capable of sustaining temperatures up to 150 degrees Celsius with an accuracy of ± 2 degrees Celsius. It also has a space for a thermometer to verify the temperature. The COD Reactor features an adjustable temperature and a timer. The reactor has two modes, 150 degrees Celsius mode and an adjustable temperature mode. For quality control and assurance a duplicate and a spike were used for validation. Table 3.2 shows the hach test method and detection limits for the total phosphorus and total nitrogen tests(Dukart 2008b).

Table 3.2: Nutrient test method and and detection limit (Dukart 2008b)

Nutrients	Test Method	Hach method number	Detection Limit (mg/L)	ASCE/EPA Database (mg/L)
Phosphorus-total	PhosVer3 with Acid Persulfate Digestion	8190	.06 mg/L PO43	0.06 mg/L PO_4^3
Nitrogen-total	Persulfate Digestion	10071	1.7 mg/L N	2.0 mg/L N

3.3.3 Chloride Testing

The chloride analysis for this project was performed using two procedures. The samples tested from November 2007 until January 2008 were tested using a High

Performance Liquid Chromoatography (HPLC). Samples tested from January 2008 until April 2009 were performed using a Systea.

The HPLC consists of the following components: a Waters Model 626 HPLC Pump with IonPac® ASII-HC Anion-Exchange Column, a Waters Model 431 Conductivity Detector, aWaters Model 600s Controller, a Waters Model 717plus Autosampler, a Dionex AMMS® IIIEluent Suppressor, Galaxie Chromatography Data System Version 1.7.4.5, IonPac ATC-3 TrapColumn 9x24mm, AG11-HC Guard Column, 4x50mm, and IonPac ASH11-HC Analytical Column, 4x250mm (Dukart 2008a).

The HPLC injected small quantities of sample into an anion exchange column that separated out the present anions. After being separated, the anions were read by a conductivity detector. The measured conductivities were then plotted and computer software integrated the area underneath the peaks for each individual anion. The area underneath the chloride peak was then related back to the calibration standard in order to determine the concentration of chloride in each sample (Dukart 2008a).

Blanks and calibration curve/checks were used as a method of quality control. Table 3.3 shows the detection limit based on chloride concentration for the chloride test performed using the HPLC.

Table 3.3:Chloride detection limits using the HPLC (Dukart 2008a).

Chloride Detection Limits				
Conductivity	Chloride Concentration			
uS/cm²	<80mg/L	150mg/L	250mg/L	250mg/L
< 430	0.5mg/L			
710		0.925mg/L		
1105			1.562mg/L	
1500				2.27mg/L

In January 2008, chlorides began being tested with the Systea. In the EasyChem methodology, a thiocyanate ion was liberated from mercuric thiocyanate through the formation of soluble mercuric chloride. In the presence of a ferric ion, free thiocyanate ion forms a highly colored ferric complex. The intensity of this complex was measured at 480 nm, and this intensity was proportional to the chloride concentration (Systea Scientific LLC 2006).

3.3.4 Metals Testing

The stormwater samples were tested for their dissolved metal concentrations using a Perkin-Elmer 4100ZL Graphite Furnace Spectrometer. The Perkin-Elmer Model 4100ZL is a high performance graphite furnace atomic absorption unit that utilizes the Zeeman effect, which allows alternation between a strong magnetic field and the heated furnace unit for background compensation, and the mitigation of interferences (Dukart 2008c).

To ensure quality control a set of three to five standards for each element were used to create an abundance-concentration curve. Standards were analyzed for at least every 10 samples, and duplicate samples were analyzed for every batch. To ensure accuracy there should not be more then a 10% difference between duplicate samples

(Dukart 2008c).

All of the calculations for the determination of the metal abundance was preformed in the AA laboratory software and recorded in an Excel spreadsheet (Dukart 2008c).

3.3.5 Total Suspended and Total Dissolved Solids

'Total Solids' is the term applied to the material residue left in the vessel after evaporation of a sample and its subsequent drying in an oven at a defined temperature. Total Solids includes 'total suspended solids,' the portion of total solids retained by a filter, and 'total dissolved solids,' the portion that passes through the filter." For this study a .45 μm HAWP filter is used to separate the TSS from the TDS particles. Accurate sample volume measurements are crucial to determine the correct concentration of the sample. Each vacuum flask is weighed empty, and then reweighed with the sample volume inside. The values are subtracted to determine the exact volume passed through the filter. Each filter is weighed to the nearest 0.0001 g prior to and after filtration/drying to determine the mass of suspended solids. Each evaporating dish is also weighed prior to and following filtration/drying to determine the mass of the dissolved solids. The concentration (mg/L) of the dissolved/suspended matter is calculated using the following equation (Dukart 2008d):

Equation 3.1: Total Suspended Solids Equation

$$TSS,TDS = \frac{(A-B)*1000}{samplevolume,mL}$$

Both the solid filter papers and the displaced liquid are dried in dishes in an oven set at

approximately 100 C for at least one hour, or until dry. Desiccators are used to cool the samples without allowing moisture to infiltrate.

3.4 Statistical Analysis

3.4.1 Stormwater samples

Each of the stormwater samples were analyzed for pH, Conductivity (con), Total Nitrogen (TN), Total Phosphorus (TP), Total Dissolved Solids (TDS), Dissolved Cadmium (DCd), Dissolved Chromium (DCr), Dissolved Copper(DCu), and Dissolved Lead (DPb). For samples that were below the detection limit for the respective test a value of half of the detection limit was used. Table 3.4 shows the detection limits for each test and the corresponding value use in the data anaylsis.

Table 3.4: Minimum detection limits, and the values used for samples that fall below the minimum detection limit.

Test Parameter	Units	Minimum Detection limit	Value Used in Data Analysis
pH		3	1.5
Conductivity	uS/Cm	0	0
Total Nitrogen	mg/L	1.7	0.85
Total Phosphorus	mg/L	0.06	0.03
Dissolved Copper	ug/L	2.8	1.4
Dissolved Lead	ug/L	4.8	2.4
Dissolved Chromium	ug/L	2.2	1.1
Dissolved Cadmium	ug/L	0.5	0.25
Total Dissolved Solids	mg/L	0	0

There were a total of nine samples that were collected on a regular basis. Those samples were 2 first flush samples for each surface (AFF1, AFF2, CFF1, CFF2), and 5 soil pore water samples between each surface (C061, C121, C181, A061, A122). In the case where there were two samples were collected for the same surface at the same depth,

the average was taken. Three samples were attempted each storm, but did not provide a consistent enough of a sample for analysis. Those samples include a grab sample from each surface (CGS1, AGS1), and a soil water sample from either of the two 46 cm (18 in) deep pore water samples under the porous asphalt surface (A181, A182).

Using SPSS the descriptive statistics were calculated. The descriptive statistics reported by SPSS were the sample count, maximum value, minimum value, mean, and standard deviation for each sample and an average first flush value for both the pervious concrete and porous asphalt surfaces.

Since the data in not normalized a standard t-test does not fit perfectly as a comparison tool. On the other hand, A nonparmetric two independent sample Man-Whitney U test was performed to compare the samples of the porous asphalt side to the samples from the pervious concrete side and determine if there is a statistical difference between the each sample.

The Man-Whitney U test determines equality of the population means between two samples. Mann-Whitney tests that two sampled populations are equivalent in location. The observations from both groups are combined and ranked, with the average rank assigned in the case of ties. The number of ties should be small relative to the total number of observations. If the populations are identical in location, the ranks should be randomly mixed between the two samples. The test calculates the number of times that a score from group 1 precedes a score from group 2 and the number of times that a score from group 2 precedes a score from group 1. The Mann-Whitney U statistic is the smaller of these two numbers. The Wilcoxon rank sum W statistic, also displayed, is the smaller

of the two rank sums. If both samples have the same number of observations, W is the rank sum of the group that is named first in the Two-Independent-Samples Define Groups dialog box. The Mann-Whitney U test also reports the Z statistic or the location of the data if the distribution was normal (2008).

The Mann-Whitney U test then reports a two-tailed significance value. Each two-tailed significance value estimates the probability of obtaining a Z statistic as or more extreme as the one displayed, if there truly is no effect of the treatment (2008). For the purpose of this study any two-tailed significance value that is below .10 the samples are considered statistically different. Any two-tailed significance value greater then .1 is considered statistically similar.

In chapter 5 the results of the PAPC comparison study will be discussed.

Chapter 4 Stormwater Comparison Results and discussion

4.1 Background

The results of the stormwater comparison from the Porous Asphalt, Pervious Concrete (PAPC) comparison study are reported in this chapter. The water quality of nine samples, AFF1, AFF2, CFF1, CFF2, A061, A122, C061, C121, and C181, were analyzed for rain events when 6.35 mm (0.25 in) of rain fell in a 8 hour period. These samples were tested for pH, Total Dissolved Solids (TDS), Conductivity (Cond), Chlorides (Cl), Total nitrogen (TN), Total Phosphorus (TP), Dissolved Copper (DCu), Dissolved Lead (DPb), Dissolved Chromium (DCr), Dissolved Cadmium (DCd), and Dissolved Zinc (DZn).

Each porous asphalt stormwater sample was compared to the pervious concrete stormwater sample for the same location using descriptive statistics, graphs, and statistical tests. For this study a total of 19 storm events were sampled starting in November 2007 and ending in October 2008. Table 4.1 shows the date, duration, maximum 10-minute intensity, and total volume for each storm sampled in the 11-month period.

Table 4.1: 19 storms where the stormwater quality was tested for the PAPC comparison study

	Storm Dates	Storm Duration (Hrs)	Max 10 min rain intensity (mm/hr)	Total volume (mm)
1	11/15-16/2007	32.7	10.7	20.3
2	12/2-4/2007	39.8	15.2	82.0
3	12/9-10/2007	24.2	16.8	6.6
4	1/10-11/2008	15.5	19.8	18.5
5	2/10-11/2008	22.8	73.2	60.2
6	3/4-5/2008	23.5	38.1	39.4
7	3/31/2008-4/2/2008	56.3	15.2	35.3
8	4/3-6/2008	61.5	6.1	14.2
9	4/11-13/2008	24.2	15.2	22.6
10	4/26-28/2008	65.9	35.6	32.3
11	5/27/08	17.3	22.9	11.2
12	5/31/08	4.0	32.0	12.2
13	6/27-28/2008	28.5	38.1	19.3
14	7/14/08	5.5	18.3	13.0
15	7/23-24/2008	30.8	15.2	43.9
16	9/5-6/2008	28.3	45.7	133.6
17	9/12-13/2008	12.2	10.7	18.3
18	9/25-29/2008	96.2	67.1	88.1
19	10/25-26/2008	33.2	61.0	52.3
	Mean	32.8	29.3	38.1
	max	96.2	73.2	133.6
	min	4.0	6.1	6.6
	standard dev.	22.9	20.1	33.0

4.2 pH

The pH value is a measure of the acidity of the water. It is a measure of the hydrogen ion concentration on a logarithmic scale. A pH of 7 is considered to be neutral, a pH below between 1 and 6.9 is considered to acidic, and a pH from 7.1 to 14 is considered to be basic. A pH between 6 and 8 is generally considered a safe range for wildlife.

The pHs from the first flush samplers are the most acidic out of all of the samples. The average for the first flush samplers on the asphalt and concrete sides are 6.85 and 6.86, respectively. The pH of the samples taken from the soil pore water samples 15 cm

(6 in) and 30 cm (12 in) below the storage bed under the porous asphalt surface is close to neutral, and have a pH value of 7.02 and 7.07 respectively. The pH from the soil pore water from 15 cm (6 in), 30 cm (12 in), and 45 cm (18 in) below the storage bed under the pervious concrete side were basic having values of 7.41, 7.42, and 7.97 respectively. Table 4.2 shows the descriptive statistics for the pH of the samples. It reports the number of samples, range of values, the average and standard deviation for the seven sample depths (A061, A122, C061, C121, C181, AVG AFF, and AVG CFF).

Table 4.2: Descriptive Statistics for pH from the 20 rain events tested. The effective range is from 3 to 14.

pH Descriptive Statistics					
Sample	**N**	**Minimum**	**Maximum**	**Mean**	**Std. Deviation**
A061	18.00	6.35	7.82	7.02	0.38
A121	15.00	6.16	7.75	7.07	0.48
C061	8.00	6.82	8.12	7.41	0.43
C121	14.00	4.71	8.3	7.42	0.90
C181	17.00	5.88	9.78	7.97	0.93
AVG_AFF	18.00	5.48	8.5	6.85	0.81
AVG_CFF	17.00	5.43	7.93	6.86	0.66

Figure 4.1 shows the average for each of the seven-sample depth. The graph shows that the pHs in the first flush samplers entering the site have the lowest pH, the pore water samples from below the asphalt are almost neutral, and the pH from the concrete side has the highest pH.

Figure 4.1: Mean pH concentration graph for the 19 storms tested. C = Concrete, A = Asphalt, 6 = 06 in below bed, 12 = 12 in below bed, 18 = 18 in below bed, FF = First Flush Surface sample

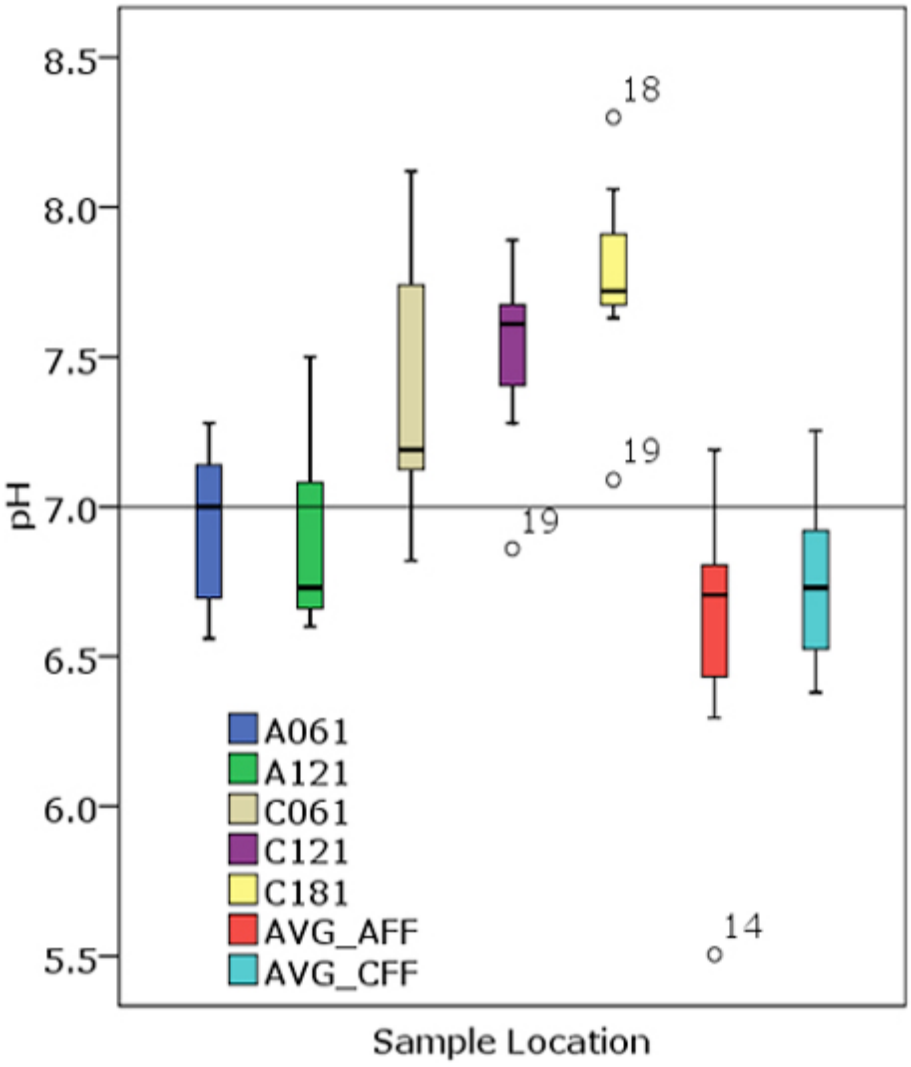

When a Mann-Whitney U test is performed to test the statistical difference between samples of the same depth but from different surfaces the pH at 15 cm (6 in) and the 30 cm (12 in) soil porewater depth are statistically different. The Mann-Whitney exact significance value for the 15 cm and the 30 cm depths are 0.043 and 0.025 respectively. For this thesis, any significance value under 0.10 is considered statistically

different. When the pHs for the average first flush samplers are compared to each other there is no statistical difference.

Finally, when the means for the 15 cm soil porewater values are compared to their respective surface's average first flush, there is no statistical difference for the asphalt side. On the other hand, there is a strong statistical difference on the concrete side with a significance of 0.036. Table 4.3 shows the results from the Mann-Whitney U tests.

Table 4.3: **pH Mann-Whitney U Test Statistics. 06, 12 and AVG FF are comparing the concrete and asphalt samples for the respective sample sites. A06_AFF and C06 _CFF compare the mean between the average first flush pH value and the 15cm (6 in) porewater pH for the two surfaces.**

pH Mann-Whitney U Test Statistics			
	D6	D12	DFF
Mann-Whitney U	35.5	53.5	146
Wilcoxon W	206.5	173.5	317
Z	-2.028	-2.248	-0.231
Asymp. Sig. (2-tailed)	0.043	0.025	0.817

4.3 Total Dissolved Solids, Conductivity and Chlorides

4.3.1 Total Dissolved Solids

The total dissolved solids (TDS) in a stormwater sample are substances that dissolve in the stormwater sample, and pass through a 0.45 μm filter. TDS particles can be composed of organic and inorganic compounds.

The results from the 19 storm events show a strong seasonal correlation. The TDS values in the colder months of November through March show high TDS values. These values are in some cases magnitudes higher than the TDS values in the non-winter months, April through October.

For each sample except C061, which was not collected and tested until April 2008, all of the sample's peak values occurred in the winter months. This is due to deicing compounds spread on the contributing watershed. Deicing compounds commonly

are ionic compounds that easily dissolve in water. Chloride (Cl^-) is a common anion found in deicing compounds. The use of chloride deicing agents in the surrounding watershed would support the high concentrations of TDS in the winter months and a lower concentration in the summer months. It is important to note that care was taken so that no deicing compounds were applied directly to porous surfaces themselves to protect the pervious concrete surface.

Figure 4.2: Total Dissolved Solids storm concentrations (mg/L). C=concrete, A=Asphalt, 6= 06 in below bed, 12= 12in below bed, 18= 18in below bed, FF=First Flush Surface sample, AVG=Average of two samples from the same surface, at the same depth, but different locations reported.

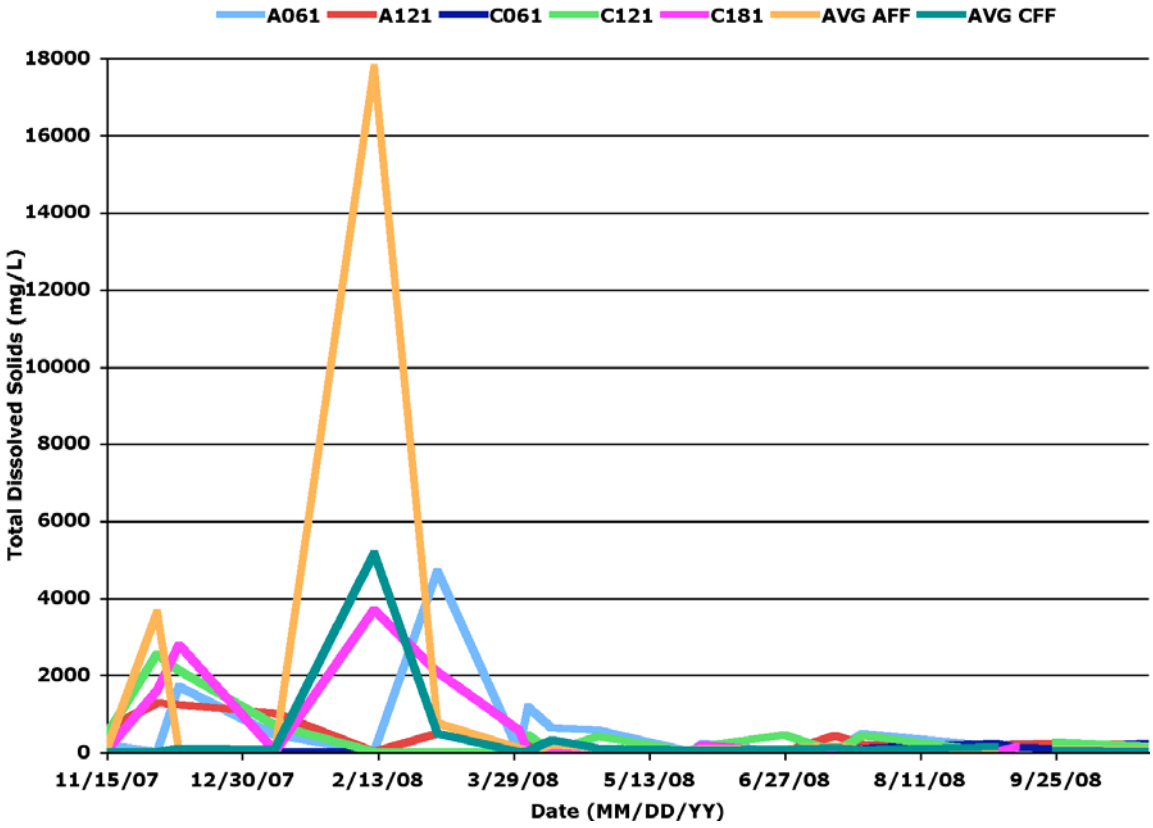

When descriptive statistics are analyzed, C181 has the highest mean concentration at 1382 mg/l, while the average asphalt first flush has the highest peak at 17743 mg/l. The standard deviations for each sample are high, and some cases much larger than the

mean. For example the average concrete first flush average is 401 mg/l, but one standard deviation is 1230 mg/l. This speaks to the large seasonal variation, where there could be high values for samples taken in the winter months, but much lower values, in some cases 0 mg/l, in the summer months. C121 is another sample where its standard deviation of 806 mg/l is greater then its average for the mean. Table 4.4 shows the descriptive statistics for each sample collected.

Table 4.4: Descriptive Statistics for Total Dissolved Solids from the 19 rain events tested. The effective range is above 0 mg/L.

TDS Descriptive Statistics					
Sample	**N**	**Minimum**	**Maximum**	**Mean (mg/L)**	**Std. Deviation**
A061	13	155.7	4687.0	838.4	1242.6
A121	12	157.6	1288.2	515.8	422.5
C061	6	0.0	219.7	125.3	82.4
C121	11	153.5	2528.2	731.3	805.9
C181	8	53.6	3680.3	1382.0	1373.1
AVG_AFF	18	0.0	17743.6	1295.0	4189.8
AVG_CFF	17	0.0	5151.3	401.2	1230.0

When the porous asphalt and pervious concrete samples are compared to one another using the Mann-Whitney U test, the 15 cm (6 in) depth samples are statistically different with a significance of 0.009. Because no 15 cm (6 in) samples were collected for the concrete side in the winter months this supports the conclusion that the seasons play a large role in the TDS concentration. When the 30 cm (12 in) and the first flush samples are compared for the two surfaces, there is no statistical difference. The 30 cm (12 in) depth samples had a significance of 0.740. Table 4.5 shows the results from the Mann-Whitney U test for the 15 cm (6 in), 30 cm (12 in), First flush samples, A061 compared to the average asphalt first flush, and C061 compared to the average first flush on the concrete side samples.

Table 4.5: Total Dissolved Solids Mann-Whitney U Test Statistics. 06, 12 and AVG FF are comparing the concrete and asphalt samples for the respective sample sites.

	06	12	AVG FF
Mann-Whitney U	9	60	130.5
Wilcoxon W	30	138	283.5
Z	-2.631	-0.369	-0.743
Asymp. Sig. (2-tailed)	0.009	0.712	0.458

4.3.2 Conductivity

The conductivity of the sample is a measure of the ions in water that carry an electrical current. A common ion is chloride (Cl^-), which is used in deicing products. In this study the conductivity was related to the season with the higher conductivities being seen in the winter months. The peak conductivity value for each first flush sample, and C181 was seen on February 12, 2008. A sample was not collected for C061 and C121 for that date because of a malfunction with the porewater sampler. The highest conductivity value for C121 came on December 2, 2008. For C061 and A061 the maximum values both came in the spring, occurring on April 11 2008 for A061, and April 26, 2008 for C061. It is worth noting that the first available sample for C061 was not collected until April 11, 2008, missing the winter months. Also, no deicing materials were applied directly to either porous surface in the first winter. Deicing materials were applied to the surrounding drainage area of the each surface.

An interesting trend, which will be discussed in the chlorides section, is the upward trend of the porewater samplers in the late summer months. This trend seems to follow the larger summer rainfall volumes. The unanswered question is where are these ions coming from, because the conductivity found in the first flush samples are some

times as much as a magnitude lower than those concentrations found in the porewater samples. Figure 4.3 shows the chloride values for the storm dates from March 31, 2008 until October 25, 2008 along with the rainfall volumes in inches.

Figure 4.3: Event conductivities (us/cm). C=Concrete, A=Asphalt, 06= 06in below bed, 12= 12in below bed, 18= 18in below bed, FF=First Flush Surface sample, AVG=Average of two samples from the same surface, at the same depth, but different locations reported.

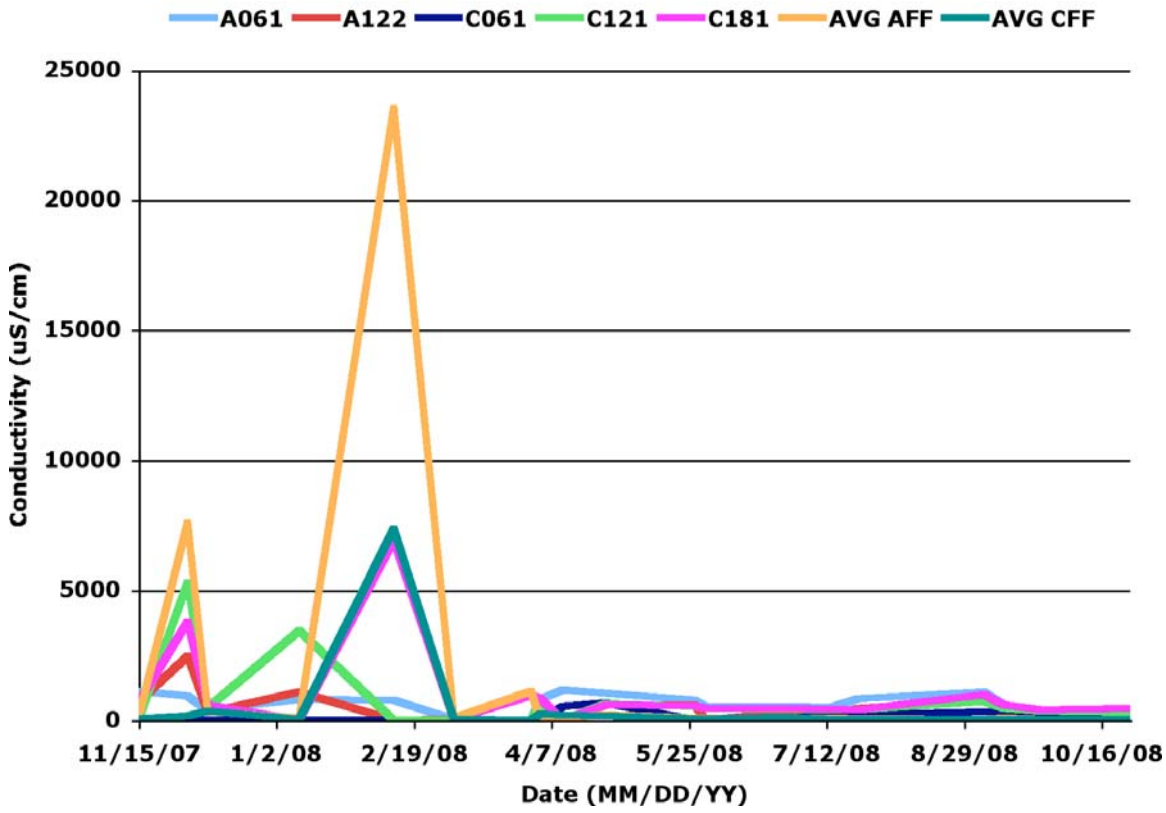

Figure 4.4: non-winter conductivity levels and rainfall.

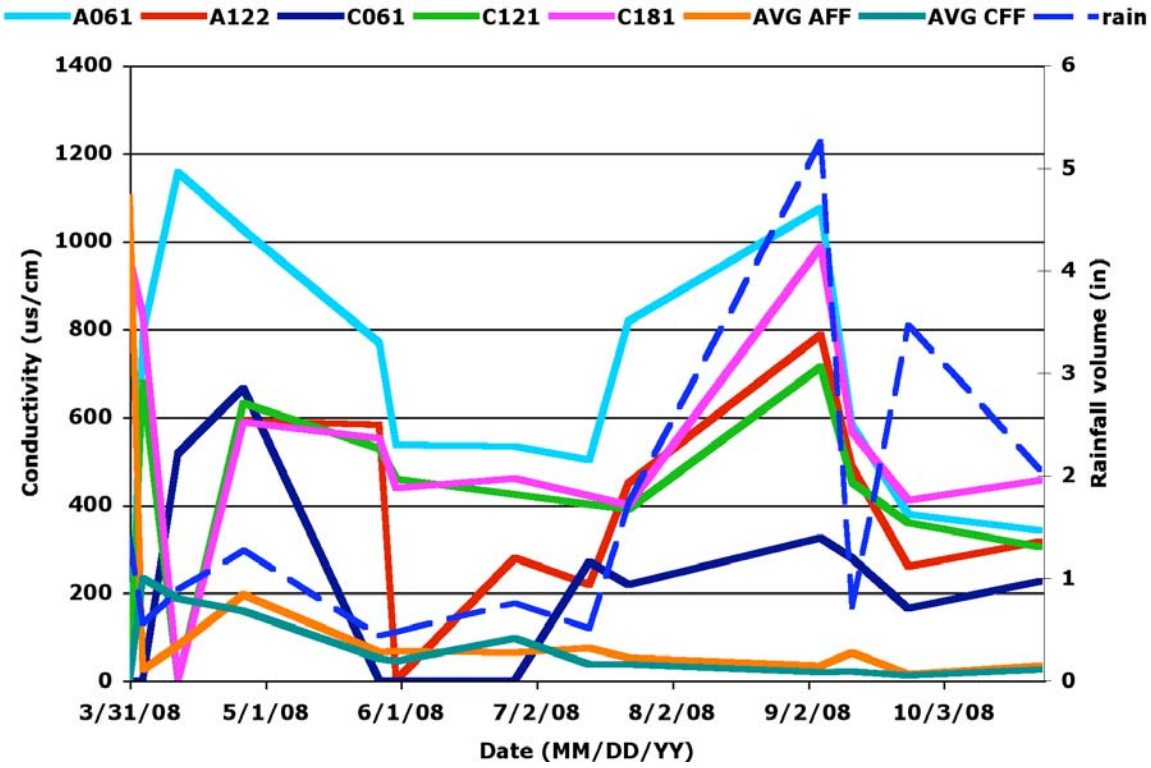

When the descriptive statistics are analyzed, C061 has the lowest mean of 333.70 μs/cm. This is due to the fact that no samples were collected through the winter months because of equipment malfunction. The average for A061 and A122 samples are in a similar range. The conductivity values for C121 and C181 are similar, but higher then the same depth on the asphalt side. The average asphalt first flush is considerably higher then the concrete first flush. This difference is mostly due to February 12, 2008 when the asphalt first flush had an average conductivity of 23,520 μs/cm while the average concrete value was only 7340.9 μs/cm. Table 4.6 shows the descriptive statistics for the conductivities of the seven samples analyzed.

Table 4.6: Descriptive Statistics for conductivity from the rain events tested. The effective range is above 0.

Conductivity Descriptive Statistics					
Sample	N	Minimum	Maximum	Mean	Std. Deviation
A061	18	19	1157	695.22	308.53
C061	8	165.6	666	333.70	170.98
A121	15	19	2470	612.80	578.30
C121	14	304	5260	1038.07	1455.82
C181	17	19.6	6900	1116.45	1695.44
AVG_AFF	19	14.04	23520	1762.64	5542.43
AVG_CFF	18	11.41	7340.9	492.08	1711.64

When the Mann-Whitney U test is performed the 15cm (6in) samples are statistically different with a significance of 0.003. This is most likely due to the fact that no C061 samples were collected in the winter months of this study. The Average first flush and the 15cm (12in) deep samples were statistically similar with significances of 0.24 and 0.50 respectively.

Table 4.7: Conductivity Mann-Whitney U Test Statistics. 06, 12 and AVG FF are comparing the concrete and asphalt samples for the respective sample sites.

	06	12	AVGFF
Mann-Whitney U	19	89.5	132.5
Wilcoxon W	55	209.5	303.5
Z	-2.944	-0.677	-1.17
Asymp. Sig. (2-tailed)	0.003	0.499	0.242

4.3.3 Chlorides

When the chloride descriptive statistics are analyzed, the chloride results follow both the TDS and conductivity trends as expected. C061 is the lowest, and that is because no C061 samples were collected during the winter months when chlorides are the highest. Each sample had high variability, and the standard deviation for the samples are once again sometimes larger than the average value. This is because the winter months have such high values and the summer months are so low. The range of every sample

except C106 is well over 1000 mg/L. The average asphalt first flush sample had the greatest range. The minimum value for the AVG FF sample was below the detection limit of 0.5 mg/l, while the maximum value was 9557 mg/L. Table 4.8 reports the descriptive statistics for the seven samples tested.

Table 4.8: Descriptive Statistics for Chlorides from the rain events tested. The effective range is above 0.5 mg/L.

Chlorides Descriptive Statistics					
Sample	**N**	**Minimum**	**Maximum**	**Mean (mg/L)**	**Std. Deviation**
A061	18	1.25	2674.17	501.48	603.32
C061	10	8.65	326	169.13	113.66
A121	16	0.25	977.15	277.76	278.08
C121	14	16.76	5471.73	853.61	1535.97
C181	17	0.25	1063.13	309.99	334.53
AVG_AFF	19	0.25	9556.9	858.45	2501.45
AVG_CFF	18	0.25	2826.96	277.87	735.91

When the samples from the porous asphalt side are compared to their pervious concrete counterparts using the Mann-Whitney U test the results follow what has been found for both TDS and conductivity. There is no significant difference between the first flush samples and the 30 cm (12 in) deep samples. The 15 cm (6in) samples are statistically different, but that is due to sampling periods, and not due to pavement properties. A sample from C061 was not collected until April of 2008 missing the winter season, and the highest chloride values.

Table 4.9: Chlorides Mann-Whitney U Test Statistics. 06, 12 and AVG FF are comparing the concrete and asphalt samples for the respective sample sites.

	D6	**D12**	**DFF**	**A06_AFF**	**C06_CFF**
Mann-Whitney U	40	85	145.5	57	49
Wilcoxon W	95	221	298.5	228	202
Z	-2.398	-0.833	-0.507	-3.322	-2.094
Asymp. Sig. (2-tailed)	0.017	0.405	0.612	0.001	0.036

As with the TDS concentration and the conductivity level, the chloride concentration is seasonal with the highest concentrations being observed in the winter months. From observing a graph of each event concentration, it appears that there is a lag in chloride concentration in the winter months when the surface first flush samples are compared with the soil porewater samples. This porewater lag effect is seen when one looks at the February 10, 2008 and March 4, 2008 Storms. The First Flush samples for both the concrete and asphalt side peak for the February storm, but the porewater samples remain low. For the March 4, 2008 storm the next rain event over 63mm (.25in) the opposite is observed. The First Flush values are low, and the porewater samples are high. This supports the theory that the chlorides are washed out of the system with the spring rains when deicing materials are no longer required. Figure 4.5 shows the chloride concentration (mg/l) for all 19-storm events tested.

Figure 4.5: Event chloride concentration. C=concrete, A=Asphalt, 6= 06 in below bed, 12= 12in below bed, 18= 18in below bed, FF=First Flush Surface sample, AVG=Average of two samples from the same surface, at the same depth, but different locations reported.

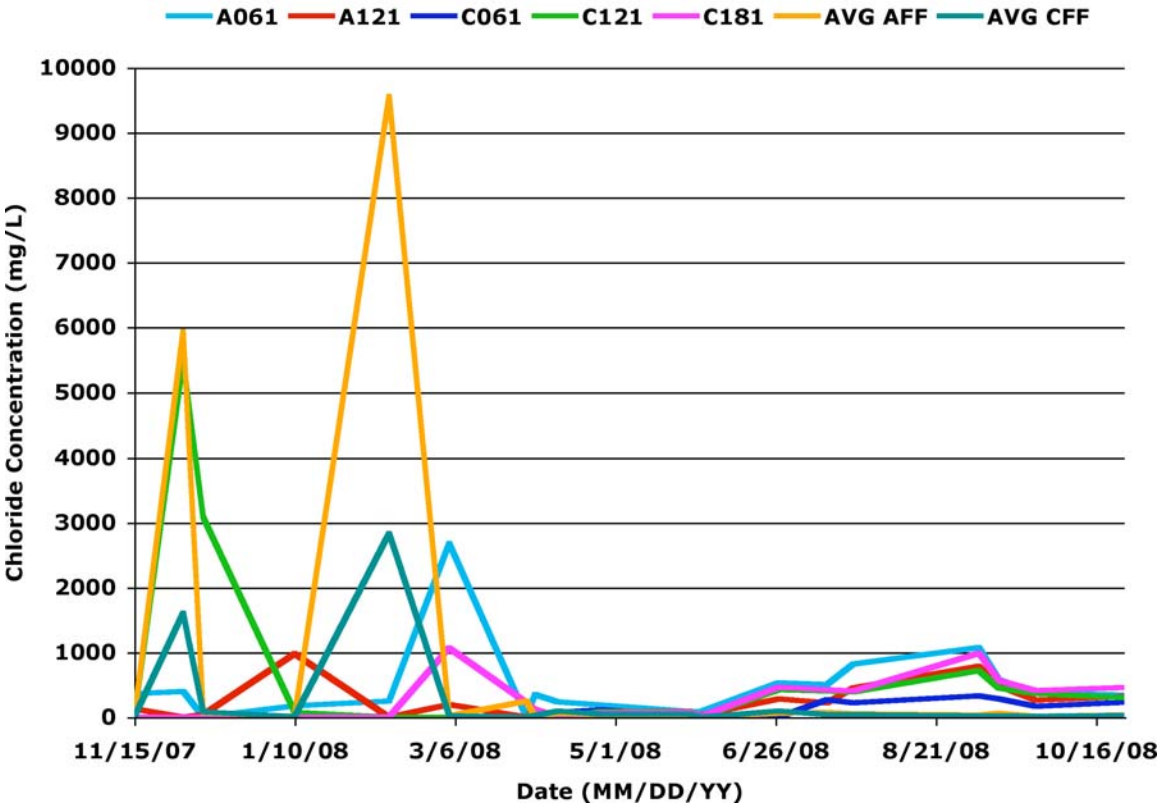

As with conductivity, an upward tend is observed through the summer months with a peak in early September. To show this effect, Figure 4.6 shows just the storm events tested from March 31, 2008 until October 25, 2008, along with the volume of rainfall for each storm event. When the storm rainfall volume is compared to the chloride concentration a strong relationship is observed for the porewater samplers. The largest rainfall event of 13.6 cm (5.36 in) resulted in the highest non-winter chloride peak for A061, A122, C061, C121, and C181. Interestingly, the first flush values for this period remain very low. Another interesting observation from the summer chloride concentration graph that is on the concrete side the chloride concentration becomes greater with depth. C061 has the lowest value, C181 has the highest and C121 is in the

middle. For the asphalt side A061 is the highest while, A122 is only slightly higher than C121.

Figure 4.6: Summer chloride values and storm rainfall volumes

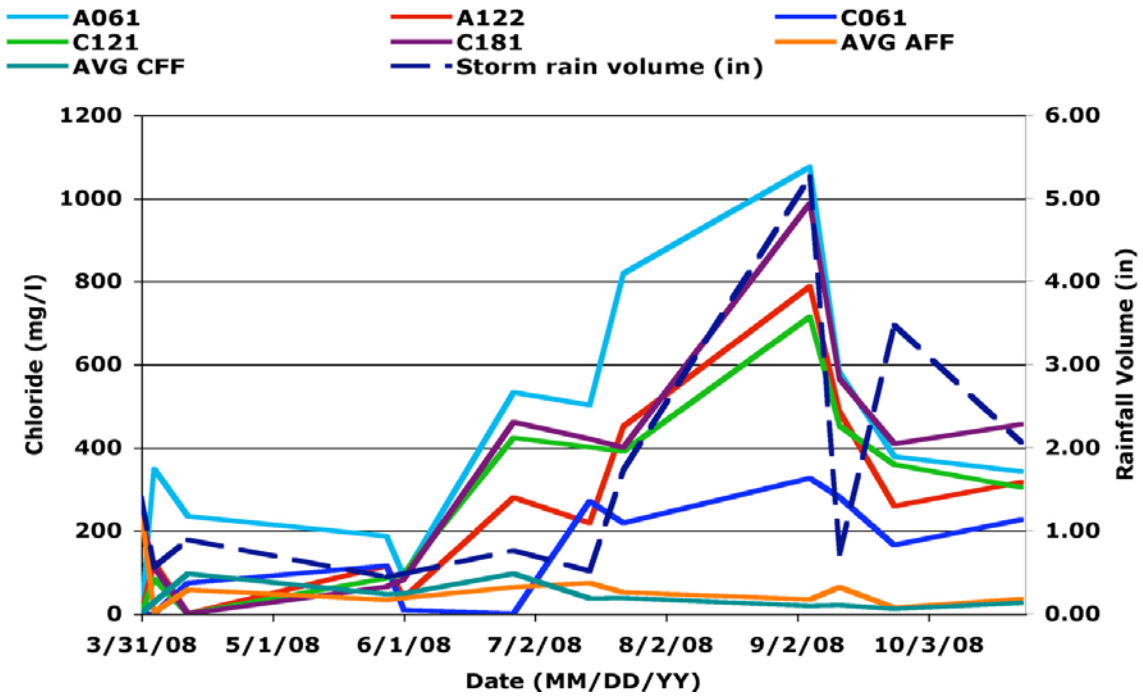

When a correlation test is performed, the porewater samples have strong correlation coefficients, C061 has the lowest coefficient at 0.49, and C181 has the strongest coefficient at 0.75. The chloride concentration of the first flush samplers on the other hand have a slight inverse relationship with the correlation coefficients being -0.14, and -0.46 for the asphalt and concrete average first flush samples. Table 4.10 shows the correlations coefficients between chloride concentration and the non-summer event rainfall volumes.

Table 4.10: Correlation coefficients of the relationship between chloride concentration and non-winter event rainfall volumes.

Sample	A061	A121	C061	C121	C181	AVG AFF	AVG CFF
Summer corelation coeff. to Rainfall Vol. 3/31-10/25/2008	0.65	0.74	0.49	0.69	0.75	-0.14	-0.46

From observing both graphs, it appears that after the September 4, 2008 storm the chloride value continues to decline; the high summer rainfall volumes may washout the remaining chlorides in the soil.

The question of what is the source of these chlorides for the non-winter upward trend needs to be asked. Up until now it was believed that the main chloride source was from the deicing material, and because chlorides are a conservative tracer they are supposedly washed out of the soil in the spring months, which is supported by the winter and early spring chloride results.

However, the observation of an upward trend that is correlated to the rainfall volume suggests that there is a chloride sink somewhere in the porous pavement system that traps and stores the chlorides in the system, and releases them during heavy rainfall events. The concentration reaching a peak value after a storm larger than 13 cm (5 in) supports the theory of a chlorides being stored in the soil, and not a continual source of chlorides. Further study is required to confirm this theory and gain a better understanding of the mechanisms that drive these observations.

4.4 Nutrients

4.4.1 Total Nitrogen

Because the total nitrogen results for only a few of A061 and A122 results were much higher than all of the other samples for the 19 storms, an outlier test was performed to see if those value were skewing the results. When the box Plot outlier test is performed for the A106 site with all of the samples include, the mild outlier range, which is 1.5 times the range between the 25 and 75 percentile, is any value above 18.4. Because the first A061 value is 18.7, it is considered an outlier and is not included in this analysis. When the 15.8 mg/l sample from the December 2, 2007 storm is tested in the same manner, the extreme outlier range is any number above 13.6 and thus this value is disregarded. The final value that classifies as an outlier is the 10.4 mg/l value on December 9, 2007. The mild outlier value for this test is 8.9 mg/l, which is less than the sample value, so it is disregarded. When this same test was preformed on the November 15, 2007 storm the A122 sample with a value of 11.7 it was found to be a mild outlier and was left out of the data set.

The reason these samples may have been so extreme is that there could have been some contamination when the porewater samplers were installed. Care was taken to rinse the samplers before installation with deionized water as recommended by the manufacturer. The manufacturer though does suggest discarding the first two samples after the sampler is installed. To expand the data set, we decided not to discard every sample from these storms; instead extreme values are tested for outliers.

When descriptive statistics are analyzed without the outlying vales included, the averages of all of the samples fall within a similar range. The asphalt samples have the highest averages with both samples being very close to 3.5 mg/l.

Table 4.11: Descriptive Statistics for Total Nitrogen for the 19 rain events tested. The effective range is above 1.7 mg/l. Outlier values from A061 and A122 are not included.

Total Nitrogen Descriptive Statistics					
Sample	**N**	**Minimum**	**Maximum**	**Mean (mg/L)**	**Std. Deviation**
A061	7	1.7	5.2	3.49	1.50
A121	9	0.8	7.1	3.52	2.22
C061	3	0.8	5.4	2.33	2.66
C121	9	0.8	4.5	2.57	1.27
C181	10	0.8	7.8	2.49	2.06
AVGAFF	14	0.8	5.6	2.28	1.25
AVGCFF	13	0.8	7.45	2.87	2.24

When the averages are compared, the nitrogen level in the native soil is equal to or higher than the total nitrogen being introduced to the system from the watershed. This result supports the findings of Kwiatkowski et al. (2007) who reported that the native soil had higher total nitrogen values than did the runoff from the surrounding watershed at a pervious concrete site

Figure 4.7: Mean total nitrogen concentration. C=concrete, A=Asphalt, 6= 06 in below bed, 12= 12in below bed, 18= 18in below bed, FF=First Flush Surface sample

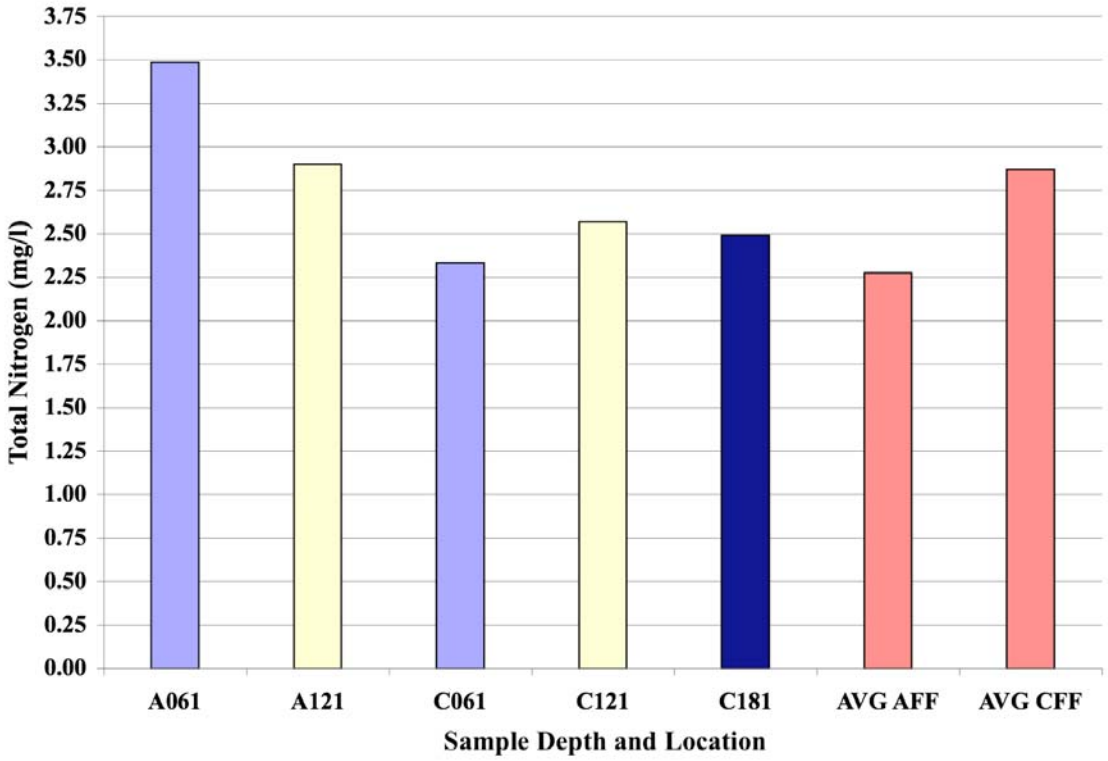

When the concrete and asphalt samples are compared using the Mann-Whitney U test, the samples at 15.24 cm , 30.5 cm and at the surface in the first flush are statistically similar. There is no statistical difference between any of these samples, from which one can conclude that neither pavement has a greater effect on the total nitrogen concentration.

Table 4.13 shows the results from the Mann-Whitney U Test. When the surfaces are compared to the 15.24 cm (6 in) samples there is no statistical difference meaning that over the 19 storms, with the early outliers disregarded from A061, that there is no statistical difference in the average First Flush total nitrogen concentration and the 15.24 cm (6 in) deep soil porewater sample for either surface.

Table 4.12: Total nitrogen Mann-Whitney U Test Statistics. 06, 12 and AVG FF are comparing the concrete and asphalt samples for the respective sample sites.

	06	12	AVG FF
Mann-Whitney U	7	28	86.5
Wilcoxon W	13	73	177.5
Z	-1.358	-1.117	-0.224
Asymp. Sig. (2-tailed)	0.175	0.264	0.823

4.4.2 Total Phosphorus

At the PAPC site, the Total Phosphorus concentrations varied quite substantially, but the average concentrations were very consistent between samples. The first flush samples had the widest variation of average concentration between pavement type, with the concrete side having an average concentration of 0.77 mg/l and the asphalt side average was 0.53 mg/l. The soil porewater samples were all between 0.22 and 0.30 mg/L. One explanation for the consistent values between the pore water samples is that the lysmeter "filters" the water preventing sediment and soil particles from entering the tubing. Because, phosphorus binds easily to soil the elimination of the soil particles decreases the insoluble phosphorus values. The first flush samples are not filtered so any soil particles that enter the container are included in the total phosphorus value. Table 4.14 shows the descriptive statistics for each of the stormwater samples collected and tested.

Table 4.13: Descriptive Statistics for Total Phosphorus from the rain events tested. The effective range is above .06 mg/L.

Total Phosphorus Descriptive Statistics					
Sample	N	Minimum	Maximum	Mean	Std. Deviation
A061	12	0.03	1.03	0.27	0.28
A121	11	0.03	0.82	0.30	0.30
C061	5	0.07	0.34	0.22	0.13
C121	11	0.03	0.58	0.24	0.17
C181	12	0.12	0.58	0.26	0.13
AVG_AFF	16	0.16	2.4	0.53	0.53
AVG_CFF	15	0.03	2.69	0.77	0.75

The results of the Mann-Whitney U test show there is no difference between the total phosphorus concentrations between surfaces, and despite being the porewater samples having lower average then the surface first flush the difference is not statistically differenent.

Table 4.14: Total phosphorus Mann-Whitney U Test Statistics. 06, 12 and AVG FF are comparing the concrete and asphalt samples for the respective sample sites.

	D6	D12	DFF	A06_AFF	C06_CFF
Mann-Whitney U	7	28	86.5	28	11
Wilcoxon W	13	73	177.5	133	17
Z	-0.805	-0.78	-0.224	-1.586	-1.178
Asymp. Sig. (2-tailed)	0.421	0.435	0.823	0.113	0.239

4.5 Dissolved Metals

The dissolved metals results were analyzed using the same methods as the other stormwater quality parameters, using descriptive statistics, average and event concentration graphs to identify any trends, and the Mann-Whitney U test to determine if there is a statistical difference in the pavement's performance.

Each dissolved metal concentration was analyzed for outliers using the outlier test discussed in the Total Nitrogen section of this chapter. The dissolved metal

concentrations that were greater than the upper mild boundary, which is 1.5 times greater then the difference between the 25th and 75th percentiles, were disregarded.

4.5.1 Dissolved Copper

The dissolved copper concentration entering each pavements surface was 7.70 μg/l for the porous asphalt and 7.07 μg/l for the pervious concrete first flush samples. The dissolved copper concentration was much lower than in the first flush. The porous asphalt 15 cm (6 in) and 30 cm (12 in) showed an average concentration of 3.07 μg/l and 3.19 μg/l. While concrete porewater samples for the 15 cm, 30 cm and 45 cm (18 in) had an average dissolved copper concentration of 1.74, 5.58 and 5.61 μg/l. The C061 sample was the only average dissolved copper concentration, which was below the detection limit of 2.8 μg/l, although all of the samples had at least one date which was below the detection limit. Table 4.16 shows the dissolved copper descriptive statistics.

Table 4.15: Dissolved copper descriptive statistics for the 19 rain events tested. The effective range is above 2.8 μg/l.

Dissolved Copper Descriptive Statistics					
	N	Minimum	Maximum	Mean	Std. Deviation
A061	12	1.40	9.23	3.07	2.45
A121	9	1.40	8.24	3.19	2.55
C061	6	1.40	3.42	1.74	0.83
C121	10	1.40	11.65	5.58	3.95
C181	10	1.40	12.87	5.61	4.53
AVG_AFF	18	1.40	15.65	7.70	3.44
AVG_CFF	18	1.40	22.18	7.07	6.01

The average dissolved copper concentration for the pavement types once they were adjusted for outliers were compared for statistical difference using the Mann-Whitney U Test. The results of the Mann-Whitney U test for the 15 cm, 30 cm, and for

the surface first flush samples all showed no statistical difference between the porous asphalt and pervious concrete for any of the samples. The significance for the 15 cm, 30 cm and surface samples was 0.2, 0.189.and 0.235 respectively. A significance of 0.10 greater is considered statistically similar. Table 4.17 shows the Mann-Whitney U test results.

Table 4.16: Dissolved Copper Mann-Whitney U Test Statistics. 06, 12 and AVG FF are comparing the concrete and asphalt samples for the respective sample sites.

	06	12	AVG_FF
Mann-Whitney U	24.5	29.5	124.5
Wilcoxon W	45.5	74.5	295.5
Z	-1.283	-1.315	-1.187
Asymp. Sig. (2-tailed)	0.2	0.189	0.235

4.5.2 Dissolved Lead

The dissolved lead average concentration, which was corrected for outliers, was calculated. The average concentration for the samples from the surface first flush, 15 cm (6 in), and 30 cm (12 in) porewater samples were all below the detection limit of 4.8 μg/l. Table 4.18 shows the descriptive statistics for the dissolved lead concentration.

Table 4.17 Dissolved Lead descriptive statistics for the rain events tested. The effective range is above 4.8 μg/l

Dissolved Lead Descriptive Statistics					
Sample	N	Minimum	Maximum	Mean	Std. Deviation
A061	13	2.4	5.00	2.60	0.72
A121	8	2.4	5.00	2.73	0.92
C061	6	2.4	2.40	2.40	0.00
C121	12	2.4	2.40	2.40	0.00
C181	9	2.4	6.00	2.80	1.20
AFF1	18	2.4	4.73	2.61	0.64
CFF1	17	2.4	6.74	2.90	1.40

Because all of the averages were below the detection limit of 4.8 μg/l there is not statistical difference between the two pavements. The significance for the 15 cm, 30 cm and the surface samples were 0.497, 0.221, and 0.551, respectively.

Table 4.18: Dissolved Lead Mann-Whitney U Test Statistics. 06, 12 and AVG FF are comparing the concrete and asphalt samples for the respective sample sites.

	06	12	AVGFF
Mann-Whitney U	36	42	142
Wilcoxon W	57	120	313
Z	-0.679	-1.225	-0.596
Asymp. Sig. (2-tailed)	0.497	0.221	0.551

4.5.3 Dissolved Chromium

The dissolved chromium concentration for all of the samples with the exception of the porewater sample at 45 cm (18 in) had an average concentration below the detection limit of 2.20 μg/l. The C181 sample had an average concentration of 2.26 μg/l.

Table 4.19: Dissolved Chromium descriptive statistics for the rain events tested. The effective range is above 2.2 μg/l.

Dissolved Chromium Descriptive Statistics					
	N	Minimum	Maximum	Mean	Std. Deviation
A061	13	1.1	1.1	1.10	0.00
A121	9	1.1	2.8	1.29	0.57
C061	5	1.1	4.52	1.78	1.53
C121	9	1.1	4.22	1.58	1.06
C181	10	1.1	5.68	2.26	1.91
AVG_AFF	18	1.1	1.71	1.13	0.14
AVG_CFF	17	1.1	2.75	1.47	0.68

When the averages for the 15 cm (6 in), 30 cm (12 in) porewater samples and the surface samples from the porous asphalt and pervious concrete surfaces are compared using the Mann-Whitney U test, there is no statistical difference between the two

surfaces. The significance for each of the sample depths tested were 0.497, 0.221, and 0.551 for the 15 cm, 30 cm pore water samples and the surface first flush samples, respectively. Table 4.21 shows the results from the Mann-Whitney U test for dissolved chromium.

Table 4.20: Dissolved Chromium Mann-Whitney U Test Statistics. 06, 12 and AVG FF are comparing the concrete and asphalt samples for the respective sample sites.

	D06	D12	AVG FF
Mann-Whitney U	36	42	142
Wilcoxon W	57	120	313
Z	-0.679	-1.225	-0.596
Asymp. Sig. (2-tailed)	0.497	0.221	0.551

4.5.4 Dissolved Cadmium

The average cadmium concentration was calculated for stormwater samples from the first flush, 15 cm (6 in), 30 cm (12 in), and 45 cm (18 In) pore water samplers below the infiltration bed. The detection level for dissolved cadmium is 0.5 μg/l. A061, C061, and C181 average concentrations were all below the detection limit. The A122, C121, and the average first flush samples were above the detection limit with concentrations of 0.96, 0.93, 1.04, and 1.33 μg/l, respectively. Table 4.22 shows the descriptive statistics

Table 4.21: Dissolved Cadmium descriptive statistics for the rain events tested. The effective range is above 0.5 μg/l.

Dissolved Cadmium Descriptive Statistics					
	N	Minimum	Maximum	Mean	Std. Deviation
A061	13	0.25	2.1	0.44	0.52
A122	8	0.25	3.3	0.96	1.15
C061	6	0.25	0.25	0.25	0.00
C121	9	0.25	5.2	0.93	1.63
C181	7	0.25	0.98	0.35	0.28
AVG_AFF	18	0.25	5.6	1.04	1.40
ACG_CFF	17	0.25	8.9	1.33	2.16

When the samples from the pervious concrete and porous asphalt are compared the 15 cm, 30 cm and the surface samples show no statistical difference. Table 4.23 shows the results from the dissolved cadmium Mann-Whitney U test.

Table 4.22: Dissolved Cadmium Mann-Whitney U Test Statistics. 06, 12 and AVG FF are comparing the concrete and asphalt samples for the respective sample sites.

	06	12	AVG FF
Mann-Whitney U	33	34	150.5
Wilcoxon W	54	79	303.5
Z	-0.987	-0.225	-0.085
Asymp. Sig. (2-tailed)	0.324	0.822	0.932

4.5.5 Dissolved Zinc

The dissolved zinc concentrations varied greatly from the surface samples to the soil porewater samples. The first flush samples had an average concentration of 190.55 μg/l and 90.42 μg/l for the average porous asphalt and average pervious concrete surface first flush samples. The soil porewater samples, A061, A122, C061, C121 and C181, were all similar with concentration of 17.51 μg/l , 23.22 μg/l, 12.53 μg/l, 20.40 μg/l, and 19.11 μg/l, respectively.

Table 4.23: Dissolved Zinc descriptive statistics for the rain events tested. The effective range is above 0.5 µg/l.

Dissolved Zinc Descriptive Statistics					
	N	Minimum	Maximum	Mean	Std. Deviation
A061	11	2.4	39	17.51	13.03
A121	6	2.4	50	23.22	18.64
C061	6	2.4	35	12.53	13.09
C121	8	2.4	66	20.40	21.38
C181	7	2.4	55	19.11	18.28
AVG_AFF	16	2.4	1436	190.55	377.13
AVG_CFF	15	2.4	557	90.42	137.73

When the Mann-Whitney U test was performed for the 15 cm, 30 cm and first flush samples there was no statistical difference for samples from the same depth, but different pavement surfaces. Table 4.25 shows the results from the dissolved zinc Mann-Whitney U test.

Table 4.24: Dissolved Zinc Mann-Whitney U Test Statistics. 06, 12 and AVG FF are comparing the concrete and asphalt samples for the respective sample sites.

	D06	D12	AVG FF
Mann-Whitney U	25.5	21.5	100
Wilcoxon W	46.5	57.5	220
Z	-0.771	-0.326	-0.792
Asymp. Sig. (2-tailed)	0.44	0.744	0.428

The dissolved zinc had the highest values, and also showed the greatest reduction in concentration from the first flush to the soil pore water samples. This reduction was also observed in the samples of dissolved copper and dissolved chromium. The observed decline in the metal concentration from the surface first flush concentration to the soil porewater samples is supported by other research analyzing the metal concentration in porous pavements and infiltration basins (Barraud et al. 1999; Boving et al. 2008; Kwiatkowski et al. 2007; Mikkelsen et al. 1997; Welker et al. 2006)

Chapter 5 Total Hydrocarbon and PAH Bench top study

5.1 Background

A bench top Polycyclic Aromatic Hydrocarbon (PAH) study was performed on samples of pervious concrete and porous asphalt. This test is designed to identify potential sources of PAH in the pavements which may increase the PAH and hydrocarbon pollutant loads of the stormwater entering the infiltration bed beneath the surface. The binder used in the Porous Asphalt surface is a PG 64-22 binder. This is a standard roadway binder that is commonly used in the mid-Atlantic region because of its ability to withstand the temperature fluctuations in this area. The bench top study attempts to identify and quantitate PAHs, which may leach from either pavement type and could lead to potential subsoil or ground water contamination.

Because the binder used in the porous asphalt bitumen mix is very similar to that used in standard asphalt mixes, the PAHs found leaching from the porous asphalt pavement should be similar to those found leaching from standard asphalt. Several studies have looked at the leaching possibility of standard bitumen asphalt (Birgisdóttir et al. 2007; Brandt and De Groot 2001; Legret et al. 2005; Sadler et al. 1999). All of these studies have, at least in part, focused on the Polycyclic Aromatic Hydrocarbon (PAH) molecules because of their potentially harmful properties. The US EPA identifies 16 different PAH molecules, seven of which are potential human carcinogens. These molecules vary from 2 to 6 aromatic rings. The molecules which have more rings are less soluble in water, and are more toxic (Bojes and Pope 2007).

Table 5.1:US EPA 16 priority-pollutant PAHs, their molecular weights, and solubility in water (ATSDR 2005).

PAH*	Structure (# of rings)	Molecular weight (g/mole)	Solubility (mg/L)
Naphthalene	2	128.17	31
Acenaphthene	3	154.21	3.8
Acenaphthylene	3	152.2	16.1
Anthracene	3	178.23	0.045
Phenanthrene	3	178.23	1.1
Fluorene	3	166.22	1.9
Fluoranthene	4	202.26	0.26
Benzo(a)anthracene	4	228.29	0.011
Chrysene	4	228.29	0.0015
Pyrene	4	202.26	0.132
Benzo(a)pyrene	5	252.32	0.0038
Benzo(b)fluoranthene	5	252.32	0.0015
Benzo(k)fluoranthene	5	252.32	0.0008
Dibenz(a,h)anthracene	6	278.35	0.0005
Benzo(g,h,i)perylene	6	276.34	0.00026
Indeno[1,2,3-cd]pyrene	6	276.34	0.062

*US EPA has classified PAHs in italics as probable human carcinogens

Sadler et al. (1999) looked at soil samples from below an asphalt lot that was paved in 1951 and used for electric trolley cars. From 1969 until the time of this study in 1997, the site was not used except for periodic access to storage sheds. Sadler et al's hypothesis was that since there was limited use of combustion engines on the lot that the majority of the PAHs below the asphalt surface should have been leached from the pavement surface. They used a solid–liquid extraction of the hydrocarbons from soil samples from eight different sites beneath the asphalt surface. The hydrocarbon extract was analyzed using a GCMS. Their results showed PAH levels between <1-19.5 mg/kg. When the authors analyzed the results they found that the level of hydrocarbons extracted from the soil had a linear relationship with the underlying soil moisture, and a logarithmic relationship with the water solubility of particular PAH molecules. The slope and correlation coefficient between the moisture content in the soil and PAH

concentration can be found in table 5.2. The positive linear relationships (slope) indicates that soils with a higher moisture contents will leach more likely to PAH's from the pavement. From these relationships they concluded that PAHs do contribute to soil PAH contamination and that level is depended on the soil moisture content (Sadler et al. 1999).

Table 5.2: Relationship between PAH levels and % moisture content at former trolley bus depot (Sadler et al. 1997)

PAH	* Slope of line	Correlation coefficient
Fluoranthene	1.42	0.94
Pyrene	1.19	0.93
Benz(a)anthracene	0.39	0.98
Chrysene	0.41	0.9
Benzo(b+k)fluoranthene	0.85	0.91
Benzo(a)pyrene	0.36	0.88
Indeno(l ,2,3-cd)pyrene	0.2	0.99
Benzo(g,h,i)perylene	0.05	0.99

*Slope of plot = [ΔPAH]/Δ% moisture.

By performing a 36 day lstatic leach test, Brant and De Groot (2001) found that only PAHs with four rings or less could be found in concentrations greater than 0.1 ng/l. They also discovered that PAH compounds with five or more rings were not found in concentrations greater then 0.4 ng/l. They found that steady state concentration for the PAHs with two or more rings was reached between 3 and 6 days (Brandt and De Groot 2001). Overall, Brant and De Groot (2001) found that the concentrations of the leach water from the bitumen products stayed well below the surface water limits in many European Union Countries, and more then a magnitude lower then the standards for potable water.

Legret et al. (2005), also looked at leaching of asphalt pavements. They studied if there was a difference between new and reclaimed asphalt pavements, and found that after three 16 hour batch leaching tests that the total hydrocarbon concentrations were 62, 52 and 52 μg/L. The only PAH molecule that was above the detection limit was Phenanthrene. Although above the detection limit, the concentration of Phenanthrene never rose above the Dutch level for ground water intervention. The concentration for benzo(a)pyrene remained below .01ppm. Also, the sum of the four PAH molecules noted in the European Union guideline for drinking water remained below the threshold value of 0.1 ppb (Legret et al. 2005).

Birgisdóttir et al. (2007) attempted to explain the source of the high PAH concentration near and under roadways. They performed a 64 day leach test to determine the amount of PAHs that leach out of bitumen pavements. Samples of the wearing and base layers of two different asphalt sites were examined. The first pavement pavement was 22 years old when it was tested; the second sample was one year old at the time of sampling. Naphthalene and Phenathrene were found in the highest concentrations in the four samples tested, which were an old wearing layer, a new wearing layer, an old base layer, and a new wearing layer. The total sum of the 16 EPA PAH molecules in the four asphalt specimens was 0.53-3.5 mg/Kg. Overall, they concluded that the high level of PAHs found under and around the bitumen asphalt pavements is unlikely caused by the leaching from the pavements (Birgisdóttir et al. 2007).

5.2 Project overview

We performed a similar static leach tests on fresh samples of both Porous Asphalt and Pervious concrete these samples were submerged in reagent-grade purified water for 100 days.

The bench top study was designed to identify and quantitfy any PAHs released into the water from either surface. A full system hydrocarbon investigation of the porous pavement comparison site was attempted, but it was determined that there were too many potential hydrocarbon sources to determine if the source of the hydrocarbons was from the pavement's surface. The next sections will describe the method of isolating and analyzing these samples for their hydrocarbon concentrations.

5.3 Sample preparation

The bench top study involved submerging two samples of new porous asphalt and two samples of new pervious concrete in reagent-grade water. Each pervious concrete and porous asphalt sample submerged in this test were from the same mixtures as used on the PAPC BMP site.

Each sample was placed in its own 1 liter glass container and reagent grade purified water was poured through the pavements surface until the 1 liter container was completely filled. A blank sample and a sample containing only a submerged PVC ring similar in dimensions to that used to contain each sample were used as controls. The samples were covered with aluminum foil to avoid contamination from dust, and stored in a closed shelf with no direct sunlight for 100 days.

After 100 days the samples were removed and 200 mL of the soaking water was extracted for this study. For the asphalt and concrete samples duplicate samples were collected for each of surface sample.

5.4 Sample extraction

The hydrocarbon extraction process is a liquid-liquid extraction, and was developed for a previous study by Salas-de la Cruz (2007), which was adapted from Rocher et al (2004).

Labeled PAH isotopes were used as the internal standard at a concentration 0.05 mg/L. The labeled PAHs were Acenaphthene-d10, Chrysene-d12, 1,4-Dichlorobenzene-d4, Naphthalene-d8, Perylene-d12, and Phenanthrene-d10.

Methylene chloride was used as the solvent to extract any hydrocarbons that are found in the samples. The sample was mixed with 100 ml of methylene chloride, and the methylene chloride and any hydrocarbons from the sample were allowed to separate from the water and were removed. Each glass container and jar was rinsed two times with 10 ml of methylene chloride before being added to the sepratory funnel. The 100 ml of methylene chloride sample was then passed through a silica gel column to remove any potential contaminants.

The sample was evaporated down using a hot water bath in which the water was at 45 degrees Celsius under nitrogen flux until the volume was between 1.7 to 1.9 ml. After this final step, the sample was transferred to a Supelco 2 mL amber vial with a screw top. The vial was closed with Supelco screw caps for 12 x 32 vials with 8 mm Teflon faced silicone septa and transferred to the GC unit for analysis (Salas-de la Cruz 2007).

Figure 5.1: Flow chart of hydrocarbon extraction procedure.

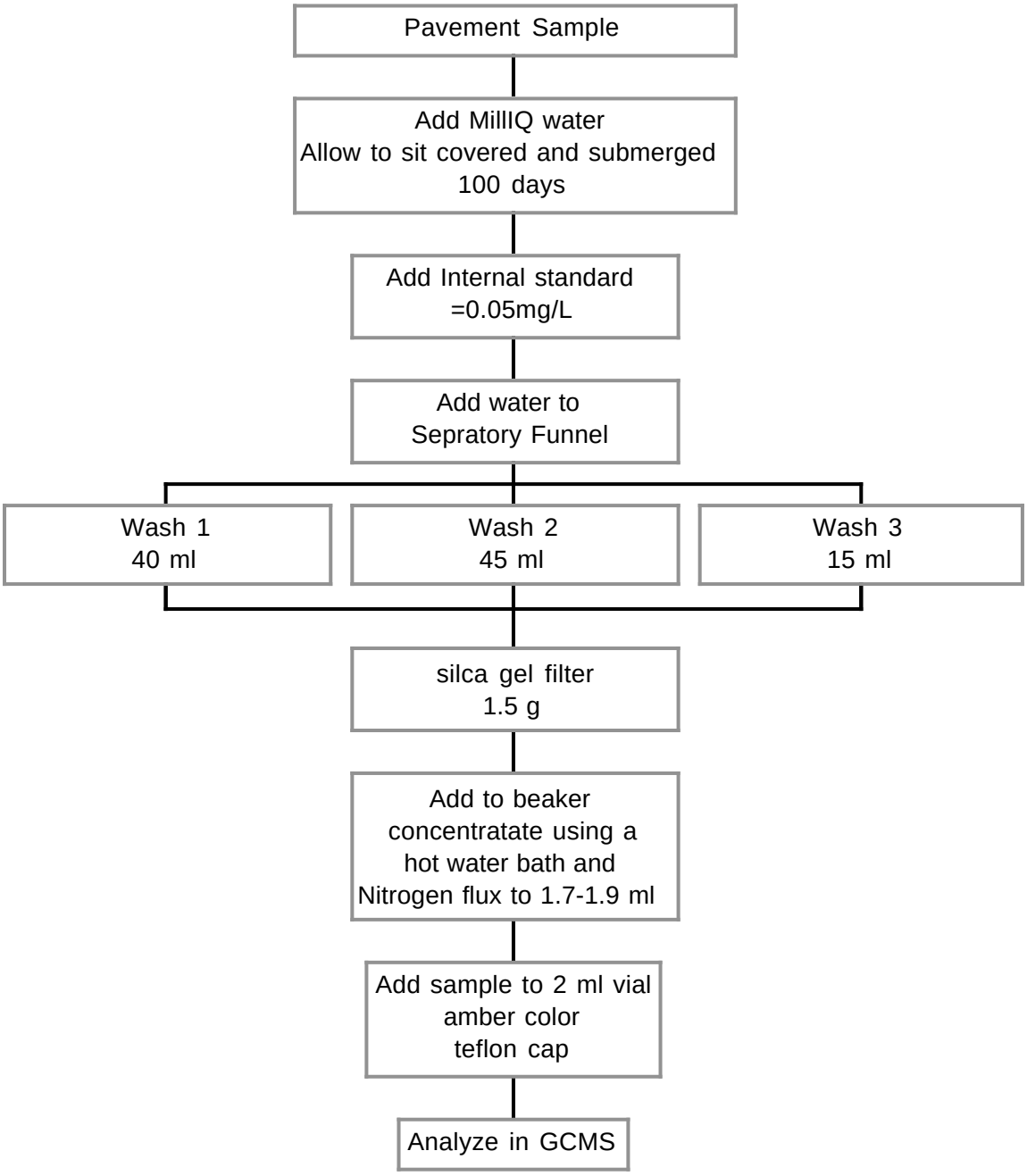

5.5 Gas Chromatography Mass Spectroscopy set up and method

Each sample was analyzed using a Agilent 6890N-5973 gas chromatograph mass spectrometer (GCMS) installed with a DB1 column (30 m x 0.32 mm x 3 um) capillary

column. The method was adapted from EPA method 8270C. The method can be found in table 5.3.

Table 5.3:Analysis Method for phase 1 of the PAPC surface Bench Top Study

PAPC Hydrocarbon Bench Top Study Analysis Method		
Parameter	**Value**	
Carrier Gas	Helium	
Constant Flow @	44cm/s	
Injection Temperature	250 ^{o}C	
Detection Temperature	280 ^{o}C	
Intial Oven Temperature	40 ^{o}C	
Solvent Delay Time	10 min	
Mode	Scan 35-800 amu	
Rate	**Oven Temperature**	**Hold Time**
^{o}C/min	**^{o}C**	**min**
----	40	4
20	220	15
10	270	60
Total Run Time (min)	90	

5.6 Hydrocarbon Characterization and GCMS method validation

The individual separated PAH compound's peak areas were established for all of the separated compounds whose retention times were above 10 min using the PAH standard. The solvent is detected at a retention time of 5 to 11 minutes. Each of the peaks were identified on the chromatograph by comparing known samples and their identifying primary and secondary ions found from EPA 8270C semi-volatile organic compound analysis method (US EPA 1996). A PAH standard containing the 16 PAH can be found in Table 5.4, which was used for the method validation.

Table 5.4: List of 16 PAHs used to test the method, and their primary ion, secondary ion, and retention time.

Compound	EPA 8270 Ret. Time (min)	Bench Top Method Ret. Time (min)	Primary ion	Secondary ions
Naphthalene	9.82	12.8	128	129,127
acenphthylene	14.57	15.1	152	151,153
Acenaphthene	15.13	15.4	154	153,152
Fluorene	16.70	16.3	166	165,167
Phenanthrene	19.62	18.2	178	179,176
anthracene	19.77	18.3	178	176,179
Fluoranthene	23.33	21.7	202	101,203
Pyrene	24.02	22.7	202	200,203
Benz(a)anthracene	27.83	30.5	228	229,226
chrysene	27.97	30.8	228	226,229
benzo(b)fluoranthene	31.45	44.6	252	253,125
benzo(k)fluoranthene	31.55	45.0	252	253,125
Benzo(a)pyrene	32.80	50.2	252	253,125
Indeno(1,2,3-d,d)pyrene	39.52	78.8	276	138,227
Dibenz(a,h)anthracene	39.82	80.8	278	139,279
benzo(g,h,i)perylene	41.43	88.0	276	138,277

The method from Table 5.3 was tested before any calibration or detection limit studies were performed to a sure that each compound is properly separated in the resulting chromatograph and provided a consistent values using a standard solution of PAH compounds found in Table 5.4.

5.7 Instrument Detection Limit

The individual PAH compound detection limit was performed using section 1030E Method Detection level (Eaton et al. 1995). The instrument detection level (IDL) was determined by analyzing the noise levels for each time period (+/- .5 sec) around each PAH peak identified in Table 5.4. The low and high levels from each retention time period were recorded for 15 blanks runs over multiple days. The difference in height between the low and high points was determined. The average noise height and the

standard deviation for each retention time were calculated by the usual method. The IDL was determined to be 3 standard deviations greater than the average height for each time. Table 5.4 shows the noise level and the IDL peak height.

The method detection level was estimated based off of the IDL values. Samples of standard and reagent grade water were mixed in a concentration of 0.001,0.005, 0.01 and 0.2 mg/l, and extracted using the extraction method. These samples were analyzed using the GCMS with the goal being to determine which concentration will be between 1 and five times the IDL.

5.8 Method Detection Level and PAH Analysis

The GC unit uses the ChemStation Program to automatically calculate the area under the curve for each of the separated compounds. Each separated compound's peak areas must meet the equipment detection limit as identified in the previous section. Any point below this detection limit is not quantified. Each of the 16 PAH compounds were quantified individually. The Method detection Limit (MDL) and the PAH concentration were calculated based off a the internal standard response (Eaton et al. 1995).

5.8.1 Internal Standard Calibration

The internal standards of Acenaphthene-d10, Chrysene-d12, 1,4-Dichlorobenzene-d4, Naphthalene-d8, Perylene-d12, and Phenanthrene-d10, and are the recommended internal standard in the EPA 8270 method (U.S. EPA 1996).

Each sample analyzed had the concentration of the internal standard equaling 0.05 mg/l added. EPA method 8270C reports which internal standard corresponds to each PAH molecule for calibration (U.S. EPA 1996). Table 5.5 describes shows which internal standards were to calibrate each PAH molecule.

Table 5.5:PAH compounds and the corresponding internal standards used to calibrate their concentrations (U.S. EPA 1996).

Napthalene d8	Acenaphthene d10	Phenanthrene d10	Chrysene d12	Perylene d12
Napthalene	Acenphthylene	Phenanthrene	Pyrene	Benzo(a)pyrene
	Acenaphthene	Anthracene	Benz(a)anthracene	Benzo(b)fluoranthene
	Fluorene	Fluoranthene	Chrysene	Benzo(k)fluoranthene
				Indeno(1,2,3-d,d)pyrene
				Dibenz(a,h)anthracene
				Benzo(g,h,i)perylene

The equation used for the internal standard calibration procedure was (Eaton et al. 1995):

Equation 5.1 Internal standard calibration

$$\text{Concentration } (\mu g/L) = \frac{(\mathrm{A_s})(I_s)}{(A_{\mathrm{is}})(RF)(V_0)}$$

where $\mathrm{A_s}$ is the response for the compound to be measure, $\mathrm{I_s}$ is the amount of internal standard added to each extract (μg), $\mathrm{A_{is}}$ is the response for the internal standard, RF is nondimensional response factor, and $\mathrm{V_0}$ is the amount of water extracted in L. $\mathrm{I_s}$ and $\mathrm{V_0}$ for each sample was 10 μg and 0.2 L, respectively.

The response factor was calculated for each compound using equation 5.2 analyzed the area of the compound response compared to the known standard concentration. The response factor was calculated as the first step of analysis by analyzing a 50 μg/L concentration of the PAH standard mixed with 50 μg/L of the internal standard. The average of three different samples was taken to be the area of each. The response factor for each compound was then calculated using the appropriate internal standard, as outlined in table 5.5, using the equation (Eaton et al. 1995):

Equation 5.2 Response factor equation

$$RF = \frac{(A_s)(C_{IS})}{(A_{IS})(C_s)}$$

Where A_s is the response area of the compound, C_{is} is the concentration of the internal standard in ng/μL, A_{IS} is the response area of the internal standard, and C_S is the concentration of the PAH compound (Eaton et al. 1995). Table 5.5 shows the concentration of the PAH compounds and the internal standards, the response area for each, and the resulting RF value.

Table 5.6: The RF values used to calculated the individual PAH concentration.

Compound	C_S ng/μL	A_S	C_{IS} ng/μL	A_{IS}	RF
Napthalene	0.05	40452848	0.05	38403099	1.05
Acenphthylene	0.05	35955263	0.05	27943041	1.29
Acenphthene	0.05	28136393	0.05	27943041	1.01
fluorene	0.05	46616829	0.05	27943041	1.67
Phenanthrene	0.05	152688631	0.05	52597594	2.90
Anthracene	0.05	115688631	0.05	52597594	2.20
fluoranthrene	0.05	76131240	0.05	52597594	1.45
Pyrene	0.05	81139161	0.05	50460966	1.61
Benz(a)anthracene	0.05	50343948	0.05	50460966	1.00
Chrysene	0.05	52979789	0.05	50460966	1.05
Benzo(b)fluoranthene	0.05	25082224	0.05	9575468	2.62
Benzo(k)anthrene	0.05	19054844	0.05	9575468	1.99
Benzo(a)pyrene	0.05	42045415	0.05	50460966	0.83
ideno(1,2,3-d,d)pyrene	0.05	6050777	0.05	9575468	0.63
dibenz(a,h)anthracene	0.05	6077800	0.05	9575468	0.63
benzo(g,h,i)perylene	0.05	5502214	0.05	9575468	0.57

5.9 Results and Discussion

No PAH compounds were found for any of the samples tested to be above the method detection limit after 2 pervious concrete samples, 2 porous asphalt samples, and a 15cm diameter PVC sample were left submerged in reagent grade water for 100 days there was no difference between the surface samples, the PVC sample, and a blank sample when the PAHs were extracted and analyzed using a GCMS following EPA

Method 8270C. The 16 individual PAH compound concentrations were calculated from the internal standard response, and the total PAH concentration was the sum of all of the individual PAH concentrations. Four samples for the pervious concrete and porous asphalt were analyzed from two different samples. Table 5.7 describes all of the samples analyzed in this leach test.

Table 5.7: Sample descriptions of the 10 samples analyzed in the porous pavement static leach test.

Sample Name	Sample Description
Blank	Reagent Grade water
PVC	15 cm (6") diameter PVC ring, reagent grade water
AVG PC1	Average of pervious concrete sample 1+ contents of PVC sample
AVG PC2	Average of pervious concrete sample 2 + contents of PVC sample
AVG PA1	Average of porous asphalt sample 1 + contents PVC sample
AVG PA2	Average of porous asphalt sample 2 + contents of PVC sample

The blank containing only reagent grade water did not show any PAH compounds. In the PVC sample, 12 out of the 16 PAH compounds were detected, all below the detection limit. there were 10, 10, 7 and 6 PAH compound identified below the detection limit respectfully. Finally, in the porous asphalt samples PA1A, PA1B, PA2A, and PA2B had 4,7,8 and 6 PAH compounds below the detection limit. Table 5.6 shows the method level detection limit, the concentrations for each individual PAH compound, and the total PAH concentration for the reagent grade water, PVC, PC1, PC2, PA1, and PA2 samples.

When all of the PAH concentrations are added together, the PVC sample had the highest overall PAH content at 2.35 μg/L. The highest pervious concrete sample was PC2A, which had a concentration of 1.94 μg/L. The highest porous asphalt sample PA2B that had a concentration 0.55 μg/L.

Table 5.8: The results from porous pavement 100 static leach test. ND concentrations shows that no response was found for that compound in the analysis, *bold and italicized* values were below the method detection limit.

Compound	LDL µg/L	Blank Water µg/L	PVC µg/L	AVG PC1 µg/L	AVG PC2 µg/L	AVG PA1 µg/L	AVG PA2 µg/L
Napthalene	1.00	ND	***0.07***	***0.04***	***0.06***	***0.04***	ND
Acenphthylene	0.86	ND	***0.07***	ND	***0.11***	*ND*	ND
Acenphthene	0.93	ND	***0.11***	***0.14***	***0.14***	***0.09***	***0.11***
fluorene	0.55	ND	ND	ND	ND	ND	ND
Phenanthrene	0.25	ND	***0.06***	***0.04***	**0.03**	***0.03***	***0.01***
Anthracene	0.33	ND	***0.08***	***0.06***	**0.04**	***0.04***	***0.01***
fluoranthrene	0.43	ND	***0.10***	***0.03***	**ND**	***0.04***	ND
Pyrene	1.21	ND	***0.11***	***0.02***	ND	ND	***0.03***
Benz(a)anthracene	1.33	ND	ND	***0.01***	ND	***0.09***	***0.05***
Chrysene	1.51	ND	***1.23***	***0.07***	ND	*ND*	***0.03***
Benzo(b)fluoranthene	4.53	ND	***0.02***	***0.05***	***0.04***	***0.06***	ND
Benzo(k)anthrene	4.73	ND	***0.10***	***0.08***	***0.06***	***0.05***	***0.05***
Benzo(a)pyrene	38.21	ND	ND	***0.05***	***0.82***	***0.14***	***0.14***
Ideno(1,2,3-d,d)pyrene	17.04	ND	***0.20***	ND	***0.78***	ND	***0.17***
Dibenz(a,h)anthracene	17.95	ND	ND	***0.13***	***0.14***	***0.10***	ND
Benzo(g,h,i)perylene	20.04	ND	***0.20***	***0.04***	***0.14***	ND	***0.23***
Total PAH	110.91	ND	***2.35***	***0.77***	***2.34***	***0.68***	***0.85***

The results from the 100 day static leach test follow the results found in Birgisdóttir et al (2007) found in their 64 day leach test of traditional asphalt. They found concentrations that ranged from 0.53 to 3.5 mg/Kg. The total PAH range in the porous asphalt samples from the 100 day static leach test was between 0.32 and 0.55 µg/L, with every compound falling below the detection limit. When all of the samples from the 100 day static leach test are compared, the range is between ND to 2.35 µg/L.

The results of this static leach test indicate that the risk of PAH contamination into the underlying soil and ground water from the pavements surface is extremely low. After 100 days of constant submersion, the Porous asphalt binder did not leach PAHs into the surrounding water. The PAH level in the porous asphalt samples was actually lower than any other sample in the test, besides the blank reagent-grade water sample.

The study of PAHs in porous pavement systems should be continued to further to understand the mechanisms that affect the mobilization of PAH from pavements. Future

studies could include effects of oil and organic spills on the pavement, and long term monitoring of PAH levels in the soil water of the site.

Chapter 6 Stormwater temperature mitigation in subsurface infiltration basins

6.1 Background

This chapter will investigate the use of underground infiltration basins as a method of reducing the harmful impacts of elevated stormwater temperatures. The temperature study in this chapter will not address any differences between the pervious concrete and porous asphalt systems. Instead this chapter will focus on the stone infiltration bed beneath each porous surface and how it mitigates large elevated temperatures from storm events.

6.2 Literature review

6.2.1 Factors governing temperature transfer

Temperature is the measurement of heat energy. “Heat is energy that flows between a system and its environment because of a temperature difference between them” (Resnick et al. 2002). The thermal conductivity of a material is the measure of that material’s ability to transfer heat energy without the motion of the material as a whole. The rate of heat transfer moves along the thermal gradient.

Equation 6.1 Rate of heat transfer equation

$$H = \frac{Q}{\Delta t} = -kA\frac{dT}{dx}$$

Where k is the thermal conductivity (W/M*K), A is the cross sectional area, H (Joules/sec) is the rate of heat transfer over time, dT/dx is the temperature gradient. DT/dx is negative because the heat will flow from the high temperature to the low

temperature (Resnick et al. 2002). The higher the thermal conductivity value, k, the better that substance is at conducting heat.

Convection is another method of heat energy transfer. Convection occurs when a fluid comes in contact with an object whose temperature is higher then the surroundings. The movement of heat will travel once again across the temperature gradient from low to high. Radiation is the third method of heat transfer, where the energy is transferred through electromagnetic waves. This is process of the sun heating the earth or a person being heated by a bonfire (Resnick et al. 2002).

6.2.2 Impervious surface and runoff temperature

In an urban watershed, the increase in development leads to the degradation of the riparian zone surrounding the stream. The lack of riparian buffers and the mature tree canopy over the stream causes an increase in summer solar radiation reaching the water and an increase in stream temperature. This especially problematic for lower order streams (Galli 1990). Figure 6.1 shows the relationship between impervious cover and stream temperature.

Figure 6.1: Relationship between stream temperature and impervious cover (Galli 1990).

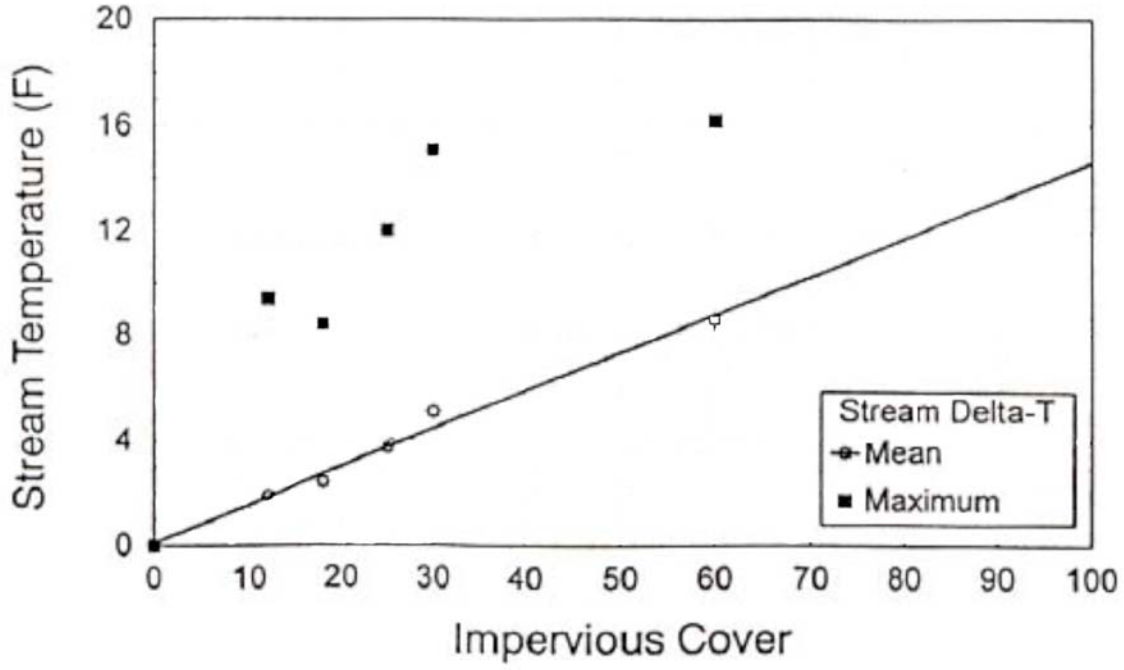

In highly developed areas, infiltration is reduced the amount of runoff is increased. This runoff travels on the surface and directly into the streams. Thus, the hydrologic cycle is disrupted (Poole and Berman 2001).

Van Buren et al. (2000) studied stormwater temperature as the water traveled across asphalt pavements. In their study it was discovered that the runoff temperature followed the same diurnal pattern as solar radiation, and a one-dimensional model was created to model the runoff temperature. The model used a heat energy balance equation to model the asphalt temperature during dry and wet weather conditions.

The one-dimensional model accurately predicted the runoff temperature well, but required the knowledge of the physical and thermal properties of the pavement, metrological data, and the initial starting conditions. When the stormwater entered a test

section of the parking lot that was 45 m long and 2 m wide, the temperature was 21.3 degrees Celsius. At the end of the 45 m section the temperature leaving the pavement was 23.0 degrees Celsius (Van Buren et al. 2000).

In a study that compared runoff from asphalt and sod plots in Wisconsin, the asphalt surface temperatures were an average of 20.3 ^{o}C warmer than the average sod surface temperature. The average initial runoff from the asphalt was 9.5 ^{o}C higher than the initial average temperature runoff from the sod plots. Ultimately it was deturmined that the heat energy of the runoff from the asphalt plot was 3.6 times greater then the runoff from the sod plot (Thompson et al. 2008).

6.2.3 Ecological effect

Increased temperatures can lead to a variety of ecological problems. The amount of oxygen that can be dissolved in water is inversely related to the water's temperature. When this relationship is combined with increased biological oxygen demand in the summer and early fall, the amount of oxygen that is available for the organisms that depend on high concentrations of dissolved oxygen are weakened or killed. Stormwater that has been heated through contact with impervious surfaces can enter a stream and cause thermal shock, which can be fatal to sensitive organisms. Trout are an example of an organism that is sensitive to the sudden change of the stream temperature. Wide fluctuations in stream temperature can negatively affect reproductive behaviors, cause species to be less tolerant to other environmental stressors, and encourage the increase in the growth of undesirable algae and pathogens (Barnes et al. 2001).

Temperature changes in an aquatic environment can impact the metabolism, behavior, enzyme function, and reproduction of aquatic organisms. In the headwaters of an urban stream the summer temperatures can increase by 7 ^{o}C (12 ^{o}F) (Jones 2008).

In Pennsylvania, stream temperatures are regulated based on designated use. The uses are designated as coldwater fisheries (CWF), warm water fisheries (WWF), and Trout Stocking Fisheries (TSF). Table 6.1 shows the maximum temperature that can be observed in each of these three uses over the course of the year. Along with the monthly temperature regulations, the Pennsylvania Code regulates that any point source can not change the stream temperature more than 1.1 ^{0}C (2 ^{0}F) in one hour (Commonwealth of Pennsylvania 2009).

Table 6.1: Pennsylvania Code §25.93 regulating stream temperatures

(Commonwealth of Pennsylvania 2009)

SYMBOL:	TEMP1 °F	TEMP2 °F	TEMP2 °F
CRITICAL USE:	CWF	WWF	TSF
January 1-31	38	40	40
February 1-29	38	40	40
March 1-31	42	46	46
April 1-15	48	52	52
April 16-30	52	58	58
May 1-15	54	64	64
May 16-31	58	72	68
June 1-15	60	80	70
June 16-30	64	84	72
July 1-31	66	87	74
August 1-15	66	87	80
August 16-30	66	87	87
September 1-15	64	84	84
September 16-30	60	78	78
October 1-15	54	72	72
October 16-31	50	66	66
November 1-15	46	58	58
November 16-30	42	50	50
December 1-31	40	42	42

6.2.4 Infiltration BMPs and watershed thermal mitigation

As mentioned in chapter 1 and 2, stormwater BMPs are more frequently focusing on runoff volume reduction through infiltration. By infiltrating the runoff, these BMP's provide two methods of temperature reduction. First, infiltration reduces the surface runoff volume, this volume of water would have would have absorbed heat energy from traveling over pavements. Having stormwater stored and infiltrated into the soil through the BMP reduces the thermal load entering a receiving waterway. Jones and Hunt

(2009) looked at bioretention cells in North Carolina and found that the retention basins were able to reduce the thermal load in the watershed by reducing the runoff volume. Second, the infiltrated ground water will recharge the underground aquifer and potentially travel to provide base flow contributions to local streams. The groundwater contribution to the stream tend to buffer the stream channel temperature year round (Poole and Berman 2001).

In the porous pavement system the air, pavements, and stormwater are heated through the same methods as in traditional stormwater systems. The difference is when the stormwater passes through the porous pavement and enters the stone storage bed. In the stone storage bed the stone that is not affected by solar radiation is cooler then the stormwater entering the bed. The stormwater transfers its heat energy to the cooler stone through conduction.

6.3 Project goals

There were two goals for this portion of the study. The first goal was to use temperature readings from the air, surface, and infiltration bed of the PAPC site to compare the average, high, and low range for storm events for a six month period to document the reduced temperature range in the infiltration bed. The second goal was to mathematically support the observations using a BMP temperature model created by Matthew Jones as part of his Ph.D work while at the North Carolina State University. The temperature model was created to be as a planning tool with bio-retention sites. Section 6.5 will discuss the specifics of the model.

6.4 Methods

6.4.1 Site description

The Porous Asphalt Pervious Concrete (PAPC) site and instrumentation is described in detail in Chapter 1. The aspects of the site which are crucial to this chapter are the traditional asphalt pavement surrounding the porous pavements, which has an area of 740 m^2, the infiltration bed which on the south side (uphill side) is 1.4 m (4.7 ft) deep on the asphalt side, 1.2 m (4 ft) deep on the concrete side, and a can store up to 0.61 (2 ft) of runoff. The bed is filled with AASHTO #2 stone. The stone used to fill each bed was limestone.

For this project, temperatures were recorded in five locations throughout the PAPC watershed. The air temperature was recorded from the roof of Mendel Hall, the classroom building adjacent to the parking lot, by the Villanova University Weather Center. The temperature of the stormwater entering the bed was observed in each of the first flush samplers on the south edge (uphill) of the pavement. The pavement surface temperatures were recorded in the center of each pavement 4.6 m from the east (concrete) and west (asphalt) edges of the porous pavements. The surface temperatures were recorded using IButton temperature loggers, section 6.4.2 will discuss the I button temperature logger in more detail. Finally, the infiltration bed temperature was recorded in the outlet boxes located on the east (concrete) and west (asphalt) of the porous pavements. An Instrumentation Northwest PT2x pressure/ temperature transducer recorded the bed temperatures.

Figure 6.2: Locations of temperature sensors. Light blue = Air Temperature, Red = First Flush temperature, Yellow = Porous Pavement surface temperature, Blue = infiltration bed temperature.

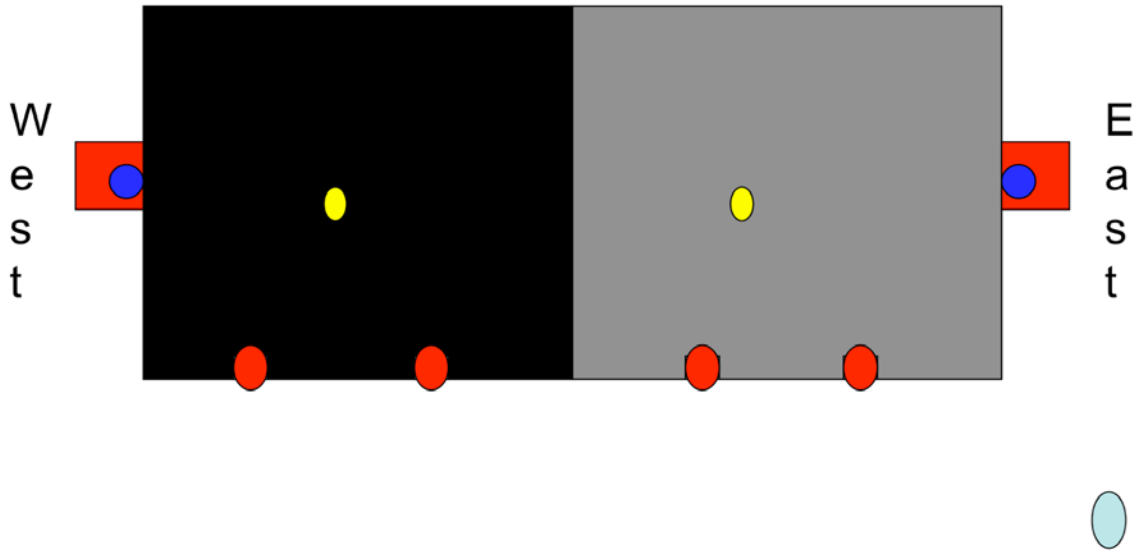

6.4.2 IButtons

IButton's were used to record the surface temperature coming off of the traditional asphalt and entering the bed and for the porous pavement's surface temperatures. The DS1921G Thermochron IButton was used because it is self data logging and has an accuracy of (+/-) 1^{o}C and a temperature range from -30 ^{o}C to 70 ^{o}C. The IButton is programmable to the recording interval, which can be set by the user. Each IButton was installed on the site in a protective waterproof case sold by the IButton manufacturer.

The IButtons were set to log data every 10 minutes. The data was downloaded using IButton-TMEX software version 3.21. The IButtons had enough memory for 14.2 days of data when logging data every 10 min.

6.4.3 Data Analysis

For the first part of the temperature study 12 storms were analyzed from March 2009 until August 2009. For each storm the average, maximum, and minimum temperature were calculated for the entire length of rainfall for the air and pavement temperatures. The stormwater runoff temperatures were analyzed for the entire length of storm plus twenty additional minutes to allow for all of the rainfall to reach the temperature sensors. Finally, the infiltration bed temperature was calculated for the entire length of time where there was water in the infiltration bed. The average and range values for the five locations were compared for each storm.

6.5 Temperature model

6.5.1 Model Background

For the second part of this study the Bioretention Thermal Model (Jones 2008) was used to model the temperature of the stormwater as it moved through the porous pavement system. The model was created to be used a planning tool to allow designers to take temperature into consideration when designing bioretention BMPs (Jones 2008).

6.5.2 Model Development

The model was created and calibrated using data from three bio-retention cells located in Ashville, Brevard, and Lenior, North Carolina. The model design focused on three branches of calculation; hydraulics, influent temperature, and the initial soil profile to calculate the thermal profiles of the infiltration and soil. The model assumes rain temperature and air temperature are equal. The model is a single event model, which has the capability of running historical or design storms. One requirement for the model is

that the rain event is continuous, because the model does not account for heat exchanges due to evaporation once the rainfall ends (Jones 2008). To account for this limitation any period where there was no rainfall the precipitation value was replaced with a value of 0.00001 in.

From a watershed hydrology perspective, the model is designed for a small impervious subcatchment. The model allows the user to input the watershed area, initial abstractions, and the bioretention surface area. The Chu and Mariño Green-Ampt method was used to calculate the infiltration of the stormwater into the bio-retention cell. This approach was selected because of its ability to account for unsteady rainfall patterns. It was adapted from its original form to calculate the infiltration of the stormwater only in the bio-retention cell, and not across the whole watershed. This was accomplished by increasing the effective rainfall intensity by dividing the inflow volume by the area of the retention cell (Jones 2008). As the wetting front progresses through the soil column the model accounts for the movement by using the Darcy equation. The model accounts for changes in soil layers and profiles by calculating the infiltration into the subsoil using of the subsoil's Green-Ampt parameters. For all Green-Ampt calculations the model uses a time step of 1 sec and grid spacing of 1 meter. Once the runoff inflow has stopped the movement of the water through the soil profile is calculated using the Darcy equation. A water balance is calculated at each time step for the surface and soil water. These volumes are used for the calculation of thermal load and surface water infiltration temperatures (Jones 2008).

6.5.3 Thermal properties and equations

For the model the surface temperature was calculated using three equations (Equation 6.2, equation 6.3, and equation 6.4). Equation 6.2 calculates the heat transfer through the pavement by calculating the transient heat conduction. These equations were presented by Van Buren et al. (2000) for the model described in section 6.2.1 including equations 6.2 and 6.3 (Jones 2008):

Equation 6.2: Transient heat conduction

$$T_m^{t+\Delta t} = T_m^t\left(1 - \frac{2\alpha\Delta t}{\Delta Z^2}\right) + \frac{\alpha\Delta t}{\Delta Z^2}\left(T_{m+1}^t + T_{m-1}^t\right)$$

Where T is the temperature within the pavement (^oC), α is the thermal diffusivity of the pavement material (m^2/s), Δt is the time step (s), Z is the depth below the pavement's surface (m), The m subscript refers to the depth at time t. Equation 6.4 calcuates the pavement's temperature during dry weather conditions, and is based on a surface heat balance (Jones 2008):

Equation 6.3: Dry weather heat balance

$$\left.\frac{\partial T}{\partial Z}\right|_{Z=0} = q_{cond} = \frac{h_c}{k}\left(T_s - T_{air}\right) - \frac{q_{rad}}{k}$$

Where k is the thermal conductivity of the pavement (W/m K), T_s is the pavement surface temperature (^oC), T_{air} is the air temperature (^oC), and q_{rad} is the solar radiation heat flux (W/m^2). Finally, Equation 6.4 calculates the pavement temperature during the storm event through another heat balance (Jones 2008):

Equation 6.4: Wet weather heat balance

$$\left.\frac{\partial T}{\partial Z}\right|_{Z=0} = \frac{h_c}{k}(T_s - T_{ro}) - \frac{q_{rad}}{k} + \frac{q_{evap}}{k}$$

Where h_c is the convective heat transfer coefficient at the pavement surface (W/m^2 K), T_{ro} is the runoff temperature (^{o}C), and q_{evap} is the evaporation heat flux (W/m^2) (Jones 2008).

To accurately predict the surface temperature, the model assumes that the pavement temperature is no longer affected by previous storms. The pavements physical and thermal properties were using values developed by Barber (1957) (table 6.2):

Table 6.2: Physical and thermal properties of asphalt pavement and gravel base layer (Barber 1957; Jones 2008).

	Asphalt	Gravel
Density (kg/m^3)	2250	1760
Thermal Conductivity (W/m K)	1.21	1.3
Specfic Heat (J/kg K)	921	837

The soil and water temperature profiles were calculated using a two phase, two equation model for heat transfer of water moving through porous media. Jones (2008) used separate equations to solve for the solid and fluid phases (equations 6.5 through 6.10) :

Equation 6.5:Fluid energy equation (Nakayama et al. 2001)

$$\rho_f C_{PF}\left[\varepsilon\frac{\partial\langle T\rangle^F}{\partial t} + \left\langle\vec{u}\right\rangle\frac{\partial\langle T\rangle^F}{\partial Z}\right] = (\varepsilon + G(1-\sigma))K_F\frac{\partial^2\langle T\rangle^F}{\partial Z^2} +$$

$$\bar{\bar{K}}_{dis}\frac{\partial^2\langle T\rangle^F}{\partial Z^2} + a_{sf}h_{sf}(\langle T\rangle^s - \langle T\rangle^F) - K_s G\left(\frac{\partial^2\langle T\rangle^s}{\partial Z^2} - \frac{\partial^2\langle T\rangle^F}{\partial Z^2}\right)$$

Equation 6.6: solid energy equation (Nakayama et al. 2001)

$$(1-\varepsilon)\rho_s C_s \frac{\partial \langle T \rangle^s}{\partial t} = \left(1-\varepsilon+G(\sigma-1)\right)* \\ k_s \frac{\partial^2 \langle T \rangle^s}{\partial Z^2} a_{sf} h_{sf}\left(\langle T \rangle^s - \langle T \rangle^F\right) + k_s G\left(\frac{\partial^2 \langle T \rangle^s}{\partial Z^2} - \frac{\partial \langle T \rangle^F}{\partial Z^2}\right)$$

Equation 6.7: Thermal conductivity ratio

$$\sigma = \frac{k_s}{k_F}$$

Equation 6.8: Tortuosity parameter (Hsu 1999)

$$G = \frac{\left(\frac{k_{stg}}{k_F}\right) - \varepsilon - (1-\varepsilon)\sigma}{(\sigma-1)^2}$$

Equation 6.9:Thermal dispersion tensor (Wakao and Kaguei 1982)

$$\overline{\overline{K}}_{dis} = k_f \left[\frac{\rho_F C_{PF} \left|\left\langle \vec{u} \right\rangle\right| d_p}{2k_F}\right]$$

Equation 6.10: Interfacial heat transfer coefficient (W/m2 K) (Wakao and Kaguei 1982)

$$h_{SF} = \frac{k_F}{d_P}\left[2 + 1.1 \mathrm{Pr}_F^{1/3}\left(\frac{\rho_F \left|\left\langle \vec{u} \right\rangle\right| d_p}{\mu_F}\right)^{.6}\right]$$

where ρ represents density (kg/m3), C_p represents specific heat capacity (kJ/kg K), ε is soil porosity, T is temperature (K), t is time (s), $\langle \vec{u} \rangle$ is the Darcian velocity of infiltrating water (m/s), Z is the depth below the soil surface (m), G is a tortuosity parameter, σ is the

thermal conductivity ratio, k is the thermal conductivity (W/m K), k_{dis} is the thermal dispersion tensor, a_{sF} is the interfacial area (m^2/m^3), h_{sF} is the interfacial heat transfer coefficient (W/m^2 K), d_p is the particle diameter (m), P_r the Prandtl number, and μ is the dynamic viscosity (Ns/m^2). In equations 6.5 and 6.6, the S subscripts apply to the solid phase, the F subscripts apply to the fluid phase, and the stg subscript applies to the combined solid and stagnant fluid.

6.5.4 Model inputs and assumptions

For the model inputs there are two categories that need to be completed by the user. The first is the site description, rainfall information, and atmospheric conditions. The site descriptions include the watershed area, initial abstractions, bio-retention area, latitude, longitude, solar transmittance, elevation, time zone, and shading coefficient. All of these inputs are site specific and are entered in by the user. The rainfall inputs can either be a design storm, or a historical storm. If it is historical storm, a comma separated file can be inputed in the format date (mm/dd/yyyy) time (HH:MM), volume for time interval. Finally, for the atmospheric conditions, the air temperature, wind speed, solar radiation, and relative humidity are required inputs. For the PAPC model, the wind speed , and relative humidity were all zero because the storage bed is beneath the porous pavement. Table 6.3 shows the site description, and known atmospheric inputs for the model.

Table 6.3:Atmospheric and site description inputs, SD are inputs which vary for each storm event.

Atmospheric Inputs		
	Units	Input
Air Temperature	^{o}C	SD
Wind speed	m/s	0
Radiation	W/m^2	SD
Relative humidity	%	70
Site Description		
Watershed area	m^2	724
Initial abstractions	mm	0.5
Bio-retension area	m^2	140
Longintude	Decimal degrees	40.02
Lattitude	Decimal degrees	75.2
Transmittance	%	100
Elavation	m	136
time zone		-5
Shading	%	100

The second sets of inputs are the hydraulic and thermal properties of the design. The hydraulic inputs are the drain depth, which, for this study, is the same as the maximum bed depth for the bed. Next, are the Green-Ampt parameters suction head of the wetting front, hydraulic conductivity, fillable porosity, surface storage capacity, gravel porosity, drain height, and sub-soil hydraulic conductivity. The hydraulic properties require the most assumptions to account for the differences between a bio-retention and a porous pavement system. For this model, the porous pavement infiltration bed was treated as the bio-retention cell, and the pavements surface is not considered. Consequently, the drain height and the surface storage capacity are the same. For the Green-Ampt parameters the bioretention soil properties are replaced with those of limestone. Because there is no under drain the drain height is set to a very low value and the gravel porosity is set to equal a silt with sand type soil. The subsoil saturated hydraulic conductivity is also set to a silt with sand.

For the thermal properties, the model required the specific heat of the limestone, limestone porosity, thermal conductivity of the limestone, contact area between limestone and the water, the saturated limestone thermal conductivity, and finally the particle size of the limestone. The American Geophysical Union reference reported the thermal properties of the limestone (Clauser and Huenges 1995). The thermal conductivity of the limestone was also used and as a model calibration parameter. Table 6.4 show the final inputs for the hydraulic and thermal properties.

Table 6.4: Hydraulic and thermal inputs

Hydraulic Properties		
	Units	Input
Bed Depth (drain depth)	m	0.61
Suction head	m	0.05
Saturated hydraulic conductivity	m/hr	0.24
Soil pore space that can be filled durring infiltration		0.4
Surface storage capapcity	m	0.61
Gravel porosiy		0.7
Drain height	m	0.001
Sub-soil saturated hydraulic conductivity	m/hr	0.4
Thermal Properties		
Specfic heat of stone	kJ/kg K	0.84
Stone porocity		0.4
Thermal conductivity of stone	W/m K	1.26
Interface area	$m^{2/}m^3$	31
Stagnant thermal conductivity	W/m K	1.33
Stone diameter	mm	63.5

6.5.5 Model Calibration

One of the limitations of the bioretension thermal model is that saturated soil conditions are required for the model to run properly. The amount of precipitation required to produce saturated conditions will vary from BMP to BMP based on soil Green-Ampt parameters, watershed size, and bed size. For the PAPC watershed it

required a storm of 48 mm (1.88 in) of rainfall in 24 hours to produce saturated conditions.

The model was calibrated using a storm on August 2, 2009, when 82.5 mm (3.25 in) of rainfall fell in 24 hours. The average solar radiation, recorded by the Mendel weather center, was 169 W/m^2.

6.5.6 Model Verification

The PAPC thermal model was validated using a storm starting August 8, 2009. The rainfall volume was 46.2 mm (1.82 in), which is lower than the required 24 hour volume. This storm was chosen because it was the largest 24 hour storm volume monitored. To have this volume of rainfall produced reasonable results, the 10 minute rain data was summed to create 30 minute data. The larger intensity volume allowed the model to produce saturation. The average solar radiation, recorded by the Mendel weather center, was 158 W/m^2.

6.6 Results

6.6.1 Observed Temperature Results and discussion

Twelve storms were analyzed for the temperature on the PAPC site from March 2009 through August 2009. The rainfall volumes and intensity varied greatly. The average, maximum, minimum and range were calculated for each of these storms for the air temperature, runoff temperature, and the bed temperature. The porous pavement surface temperature was analyzed for these parameters for nine out of the twelve storms; the three storms that were not analyzed were missed due to equipment error.

The temperature results of each of these storms have one very clear observation. The infiltration bed temperature remains fairly consistent through out the storm event and as the bed empties through infiltration. Figure 6.3 shows the event graph for the August 2, 2009 storm, which is representative of the twelve storms observed.

Figure 6.3: August 2, 2009 temperature graph.

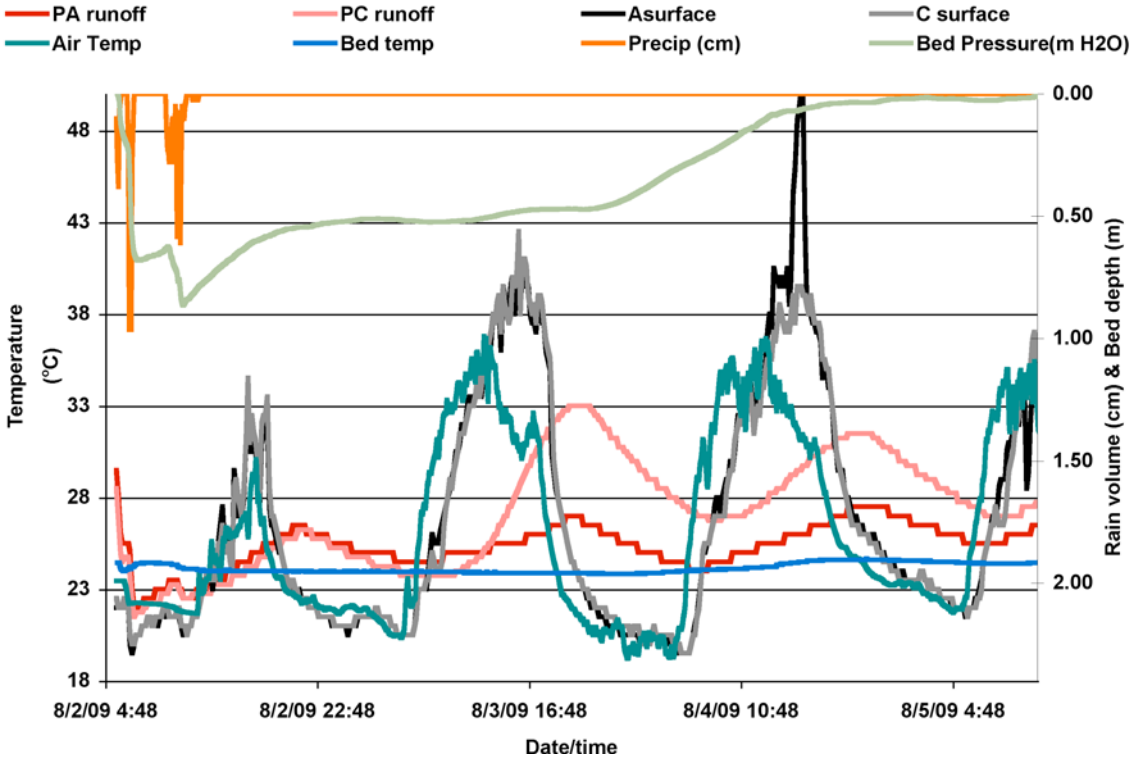

The average range for each parameter shows distinct temperature range mitigation for the twelve storms. Table 6.5 shows that the average range for the storm temperature in the infiltration bed is much lower then the temperature of the recorded runoff entering the bed. The average maximum temperature entering the bed is 20.9 ^{o}C, and decreases by an average 5.7 ^{o}C over the course of the storm. The average maximum temperature in the infiltration basin is 15.9 ^{o}C and decreases only by an average of 1.4 ^{o}C. When the runoff temperature is compared to the infiltration bed temperature, there is a temperature reduction of 24.1% of the average maximum temperature and 75% of the range from the

runoff entering the bed and in the infiltration basin. This observation supports the hypothesis that the interaction between stone in the infiltration basin and the warm stormwater reduces the stormwater's high-end thermal energy. This is supported as well by Figure 6.4 where the average maximum value is much lower then runoff entering the bed on either the concrete or asphalt side.

Table 6.5: Average temperature range (^{o}C) and standard deviation for the 12 storms analyzed.

^{o}C	Air	PA surface	PC surface	PA Runoff	PC Runoff	Bed
Average range	6.0	9.9	9.8	5.7	5.3	1.1
Standard deviation	5.6	7.5	7.7	3.3	3.2	0.5

Figure 6.4: Average range and mean temperature (^{o}C) for the 12 storms analyzed. The Blue block represents the range between the average high and low temperatures. The Orange diamond represents the average storm temperature for the 12 storms.

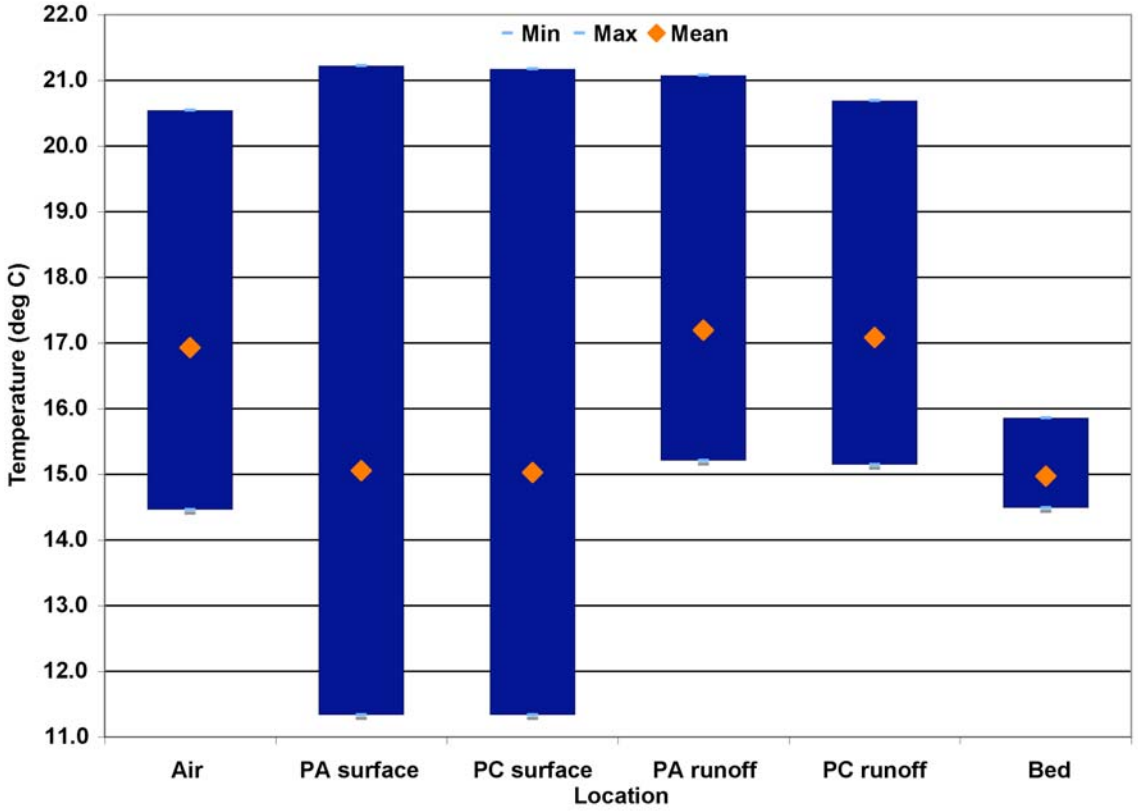

When the average storm temperature is compared in Figure 6.4, the water temperature in the infiltration bed, 15.0^{o}C, is significantly lower than the runoff temperature entering the bed on either the asphalt or concrete sides, 17.2 ^{o}C and 17.1^{o}C. An interesting observation when the averages are compared is that the runoff entering the bed has a higher average than both porous surfaces and the air temperature. Table 6.6 and Figure 6.4 shows the average temperature for the six locations monitored for temperature.

Table 6.6: Average temperatures for the runoff entering the bed, air temperature, porous pavement surfaces, and the infiltration bed.

^{o}C	Air	PA surface	PC surface	PA runoff	PC runoff	Bed
Average	16.9	15.1	15.0	17.2	17.1	15.0
Standard deviation	6.2	8.0	8.0	7.2	7.2	6.7

When the average temperature is plotted on an event basis for the air, runoff, and infiltration bed temperatures, there is an increase in temperature for all of the parameters over the course of the summer, but the infiltration bed is cooler than the runoff for all but two storm events. The highest average runoff temperature was for the July 31, 2009 storm. For this storm the runoff temperature was 27.1 ^{o}C. When the average runoff and infiltration bed temperatures are compared to the Pennsylvania regulations for temperatures in Cold Water Fisheries (CWF), Warm Water Fisheries (WWF), and Trout Stocking Fisheries (TSF), the infiltration bed temperature is consistently below the regulations for WWF and TSF. This means that if any overflow left the infiltration bed at the same temperature and entered one of these regulated streams, the temperature would decrease slightly. However, stream temperature is a function of stream volume, overflow volume, and the temperature gradient between the overflow and the stream. The runoff temperature is higher than the TSF and WWF regulatory values. If the runoff were to enter the stream directly it would increase the temperature of the receiving stream slightly. Both the infiltration bed and runoff were higher than the maximum temperature for a CWF. Figure 6.5 shows the comparison of the average runoff, infiltration bed, and air temperatures versus the Pennsylvania regulations.

Figure 6.5: Average temperature for each monitored event

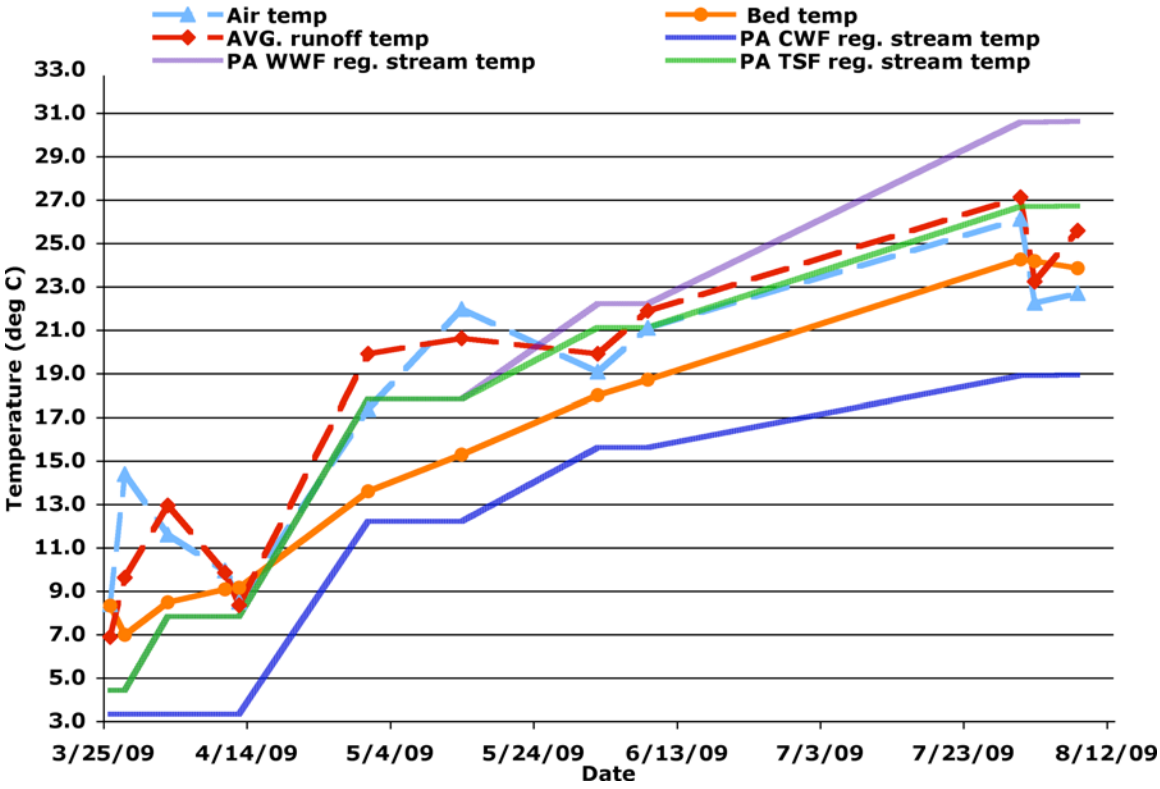

The reduced average temperature and range both support the hypothesis that there is a reduction in the heat energy as the stormwater passes through the stone filled infiltration bed. As the thermally enhanced stormwater moved through the bed it passed over the surface of the stone, in this contact there was a transfer of heat from the warmer stormwater to the limestone through conduction. Because the air temperature surrounding the stone bed remains fairly constant, and the porous pavement absorbs the solar radiation, the stone remains cooler then the surrounding area, which can be influenced by the sun's radiation.

6.6.2 Model results

6.6.2.1 Calibration

Figure 6.6 shows the results of the calibration of the model using the August 2, 2009 storm. The model overestimates the bed temperature early, but not severely, and the prediction improves with time. The model cannot predict bed temperature changes which are influenced by factors other than the thermal properties (Table 6.4). The observed infiltration basin temperature increases slightly over time due to the air temperature two day after the rainfall had finished falling. Because the model can not account for the air temperature input after the storm, the analysis of the model and the observed values were carried out from the beginning of the storm until the observed bed temperature began to rise on August 4, 2009 at 1:00 am.

Figure 6.6: Results of the August 2, 2009 storm. Observed temperature (green), predicted model temperature (red), air temperature (light blue), and rain volume (blue)

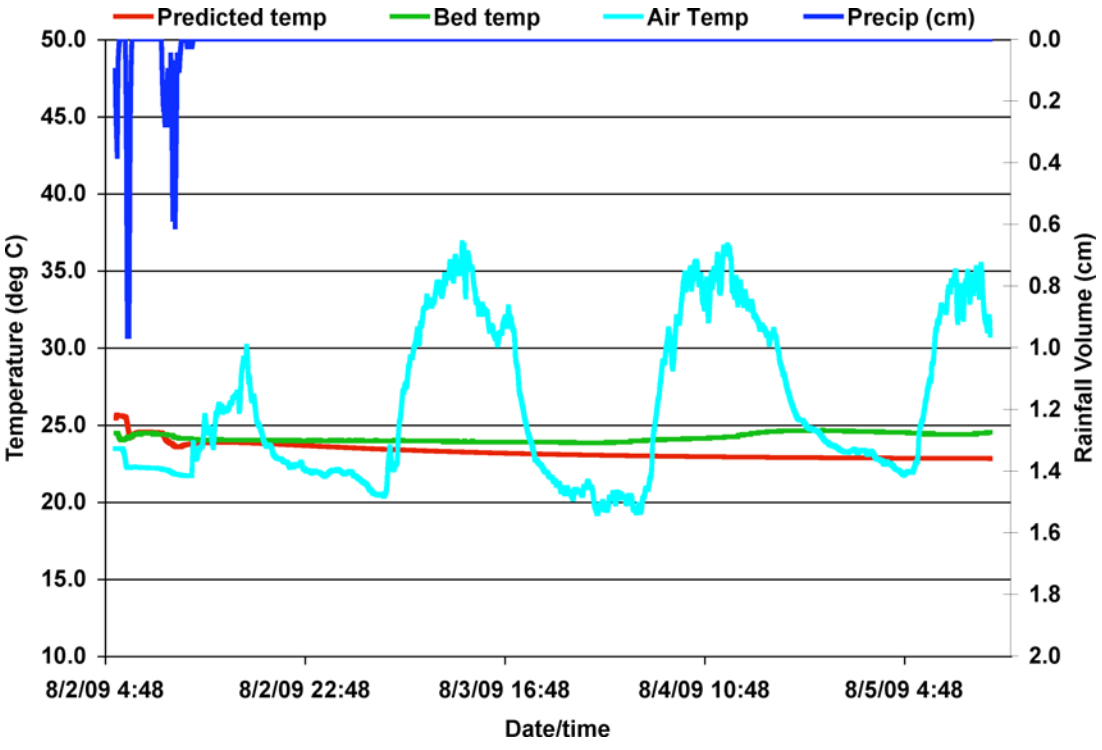

The correlation coefficient, standard error (%), absolute error (^{o}C), root mean square error (RMSE) (^{o}C), and the R^2 we used to compare the model values to the observed values.

Table 6.7 shows the results for each of these comparisons for the August 2, 2009 storm. The standard error for the average, maximums and minimum temperatures are all within +/- 5%. The RMSE and absolute error is 0.33 ^{o}C and 0.51 ^{o}C. Finally, model and observed values have a correlation coefficient and R^2 of 0.78 and 0.6, respectively.

Table 6.7: Observed and Model results for the August 2, 2009 storm

	Average temp ^{o}C	Max temp ^{0}C	Min temp ^{o}C
Observed	24.0	24.4	23.8
Predicted Model	23.6	25.7	23.0
Error %	1.77	-4.93	3.42
RMSE ^{o}C	**Abs error ^{o}C**	**Correl coef.**	**R^2**
0.33	0.51	0.78	0.60

6.6.3 Model verification

To verify the model the rainfall, starting air temperature, and average solar radiation for a storm on August 8, 2009, when 46.2 mm of rain fell over an 18 hour period. This rainfall had to be adjusted from 10 minute to 30 minute increments in order to produce saturation, as required by the model.

The results of the modeled and observed values from the August 8, 2009 storm can be found in Figure 6.7. Since, the rainfall values were summed from 10 minute to 30 minutes the model overestimated the amount of time it takes for the bed to empty. The model was compared to the observed values from the beginning of rainfall until the predicted model bed empties.

Figure 6.7: August 9, 2009 storm. Observed temperature (green), Predicted model temperature (red), air temperature (light blue), rain volume (blue)

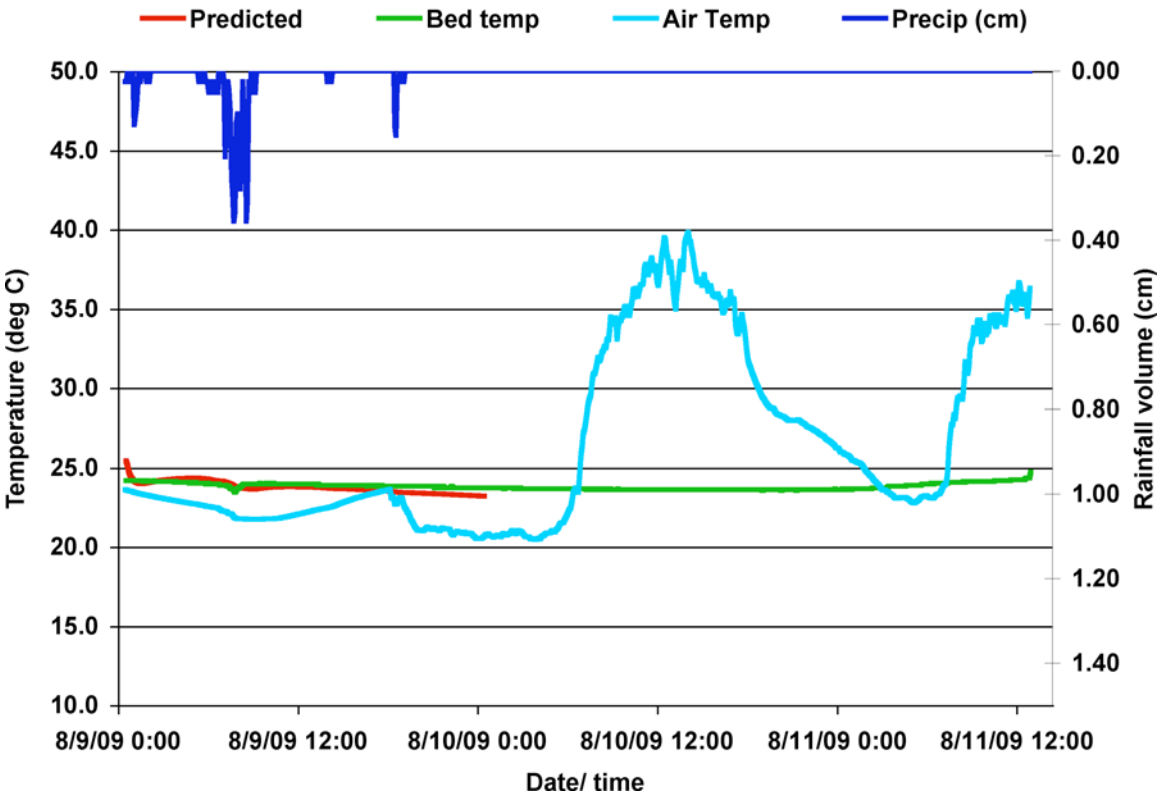

The temperatures predicted by the model do match the observed values well. As with the August 2, 2009 storm the initial temperature is slightly higher than the observed values. When the standard error is calculated for the average, maximum, and minimum temperature the error is under +/- 6%. The standard error for the average temperature error was only 0.65%. The RMSE and absolute error was 0.10 ^{o}C and 0.28 ^{o}C, respectively. The predicted model and observed values have a correlation coefficient of 0.76, and a R^2 value of 0.57. Table 6.8 shows the results from the calculation of the comparison parameters mentioned above.

Table 6.8:Observed and model results for the August 8, 2009 storm

	Average temp ^{o}C	Max temp ^{0}C	Min temp ^{o}C
Observed	24.0	24.4	23.8
Predicted Model	23.6	25.7	23.0
Error %	1.77	-4.93	3.42
RMSE ^{o}C	**Abs error ^{o}C**	**Correl coef.**	**R^2**
0.33	0.51	0.78	0.60

The results from the model show that the thermally enhanced stormwater transfers its heat energy to the limestone in the infiltration bed. The stone in the infiltration bed is cooler because it is not directly affected by the solar radiation. The model cannot take environmental influences from after the storm into account that can limit usefulness of the model in situations when it takes more then two days for the infiltration bed to empty. In both storm models, the initial temperature entering the bed was higher than what was observed. This could be due to several factors: the storm start time, and that the solar radiation value was averaged to account for the time of day when there is limited to no solar radiation. Jones (2008) also reported that the initial values were high for his calibration and verification of the model.

6.7 Conclusion

Overall, the temperature data from the infiltration bed support the hypothesis that the thermal properties of limestone in the infiltration bed reduce the runoff temperature. The physical observations were from the summer of 2009, summer was selected because it is when the pavements are heated the most. The data shows a significant reduction in the maximum and average temperature when the runoff temperature is compared from the surface to the bottom of the infiltration bed. When the Bioretention Thermal Model is used to model the system, there is a strong correlation between the model and observed

values. This supports the conclusion that the thermal properties of specific heat and thermal conductivity accurately reproduce the observed temperatures in the bed.

The infiltration bed in the porous pavement system is capable of reducing a nonpoint source pollutant, temperature. Infiltration reduces the volume of thermally enhanced stormwater entering the stormwater system and entering the stream. Over time a percentage of the infiltrated water will enter the stream in the form of baseflow, which is cooler and in most cases does not negatively impact the stream temperature. When overflow does there is a temperature mitigation because the stormwater is coming into contact with the stone in the infiltration basin. The temperature in the infiltration bed would be acceptable for a Trout Stocking Fishery or a Warm Water Fishery under the Pennsylvania regulations.

Chapter 7 Conclusions

The PAPC site on Villanova University's campus is an ideal location for a porous pavement retrofit site location. The drainage area is 100% impervious, and surrounded by curbing preventing sediment from outside the drainage area from entering the system and clogging the surfaces. Porous asphalt and pervious concrete when constructed, installed, and maintained properly provide an excellent method of removing stormwater from traditional conveyance systems by storing it and allowing the stormwater to infiltrate and be filtered by the soil.

When the stormwater quality performance of pervious concrete and porous asphalt were compared for 19 different storm events over a 1 year period, only pH was found to be statistically different between the two surfaces. This is due to the components of the Portland cement used in the pervious concrete mix.

As expected there was a season relationship found for the chloride concentration with high concentrations in the winter months. There was also an unexpected high correlation between the summer chloride concentration in the soil water and the rainfall volume, suggesting that the system is storing chlorides that are then washed out with the high volume storms in the summer.

Overall, both porous asphalt and pervious concrete provide similar levels of performance in terms of water quality. Neither of these surfaces have any water quality treatment properties.

Polyatomic Aromatic Hydrocarbons (PAHs) were tested by soaking new samples of both porous asphalt and pervious concrete in reagent grade water for 100 days, and analyzing the extracted hydrocarbons using a GC-MS. No individual PAH compounds

were found in a concentration above the detection limit, indicating that the potential for PAH contamination from either surface is low.

The study of PAHs should be expanded to look at the porous pavement system as a whole to study the long-term effects of automotive and atmospheric inputs into the system.

Finally, a study of the temperature relationships between stormwater runoff and the porous pavement infiltration bed revealed that the limestone, which provides the support for the porous pavement surfaces, also mitigates the high stormwater runoff. The temperature of the stone is not impacted by solar radiation keeping the temperature relatively constant. When the warmer stormwater enters the bed the heat energy follows the temperature gradient moving from the warm water to the cooler stone. The Bioretention Thermal Model was used to model the system, using the thermal properties of the stone; specific heat, and thermal conductivity. Using the thermal properties of the stone the model represented the temperature observations well supporting the hypothesis that the heat is being transferred from the water to the stone.

In the future temperature should be looked at on a watershed level to determine the affects of stormwater BMPs. Villanova University's campus would provide a good location for a full watershed temperature study, because it has a mix of traditional and green stormwater techniques directly connecting to a stormwater wetland, which contributes to the headwaters of Mill Creek.

References

(2008). "SPSS 16.0 for windows, release 16.0.2." SPSS Inc., Chicago, IL.

Arnold, C. J., and Gibons, C. J. (1996). "Impervious surface coverage: The emergence of a key environmental indicator." *Journal of the American Planning Association*, 62(2), 243-258.

ATSDR. (2005). "Toxicology profile for polyatomic aromatic hydrocarbons." Atsdr's toxicological profiles on cd-rom, CRC Press, Boca Raton, FL.

Barber, E. S. (1957). "Calculation of maxi um pavement temperatures from weather reports." *Highway Research Bulletin*, 168, 1-8.

Barnes, K., Morgan, J., and Roberge, M. (2001). "Impervious surfaces and the quality of natural and built environments." Department of Geography and Environmental Planning Towson University, Baltimore MD, 28.

Barraud, S., Guatier, A., Bardin, J. P., and Riou, V. (1999). "The impact of intentional stormwater infiltration on soil and groundwater." *Water Science and Technology*, 39, 185-192.

Barrett, M. E., Zuber, R. D., Collins, E. R. I., Mailina, J. F. j., Charbeneau, R. J., and Ward, G. H. (1995). "A review and evaluation of literature pertaining to the quantity and control of pollution from highway runoff and construction." The University of Texas at Austin., Austin, TX.

Birgisdóttir, H., Gamst, J., and Christensen, T. H. (2007). "Leaching of PAHs from hot mix asphalt pavements." *Environmental Engineering Science*, 24(10), 1409-1421.

Bojes, H. K., and Pope, P. G. (2007). "Characterization of the EPA's 16 priority pollutant polycyclic aromatic hydrocarbons (PAHs) in tank bottom solids and associated contaminated soils at oil exploration and production sites in Texas." *Regulatory, Toxicology, and Pharmacology*, 47, 288-295.

Boving, T. B., Stolt, M. H., Augenstern, J., and Bronsnan, B. (2008). "Potential for localized groundwater contamination in a porous pavement parking lot setting in Rhode Island." *Environmental Geology*, 55, 571-582.

Brandt, H. C. A., and De Groot, P. C. (2001). "Aqueous leaching of polycyclic aromatic hydrocarbons from bitumen and asphalt." *Water research*, 35(17), 4200-4207.

Bratteboro, B. O., and Booth, B. B. (2003). "Long term quantity and quality performance of permeable pavement systems." *Water research*, 37, 4369-4376.

Center For Watershed Protection. (2003). "Impacts of impervious cover on aquatic systems ", Center for Watershed Protection, Ellicott City, MD.

Clauser, C., and Huenges, E. (1995). "Thermal conductivity of rocks and minerals, rock physics and phase relations." A Handbook of Physical Constants, American Geophysical Union.

Commonwealth of Pennsylvania. (2009). "Environmental protection water quality standards." 25.93.

Delatte, N., Miller, D., and Mrkajic, A. (2007). "Portland cement pervious concrete pavement: Field performance investigation on parking lot and roadway pavements." Cleveland State University, Cleveland, Ohio.

Dukart, M. E. (2008a). "Standard operating procedure-VUSP-c-chloride, nitrate, nitrite, phosphate determination." Quality Assurance Project Plans, Villanova Urban Stormwater Partnership, ed., Villanova University, Villanova PA.

Dukart, M. E. (2008b). "Standard operating procedure-VUSP-b-total p-total orthophosphate-total n, hach dr/400 spectrophotometer procedures." Quality Assurance Project Plans, Villanova Urban Stormwater Partnership, ed., Villanova University, Villanova PA.

Dukart, M. E. (2008c). "Standard operating procedure-VUSP-g-metal determination, perkin elmer 4100zl graphite furnace procedures." Quality Assurance Project Plans, Villanova Urban Stormwater Partnership, ed., Villanova University, Villanova PA.

Dukart, M. E. (2008d). "Standard operating procedure-VUSP-d-total suspended/ total solids/ metals preservation procedures." Quality Assurance Project Plans, Villanova Urban Stormwater Partnership, ed., Villanova University, Villanova PA.

Eaton, A. D., Clescery, L. S., and Greenberg, A. E. (1995). *Standard methods for the examination of water and wastewater*, American Public Health Association.

Ferguson, B. K. (2005). *Porous pavements*, CRC Press, Boca Raton, Florida.

Galli, J. (1990). *Thermal impacts associated with urbanization and stormwater management best management practices*, Dept. of Environmental Programs, Metropolitan Washington Council of Governments, Washington, DC.

GKY and Associates inc. (2000). *Firstflush sampler*, GKY and Associates, McLean,VA.

Hsu, C. T. (1999). "A closure model for transient heat conduction in porous media." *Journal of Heat Transfer*, 121(3), 733-721.

Irish, L. J., Lesso, W. G., Barrett, M. E., Malina, J. F., Charbeneau, R. J., and Ward, G. H. (1995). "An evaluation of the factors affecting the quality of highway runoff in the Austin Texas area." The University of Texas at Austin, Austin, TX.

Jackson, N. (2003). *Porous asphalt pavements*, National Asphalt Pavement Association, Lanham, MD.

Jeffers, P. (2009). "Water quantity comparison of pervious concrete and porous asphalt products for infiltration best management practices," Masters Thesis, Villanova University, Villanova, PA.

Jones, M. P. (2008). "Effect of urban stormwater bmps on runoff temperature in trout sensitive regions," Doctor of Philosophy Thesis, North Carolina State University, Raleigh, NC.

Kwiatkowski, M. (2004). "Water quality study of a porous concrete infiltration best management practice," Masters Thesis, Villanova University, Villanova, Pennsylvania.

Kwiatkowski, M., Welker, A. L., Traver, R. G., Vanacore, M., and Ladd, T. (2007). "Evaluation of a infiltration best management practice utilizing pervious concrete." *Journal of the American Water Resources Association*, 43(5), 1208-1222.

Legret, M., Odie, L., Demare, D., and Jullien, A. (2005). "Leaching of heavy metals and polycyclic aromatic hydrocarbons from reclaimed asphalt pavement." *Water Research*, 39, 3675-3685.

McClintock, N. L., Turner, M., Gosselink, L., and Scoggins, M. (2005). "PAHs in Austin, Texas. Sediments and coal-tar based pavement sealants polycyclic aromatic hydrocarbons." Watershed Protection and Development Review Department Environmental Resources Management division, Austin, TX

Mikkelsen, P. S., Hafliger, M., Ochs, M., Jacobsen, P., Tjell, J. C., and Boller, M. (1997). "Pollution of soils and ground water from infiltration of highly contaminated stormwater: A case study." *Water Science and Technology*, 36, 325-330.

Nakayama, A., Kuwahara, F., Sugiyama, M., and Xu, G. (2001). "A two-energy equation model for conduction and convection in porous media." *International Journal of Heat and Mass Transfer*, 44(22), 4375-4379.

National Asphalt Pavement Association. (2007). *Porous asphalt pavements*, National Asphalt Pavement Association, Lanham, Maryland.

Newman, A. P., Pratt, C. J., Coupe, S. J., and Cresswel, N. (2002). "Oil bio-degradation in permeable pavements by microbial communities." *Water Science and Technology*, 45, 51-56.

PADEP. (2007). "Pennsylvania stormwater best management practices manual." Harrisburg, Pennsylvania.

Poole, G. C., and Berman, C. H. (2001). "An ecological perspective on in-stream temperature: Natural heat dynamics and mechanisms of human-caused thermal degradation." *Environmental Management*, 27(6), 787-802.

Pratt et al. (1999). "Mineral oil bio-degradation within a permeable pavement: Long term observations " *Water Science and Technology*, 39, 103-109.

Resnick, R., Halliday, D., and Krane, K. S. (2002). *Physics 5th ed.*, John Wiley and Sons, INC., NY.

Sadler, R., Delamont, C., White, P., and Connell, D. (1997). "Contaminants in soil as a result of leaching from asphalt." *Toxicological and Environmental Chemistry*, 68, 71-81.

Sadler, R., Delamont, C., White, P., and Connell, D. (1999). "Contaminants in soil as a result of leaching from asphalt." *Toxicological and Environmental Chemistry*, 68, 71-81.

Salas-de la Cruz, D. (2007). "Stormwater total hydrocarbon and hydrologic mass balance and a chloride mass balance of the Villanova University stormwater wetland.," Master Thesis, Villanova University, Villanova PA.

Schaus, L. K. (2007). "Porous asphalt pavement designs: Proactive design for cold climate use," Masters Thesis, University of Waterloo, Waterloo, Ontario.

Stankowski, S. J. (1972). "Population density as an indirect indicator of urban and suburban land-surface modifications." 800-B:B129-B224, USGS, ed.

Systea Scientific LLC. (2006). "Chloride, US EPA by discrete analysis method easy chloride 325.2-01 (colorimetric, automated, ferricyanide)." Easychem methodology, Oak Brook.

Tennis, P. D., Leming, M. L., and Akers, D. J. (2004). "Pervious concrete pavements." Portland Cement Association, Skokie, Illinois.

Thompson, A., Kim, K., and Vandermuss, A. J. (2008). "Thermal characteristics of stormwater runoff from asphalt and sod surfaces." *Journal of the American Water Resources Association*, 44(5), 1325-1336.

Thompson Materials Engineers. (2008). "Pervious concrete evaluation materials investigation Denver, Colorado." *CT14,571-356*, Urban Drainage and Flood Control District, Denver, Co.

U.S. EPA. (1983). "Results of the nationwide urban runoff program, volume i - final report." Washington, D.C.

U.S. EPA. (1996). "Method 8270c: Semivolitile organic compounds by gas chromatography / mass spectrometry (GC/MS)."
UMS GmbH. (2005). *Spe20 pore water sampler (suction cup)*, UMS GmBH, Munchen, Germany.
University of Rhode Island Corporative Extension. (2006). "Porous pavement and groundwater quality technical bulletin."
US EPA. (1996). "Method 8270c: Semivolitile organic compounds by gas chromatography / mass spectrometry (GC/MS)."
Van Buren, M. A., Watt, W. E., Marsalek, J., and Anderson, B. E. (2000). "Thermal enhancement of stormwater runoff by paved surfaces." *Water research*, 34(3), 1359-1371.
Villanova Urban Stormwater Partnership. (2008). "Quality management plan for Villanova urban stormwater partnership." Villanova University, Villanova, PA.
Wakao, N., and Kaguei, S. (1982). *Heat and mass transfer in packed beds*, Gordon and Breach Science Publishers, New York.
Welker, A., Gore, M., and Traver, R. (2006). "Evaluation of the long term impacts of an infiltration bmp." The 7th International Conference on Hydroscience and Engineering (IHCE-2006), Philadelphia, PA.

Appendicies

Appendix A Stormwater Quality results

A.1

	pH Lower level detection limit above 0, Upper level Detection Limit below 14											
	DATE	**A061**	**A121**	**AFF1**	**AFF2**	**C061**	**C121**	**C181**	**CFF1**	**CFF2**	**AVG AFF**	**AVG CFF**
PP	11/15/07	6.71	7.05	9.96	7.05	N	N	9.78	7.07	7.18	8.51	7.13
PP	12/2/07	7.55	6.65	7.13	7.51	N	7.19	9.69	7.48	N	7.32	7.48
PP	12/9/07	7.64	7.75	7.09	6.87	N	4.71	5.88	N	7.00	6.98	7.00
PP	1/10/08	6.35	6.16	5.60	5.35	N	8.30	N	5.45	5.40	5.48	5.43
PP	2/12/08	7.82	N	7.68	8.04	N	N	6.90	7.80	8.06	7.86	7.93
PP	3/4/08	7.02	7.61	7.87	7.75	N	N	8.75	7.88	7.92	7.81	7.90
PP	3/31/08	N	N	3.36	2.35	N	N	7.92	N	N	2.86	N
PP	4/3/08	6.84	7.46	7.74	7.68	N	8.28	8.27	N	3.49	7.71	3.49
PP	4/11/08	6.90	N	5.86	5.65	7.43	N	N	5.43	6.06	5.76	5.75
PP	4/26/08	7.28	7.5	7.0	6.2	7.7	7.5	8.1	6.3	6.9	6.57	6.58
PP	5/27/08	6.97	7.72	6.62	6.57	N	8.08	8.27	6.71	7.87	6.60	7.29
PP	5/31/08	6.82	N	6.76	6.82	N	6.96	7.62	6.85	6.81	6.79	6.83
PP	6/27/08	7.25	7.30	6.67	6.68	N	7.90	8.18	6.72	6.72	6.68	6.72
PP	7/14/08	7.00	6.6	4.4	6.7	7.1	7.3	7.6	N	6.8	5.51	6.77
PP	7/23/08	7.12	6.99	6.9	6.83	7.78	7.62	7.72	7.11	7.03	6.87	7.07
PP	9/5/08	6.69	6.6	6.91	6.58	8.12	7.61	7.72	6.35	7.11	6.75	6.73
PP	9/12/08	6.56	6.73	6.32	6.27	7.19	7.89	7.76	N	6.38	6.30	6.38
PP	9/25/08	7.16	7.17	7.2	7.18	7.15	7.73	8.3	7.25	7.26	7.19	7.26
PP	10/25/08	6.70	6.69	6.72	6.69	6.82	6.86	7.09	6.40	6.55	6.71	6.48

A.2 Total Dissolved Solids

Total Dissolved Solids Detection Limit above 0 mg/L												
	DATE	**A061**	**A121**	**AFF1**	**AFF2**	**C061**	**C121**	**C181**	**CFF1**	**CFF2**	**AVG AFF**	**AVG CFF**
PP	11/15/07	187.32	583.48	0.00	0.00	N	400.66	N	0.00	0.00	0.00	0.00
PP	12/2/07	N	1288.22	2894.73	4338.79	N	2528.15	1585.83	1.01	N	3616.76	1.01
PP	12/9/07	1709.41	1221.17	27.92	41.35	N	2117.11	2772.31	N	106.52	34.63	106.52
PP	1/10/08	453.30	1006.00	67.06	60.61	N	685.80	N	88.50	61.90	63.84	75.20
PP	2/12/08	N	N	28644.90	6842.20	N	N	3680.30	10302.60	0.00	17743.55	5151.30
PP	3/4/08	4687.00	484.90	729.10	778.20	N	N	2089.00	484.90	480.50	753.65	482.70
PP	3/31/08	N	N	N	100.19	N	N	559.41	N	N	100.19	N
PP	4/3/08	1174.41	212.67	29.11	18.74	N	453.93	N	N	19.83	23.92	19.83
PP	4/11/08	620.70	N	155.39	222.75	0.00	N	N	N	311.17	189.07	311.17
PP	4/26/08	571.51	N	119.10	93.90	N	400.72	N	102.90	95.30	106.50	99.10
PP	5/27/08	0.00	N	33.47	74.04	N	N	0.00	26.55	101.02	53.76	63.78
PP	5/31/08	213.18	N	94.23	93.30	N	153.47	192.78	63.70	42.16	93.77	52.93
PP	6/27/08	N	N	69.43	95.54	N	449.15	N	109.56	47.45	82.49	78.51
PP	7/14/08	N	427.69	188.31	112.82	N	392.74.	N	N	112.30	150.57	112.30
PP	7/23/08	487.76	188.28	54.67	77.84	93.47	430.60	N	83.33	38.63	66.25	60.98
PP	9/5/08	155.73	157.57	99.51	97.76	214.37	N	N	92.15	172.66	98.64	132.40
PP	9/12/08	222.79	205.07	N	N	118.69	N	122.64	N	N	N	N
PP	9/25/08	217.12	234.82	46.83	110.63	105.61	267.62	N	56.50	46.53	78.73	51.51
PP	10/25/08	198.68	180.16	60.69	45.57	219.66	157.34	53.61	34.13	8.24	53.13	21.19

A.3 Conductivity

	Conductivity Detection Limit above 0											
	DATE	**A061**	**A121**	**AFF1**	**AFF2**	**C061**	**C121**	**C181**	**CFF1**	**CFF2**	**AVG AFF**	**AVG CFF**
PP	11/15/07	1109.0	704.0	69.2	64.0	N	N	647.0	47.9	42.2	66.6	45.1
PP	12/2/07	925.0	2470.0	6310.0	8840.0	N	5260.0	3760.0	160.0	N	7575.0	160.0
PP	12/9/07	385.0	285.0	241.0	386.0	N	471.0	588.0	N	335.0	313.5	335.0
PP	1/10/08	801.0	1066.0	95.3	37.8	N	3460.0	N	36.8	32.6	66.6	34.7
PP	2/12/08	768.0	N	34300.0	12740.0	N	N	6900.0	14550.0	131.8	23520.0	7340.9
PP	3/4/08	19.0	19.0	69.1	96.3	N	N	19.6	18.8	18.4	82.7	18.6
PP	3/31/08	N	N	244.0	1953.0	N	N	959.0	N	N	1098.5	N
PP	4/3/08	789.0	677.0	25.2	25.3	N	677.0	832.0	N	234.0	25.3	234.0
PP	4/11/08	1157.0	N	104.9	54.2	518.0	N	N	95.3	280.0	79.6	187.7
PP	4/26/08	1026.0	592.0	206.0	185.0	666.0	632.0	588.0	122.5	195.3	195.5	158.9
PP	5/27/08	770.0	582.0	50.3	80.4	N	529.0	551.0	39.3	61.2	65.4	50.3
PP	5/31/08	536.0	N	76.5	56.3	N	459.0	438.0	38.9	49.5	66.4	44.2
PP	6/27/08	533.0	279.0	85.2	41.9	N	423.0	461.0	123.3	69.2	63.6	96.3
PP	7/14/08	502.0	218.0	82.0	65.8	270.0	401.0	420.0	N	37.2	73.9	37.2
PP	7/23/08	819.0	451.0	42.3	60.5	218.0	391.0	400.0	36.8	39.0	51.4	37.9
PP	9/5/08	1075.0	788.0	33.8	34.3	326.0	715.0	987.0	18.4	19.6	34.1	19.0
PP	9/12/08	580.0	486.0	66.8	60.4	280.0	452.0	565.0	N	20.9	63.6	20.9
PP	9/25/08	378.0	259.0	15.1	13.0	165.6	359.0	409.0	11.6	11.2	14.0	11.4
PP	10/25/08	342.0	316.0	41.3	28.1	226.0	304.0	455.0	25.6	25.6	34.7	25.6

*A.4 Total Chloride (values in red are below the detection limit = 0.5*DL)*

		Total Chlorides Detection limit above 0.5 mg/L										
site	**DATE**	**A061**	**A121**	**AFF1**	**AFF2**	**C061**	**C121**	**C181**	**CFF1**	**CFF2**	**AVG AFF**	**AVG CFF**
PP	11/15/07	360.53	125.08	4.45	1.52	N	N	1.25	1.21	0.89	2.98	1.05
PP	12/2/07	397.45	***0.25***	8,198.12	3,668.97	N	5,471.73	1.25	1,603.01	N	5,933.54	1,603.01
PP	12/9/07	1.25	37.05	49.89	88.46	N	3,077.68	1.25	N	81.45	69.17	81.45
PP	1/10/08	171.41	977.15	20.81	4.17	N	75.20	N	4.88	3.12	12.49	4.00
PP	2/12/08	245.31	N	14,242.80	4,871.00	N	N	***0.25***	5,570.10	83.83	9,556.90	2,826.96
PP	3/4/08	2,674.17	196.61	24.22	18.19	N	M	1,063.13	11.35	25.06	21.20	18.21
PP	3/31/08	N	N	236.63	256.01	N	N	231.27	N	N	246.32	N
PP	4/3/08	348.85	123.10	4.37	2.57	N	83.47	111.80	N	27.52	3.47	27.52
PP	4/11/08	234.06	N	55.65	58.72	73.85	N	N	60.83	130.95	57.18	95.89
PP	4/26/08	186.80	114.96	39.04	28.31	114.57	85.71	64.83	13.57	80.19	33.68	46.88
PP	5/27/08	88.91	36.51	36.64	39.66	8.65	94.99	82.54	44.61	51.67	38.15	48.14
PP	5/31/08	88.91	36.51	***0.25***	***0.25***	8.65	16.76	15.18	***0.25***	***0.25***	***0.25***	***0.25***
PP	6/27/08	533.00	279.00	85.20	41.90	N	423.00	461.00	123.30	69.20	63.55	96.25
PP	7/14/08	502.00	218.00	82.00	65.80	270.00	401.00	420.00	N	37.20	73.90	37.20
PP	7/23/08	819.00	451.00	42.30	60.50	218.00	391.00	400.00	36.80	39.00	51.40	37.90
PP	9/5/08	1,075.00	788.00	33.80	34.30	326.00	715.00	987.00	18.40	19.62	34.05	19.01
PP	9/12/08	580.00	486.00	66.80	60.40	280.00	452.00	565.00	N	20.90	63.60	20.90
PP	9/25/08	378.00	259.00	15.05	13.04	165.60	359.00	409.00	11.59	11.22	14.05	11.41
PP	10/25/08	342.00	316.00	41.30	28.10	226.00	304.00	455.00	25.60	25.60	34.70	25.60

*A.5 Total Nitrogen (values in red are below the detection limit = 0.5*DL)*

Total nitrogen test detection limit is above 1.7 PPM												
	DATE	**A061**	**A121**	**AFF1**	**AFF2**	**C061**	**C121**	**C181**	**CFF1**	**CFF2**	**AVG AFF**	**AVG CFF**
PP	11/15/07	*18.5	*11.7	2.2	1.7	N	**N**	1.8	1.7	1.7	1.95	1.7
PP	12/2/07	*15.8	5	1.7	1.7	N	1.7	1.7	1.7	N	1.7	1.7
PP	12/9/07	*10.4	5.7	3.9	3.8	N	2.8	N	6.4	7.7	3.85	7.05
PP	1/10/08	1.7	1.7	1.7	1.7	N	1.7	N	1.7	1.7	1.7	1.7
PP	1/17/08	N	N	N	N	N	N	N	N	N	N	N
PP	2/12/08	4.3	N	1.8	1.7	N	N	2.9	1.7	1.7	1.75	1.7
PP	3/4/08	1.7	1.7	1.7	1.7	N	N	1.7	1.7	1.7	1.7	1.7
PP	3/31/08	**N**	N	2.2	2.5	N	N	2	N	N	2.35	N
PP	4/3/08	2.4	3.4	1.7	1.7	N	1.7	1.7	N	1.7	1.7	1.7
PP	4/11/08	4.8	N	4	***0.85***	***0.85***	N	N	2.3	1.9	2.425	2.1
PP	4/26/08	N	7.1	6.3	4.9	5.4	4.5	7.8	10.9	4	5.6	7.45
PP	5/27/08	N	N	N	N	N	N	N	N	N	N	N
PP	5/31/08	4.3	N	***1***	***0.85***	N	3.4	***0.85***	2.5	***0.85***	***0.85***	1.7
PP	6/27/08	N	N	4.1	2.3	N	4.3	3.7	7.9	3.1	3.2	5.5
PP	7/14/08	N	***0.85***	***0.85***	***0.85***	N	***0.85***	N	N	***0.85***	***0.85***	***0.85***
PP	7/23/08	5.2	***0.85***	***0.85***	3.1	***0.85***	2.2	***0.85***	2.5	2.6	1.975	2.55

* removed due to failing outlier test see appendix 1E-1

A.5.1 Test for outliers Total Nitrogen

Outlier Test for Total Nitrogen							
A061							
Date	**Potential outlying value mg/l**	**Range between 25 and 75 quartile mg/l**	**Lower extreme boundary mg/l**	**Lower Mild Boundary mg/l**	**Upper Mild Boundary mg/l**	**Upper extreme boundary mg/l**	**Result**
11/15/07	18.7	6.23	<LDL	<LDL	18.44	27.78	diregarded
12/2/07	15.8	2.8	<LDL	<LDL	9.4	13.6	diregarded
12/9/07	10.4	2.7	<LDL	<LDL	8.91	12.92	diregarded
A122							
Date	**Potential outlying value mg/l**	**Range between 25 and 75 quartile mg/l**	**Lower extreme boundary mg/l**	**Lower Mild Boundary mg/l**	**Upper Mild Boundary mg/l**	**Upper extreme boundary mg/l**	**Result**
11/15/07	11.7	4	<LDL	<LDL	11.7	17.7	diregarded

*A.6 Total Phosphorus (values in red are below the detection limit = 0.5*DL)*

Total Phosphorus- Detection Limit is above 0.06 mg/L												
Site	**DATE**	**A061**	**A121**	**AFF1**	**AFF2**	**C061**	**C121**	**C181**	**CFF1**	**CFF2**	**AVG AFF**	**AVG CFF**
PP	11/15/07	0.12	***0.03***	0.71	0.08	N	N	0.18	0.79	0.57	0.395	0.68
PP	12/2/07	0.28	***0.03***	0.18	0.21	N	0.08	0.3	***0.03***	N	0.195	***0.03***
PP	12/9/07	***0.03***	0.55	0.67	0.27	N	0.58	0.18	N	0.77	0.47	0.77
PP	1/10/08	0.5	0.13	0.57	0.38	N	0.21	0.3	1.02	0.72	0.475	0.87
PP	1/1708	N	N	N	N	N	N	N	N	N	N	N
PP	2/12/08	0.24	N	0.18	0.15	N	N	0.16	0.08	0.28	0.165	0.18
PP	3/4/08	0.2	0.82	0.39	0.94	N	N	0.12	0.62	0.69	0.665	0.655
PP	3/31/08	N	N	0.15	0.28	N	N	N	N	N	0.215	N
PP	4/3/08	0.16	0.08	0.3	0.26	N	0.25	N	N	0.22	0.28	0.22
PP	4/11/08	0.08	N	1.05	***0.03***	0.07	N	N	N	2.69	0.54	2.69
PP	4/26/08	0.13	0.79	2.4	1.68	0.31	***0.03***	0.22	2.34	2.13	2.4	2.235
PP	5/27/08	***0.03***	0.08	0.5	0.57	0.1	0.09	0.22	0.81	N	0.535	0.81
PP	5/31/08	0.08	N	0.3	N	N	0.21	0.17	0.21	0.39	0.3	0.3
PP	6/27/08	N	N	0.33	0.34	N	0.15	0.38	1.33	0.65	0.335	0.99
PP	7/14/08	N	0.09	0.44	0.53	N	0.15	N	N	0.25	0.485	0.25
PP	9/5/08	1.03	0.49	0.62	0.89	0.3	0.42	0.31	0.47	0.39	0.755	0.43
PP	9/12/08	0.41	0.25	0.38	0.25	0.34	0.42	0.58	N	0.43	0.315	0.43

*A.7 Total Dissolved Copper (values in red are below the detection limit = 0.5*DL)*

Dissolved Copper Detection Limit above												
Site	**Date**	**A06**	**A12**	**AFF**	**AFF**	**C06**	**C12**	**C18**	**CFF**	**CFF**	**AVG**	**AVG**
PP	11/15/0	*1.4*	4.1	8.9	6.3	N	N	11.7	4.8	3.4	7.6	4.1
PP	12/2/0	N	3.1	7.2	24.1	N	*1.4*	10.9	4.4	N	7.2	4.4
PP	12/9/0	5.0	6.3	5.9	5.4	N	7.4	5.9	N	5.6	5.7	5.6
PP	1/10/0	12.1	16.7	6.5	4.6	N	7.1	N	6.5	8.4	5.6	7.5
PP	2/12/0	N	N	4.0	3.4	N	N	*1.4*	3.2	4.4	3.7	3.8
PP	3/4/0	*1.4*	*1.4*	4.1	3.0	*1.4*	N	*1.4*	*1.4*	*1.4*	3.5	*1.4*
PP	3/31/0	N	N	28.98	11.2	N	N	2.9	N	N	11.2	N
PP	4/3/0	*1.4*	8.2	37.4	6.6	N	11.2	N	N	12.8	6.6	12.8
PP	4/11/0	3.8	N	9.2	5.9	3.4	N	N	30.31	8.2	7.5	8.2
PP	4/26/0	4.4	N	12.9	10.0	N	7.5	N	40.64	19.4	11.4	19.4
PP	5/27/0	9.2*	N	N	9.2	N	N	*1.4*	10.8	12.5	9.2	11.7
PP	5/31/0	*1.4*	N	4.5	11.3	N	11.7	3.8	*1.4*	4.0	7.9	*2.7*
PP	6/27/0	N	N	33.78	31.86	N	32.48	N	53.42	22.2	N	22.2
PP	7/14/0	N	*1.4*	26.29	10.6	N	2.8	N	19.2	3.2	10.6	11.2
PP	7/23/0	*1.4*	*1.4*	13.5	7.4	*1.4*	*1.4*	3.8	5.8	12.6	10.5	9.2
PP	9/5/0	*1.4*	*1.4*	*1.4*	*1.4*	*1.4*	*1.4*	N	*1.4*	*1.4*	*1.4*	*1.4*
PP	9/12/0	*1.4*	*1.4*	5.1	4.9	*1.4*	N	12.9	N	*1.4*	5.0	*1.4*
PP	9/25/0	4.6	41.96	9.0	4.2	*1.4*	3.9	6.9	3.2	6.6	6.6	4.9
PP	10/25/0	N	N	5.2	12.9	N	N	N	*1.4*	5.6	*1.4*	3.5

*Values disregarded in outlier test - see

A.7.1 Dissolved Copper test for outliers

Outlier Test for Dissolved Copper							
A061							
Date	**Potential outlying value**	**Range between 25 and 75 quartile**	**Lower extreme B boundary**	**Lower Mild boundary**	**Upper Mild boundary**	**Upper extreme boundary**	**Result**
	ug/l	**ug/l**	**ug/l**	**ug/l**	**ug/l**	**ug/l**	
1/10/08	12.1	3.24	<LDL	<LDL	9.51	14.38	disregarded
5/27/08	9.2	3.03	<LDL	<LDL	8.98	13.53	disregarded
A122							
Date	**Potential outlying value**	**Range between 25 and 75 quartile**	**Lower extreme boundary**	**Lower Mild boundary**	**Upper Mild Boundary**	**Upper extreme boundary**	**Result**
	ug/l	**ug/l**	**ug/l**	**ug/l**	**ug/l**	**ug/l**	

1/10/08	16.7	5.86	<LDL	<LDL	16.07	24.88	disregarded
9/25/08	41.96	4.35	<LDL	<LDL	12.28	18.8	Disregarded

AFF1

Date	Potential outlying value	Range between 25 and 75 quartile	Lower extreme boundary	Lower Mild Boundary	Upper Mild Boundary	Upper extreme boundary	Result
	ug/l	ug/l	ug/l	ug/l	ug/l	ug/l	
4/3/08	37.4	8.23	<LDL	<LDL	25.72	38.07	disregarded
6/27/08	33.78	7.74	<LDL	<LDL	24.48	36.1	disregarded
3/31/08	28.98	5.13	<LDL	<LDL	17.81	25.51	disregarded
7/14/08	26.29	4.29	<LDL	<LDL	15.55	22	disregarded

AFF2

Date	Potential outlying value	Range between 25 and 75 quartile	Lower extreme boundary	Lower Mild Boundary	Upper Mild Boundary	Upper extreme boundary	Result
	ug/l	ug/l	ug/l	ug/l	ug/l	ug/l	
6/27/08	31.87	6.12	<LDL	<LDL	20.08	29.27	disregarded
12/2/07	24.1	5.72	<LDL	<LDL	18.99	2758	disregarded

C121							
Date	**Potential outlying value**	**Range between 25 and 75 quartile**	**Lower extreme boundary**	**Lower Mild Boundary**	**Upper Mild Boundary**	**Upper extreme boundary**	**Result**
	ug/l	**ug/l**	**ug/l**	**ug/l**	**ug/l**	**ug/l**	
6/27/08	32.28	7.23	<LDL	<LDL	20.19	31.04	disregarded

CFF1							
Date	**Potential outlying value**	**Range between 25 and 75 quartile**	**Lower extreme boundary**	**Lower Mild Boundary**	**Upper Mild Boundary**	**Upper extreme boundary**	**Result**
	ug/l	**ug/l**	**ug/l**	**ug/l**	**ug/l**	**ug/l**	
6/27/08	53.42	12.71	<LDL	<LDL	34.06	53.12	disregarded
4/26/08	40.64	8	<LDL	<LDL	21.79	33.74	disregarded
4/11/08	30.31	5.53	<LDL	<LDL	15.22	23.51	disregarded

*A.8 Total Dissolved Lead (values in red are below the detection limit = 0.5*DL)*

Dissolved Lead Detection Limit above 4.8 ug/L												
Site	**Date**	**A061**	**A121**	**AFF1**	**AFF2**	**C061**	**C121**	**C181**	**CFF1**	**CFF2**	**AVG AFF**	**AVG CFF**
PP	11/15/07	*2.40*	N	*2.40*	*2.40*	N	N	14.6*	*2.40*	*2.40*	*2.40*	*2.40*
PP	12/2/07	N	*2.40*	*2.40*	*2.40*	N	*2.40*	*2.40*	*2.40*	N	*2.40*	*2.40*
PP	12/9/07	*2.40*	*2.40*	*2.40*	*2.40*	N	*2.40*	*2.40*	N	6.50	*2.40*	6.50
PP	1/10/08	*2.40*	19.2*	11.8*	*2.40*	N	*2.40*	N	*2.40*	*2.40*	*2.40*	*2.40*
PP	2/12/08	N	N	*2.40*	*2.40*	N	N	*2.40*	*2.40*	*2.40*	*2.40*	*2.40*
PP	3/4/08	5.00	5.00	*2.40*	*2.40*	*2.40*	N	6.00	*2.40*	*2.40*	*2.40*	*2.40*
PP	3/31/08	N	N	*2.40*	*2.40*	N	N	*2.40*	N	N	*2.40*	N
PP	4/3/08	*2.40*	*2.40*	14.01*	*2.40*	N	*2.40*	N	N	*2.40*	*2.40*	*2.40*
PP	4/11/08	*2.40*	N	19.86*	*2.40*	*2.40*	*2.40*	N	*2.40*	*2.40*	*2.40*	*2.40*
PP	4/26/08	*2.40*	N	*2.40*	*2.40*		*2.40*	N	*2.40*	*2.40*	*2.40*	*2.40*
PP	5/27/08	*2.40*	N	N	*2.40*	N	N	*2.40*	*2.40*	*2.40*	*2.40*	*2.40*
PP	5/31/08	*2.40*	N	*2.40*	*2.40*	N	*2.40*	*2.40*	*2.40*	*2.40*	*2.40*	*2.40*
PP	6/27/08	N	N	*2.40*	*2.40*	N	*2.40*	N	*2.40*	*2.40*	*2.40*	*2.40*
PP	7/14/08	N	N	*2.40*	*2.40*	N	*2.40*	N	*2.40*	*2.40*	*2.40*	*2.40*
PP	7/23/08	*2.40*	*2.40*	7.05	*2.40*	*2.40*	*2.40*	*2.40*	7.60	5.88	*4.73*	6.74
PP	9/5/08	*2.40*	*2.40*	*2.40*	*2.40*	*2.40*	*2.40*	N	*2.40*	*2.40*	*2.40*	*2.40*
PP	9/12/08	*2.40*	*2.40*	*2.40*	5.42	*2.40*		*2.40*	N	*2.40*	*3.91*	*2.40*
PP	9/25/08	*2.40*	*2.40*	*2.40*	*2.40*	*2.40*	*2.40*	N	*2.40*	*2.40*	*2.40*	*2.40*
PP	10/25/08	*2.40*	*2.40*	*2.40*	*2.40*	*2.40*	*2.40*	N	*2.40*	*2.40*	*2.40*	*2.40*

*Values disregraded in outlier test see Appendix 1H-1

A.8.1 Dissolved Lead test for outliers

Outlier Test for Dissolved Lead							
A122							
Date	**Potential outlying value**	**Range between 25 and 75 quartile**	**Lower extreme boundary**	**Lower Mild Boundary**	**Upper Mild Boundary**	**Upper extreme boundary**	**Result**
	ug/l	**ug/l**	**ug/l**	**ug/l**	**ug/l**	**ug/l**	
1/10/08	19.2	0	<LDL	<LDL	2.4	2.4	disregarded
AFF1							
Date	**Potential outlying value**	**Range between 25 and 75 quartile**	**Lower extreme boundary**	**Lower Mild Boundary**	**Upper Mild Boundary**	**Upper extreme boundary**	**Result**
	ug/l	**ug/l**	**ug/l**	**ug/l**	**ug/l**	**ug/l**	
4/11/08	19.86	0	<LDL	<LDL	2.4	2.4	disregarded
4/3/08	14.01	0	<LDL	<LDL	2.4	2.4	disregarded
3/31/08	11.8	0	<LDL	<LDL	24	2.4	disregarded
C181							
Date	**Potential outlying value**	**Range between 25 and 75 quartile**	**Lower extreme boundary**	**Lower Mild Boundary**	**Upper Mild Boundary**	**Upper extreme boundary**	**Result**
	ug/l	**ug/l**	**ug/l**	**ug/l**	**ug/l**	**ug/l**	
11/15/07	14.6	0	<LDL	<LDL	2.4	2.4	disregarded
12/2/07	24.1	5.72	<LDL	<LDL	18.99	2758	disregarded

*A.9 Total Dissolved Cadmium (values in red are below the detection limit = 0.5*DL)*

Total Dissolved Cadmium detection limit above 0.5 ug/L												
		A061	**A122**	**AFF1**	**AFF2**	**C061**	**C121**	**C181**	**CFF1**	**CFF2**	**AVG AFF**	**AVG CFF**
PP	11/15/07	2.1	3.3	5.000	2.200	N	N	21.4	3.100	3.500	3.6	3.3
PP	12/2/07	N	31.6*	2.800	***0.250***	N	15.9*	14.3	***0.250***	N	1.525	***0.25***
PP	12/9/07	***0.25***	21.1*	2.000	***0.250***	N	11.9*	15.1	N	8.900	1.125	8.9
PP	1/10/08	***0.25***	2.1	***0.250***	***0.250***	N	5.200	N	***0.250***	***0.250***	***0.25***	***0.25***
PP	2/12/08	N	N	6.287	4.921	N	N	***0.25***	5.319	***0.25***	5.604	2.7845
PP	3/4/08	***0.25***	***0.25***	***0.25***	***0.25***	***0.25***	N	***0.25***	***0.25***	***0.25***	***0.25***	***0.25***
PP	3/31/08	N	N	***0.25***	***0.25***	N	N	***0.25***	N	N	***0.25***	N
PP	4/3/08	***0.25***	***0.25***	1.195	***0.25***	N	***0.25***	N	N	1.31	0.7225	1.31
PP	4/11/08	***0.25***	N	***0.25***	***0.25***	***0.25***	N	N	3.115	***0.25***	***0.25***	1.6825
PP	4/26/08	***0.25***	N	1.169	***0.254***	N	***0.25***	N	***0.25***	0.557	0.7115	***0.4035***
PP	5/27/08	***0.25***	N	N	***0.25***	N	N	***0.25***	***0.25***	0.929	***0.25***	0.5895
PP	5/31/08	***0.25***	N	***0.25***	***0.25***	N	***0.25***	***0.25***	0.623	***0.25***	***0.25***	***0.4365***
PP	6/27/08	N	N	***0.25***	***0.25***	N	***0.25***	N	***0.25***	***0.25***	***0.25***	***0.25***
PP	7/14/08	N	30*	0.585	***0.25***		***0.25***	N	***0.25***	***0.25***	***0.4175***	***0.25***
PP	7/23/08	0.815	1.058	1.934	0.692	***0.25***	***0.25***	***0.25***	1.566	***0.25***	1.313	0.908
PP	9/5/08	***0.25***	***0.25***	0.613	***0.25***	***0.25***	1.216	N	***0.25***	0.957	***0.4315***	0.6035
PP	9/12/08	***0.25***	***0.25***	0.71	0.588	***0.25***	N	0.981	N	***0.25***	0.649	***0.25***
PP	9/25/08	***0.386***	***0.25***	1.619	***0.25***	***0.25***	***0.434***	N	***0.434***	***0.25***	0.9345	***0.342***
PP	10/25/08	N	N	***0.250***	***0.250***	N	N	N	***0.250***	***0.250***	N	N

* Value disregarded in test for outliers see Appendix 1I-1

A.9.1 Dissolved Cadmium test for outliers

Outlier Test for Dissolved Cadmium

A122

Date	Potential outlying value	Range between 25 and 75 quartile	Lower extreme boundary	Lower Mild Boundary	Upper Mild Boundary	Upper extreme boundary	Result
	ug/l	ug/l	ug/l	ug/l	ug/l	ug/l	
12/2/07	31.6	11.95	<LDL	<LDL	30.12	48.05	disregarded
7/14/08	30	2.75	<LDL	<LDL	7.12	11.25	disregarded
12/9/07	21.1	1.85	<LDL	<LDL	4.88	7.65	disregarded

C121

Date	Potential outlying value	Range between 25 and 75 quartile	Lower extreme boundary	Lower Mild Boundary	Upper Mild Boundary	Upper extreme boundary	Result
	ug/l	ug/l	ug/l	ug/l	ug/l	ug/l	
12/2/07	15.9	2.96	<LDL	<LDL	7.65	12.08	disregarded
12/9/07	11.9	0.77	<LDL	<LDL	2.17	3.33	disregarded

C181

Date	Potential outlying value	Range between 25 and 75 quartile	Lower extreme boundary	Lower Mild Boundary	Upper Mild Boundary	Upper extreme boundary	Result
	ug/l	ug/l	ug/l	ug/l	ug/l	ug/l	
11/15/07	21.4	10.72	<LDL	<LDL	27.05	43.13	Kept
12/9/07	15.1	10.72	<LDL	<LDL	27.05	43.13	Kept
4/11/08	14.3	10.72	<LDL	<LDL	27.05	43.13	Kept

*A.10 Total Dissolved Chromium (values in red are below the detection limit = 0.5*DL)*

		Total Dissolved Chromium detection limit above 2.2 ug/l										
		A061	**A121**	**AFF1**	**AFF2**	**C061**	**C121**	**C181**	**CFF1**	**CFF2**	**AVG AFF**	**AVG CFF**
PP	11/15/07	***1.1***	***1.1***	***1.1***	***1.1***	N	N	***1.1***	***1.1***	***1.1***	***1.1***	***1.1***
PP	12/2/07	N	***1.1***	***1.1***	***1.1***	N	***1.1***	***1.1***	***1.1***	N	N	N
PP	12/9/07	***1.1***	***1.1***	***1.1***	***1.1***	N	***1.1***	***1.1***	N	***1.1***	***1.1***	***1.1***
PP	1/10/08	***1.1***	N	***1.1***	***1.1***	N	***1.1***	N	***1.1***	***1.1***	***1.1***	***1.1***
PP	2/12/08	N	N	***1.1***	***1.1***	N	N	3.9	***1.1***	4.4	***1.1***	2.8
PP	3/4/08	***1.1***	***1.1***	2.3	***1.1***	4.5	N	5.3	***1.1***	***1.1***	***1.7***	***1.1***
PP	3/31/08	N	N	***1.1***	***1.1***	N	N	***1.1***	N	N	***1.1***	N
PP	4/3/08	***1.1***	***1.1***	***1.1***	***1.1***	N	9.682*	N	N	***1.1***	***1.1***	***1.1***
PP	4/11/08	***1.1***	N	***1.1***	***1.1***	34.12*	N	N	***1.1***	***1.1***	***1.1***	***1.1***
PP	4/26/08	***1.1***	N	***1.1***	***1.1***	N	***1.1***	N	***1.1***	***1.1***	***1.1***	***1.1***
PP	5/27/08	***1.1***	N	N	***1.1***	N	N	***1.1***	***1.1***	***1.1***	***1.1***	***1.1***
PP	5/31/08	***1.1***	N	***1.1***	***1.1***	N	4.2	5.7	***1.1***	***1.1***	***1.1***	***1.1***
PP	6/27/08	N	N	***1.1***	***1.1***	N	2.3	N	3.7	***1.1***	***1.1***	2.4
PP	7/14/08	N	N	***1.1***	***1.1***	N	9.01*	N	3.0	2.5	***1.1***	2.7
PP	7/23/08	***1.1***	***1.1***	***1.1***	***1.1***	***1.1***	***1.1***	***1.1***	***1.1***	***1.1***	***1.1***	***1.1***
PP	9/5/08	***1.1***	***0.3***	***1.1***	***1.1***	***1.1***	***1.1***	N	***1.1***	***1.1***	***1.1***	***1.1***
PP	9/12/08	***1.1***	2.8	***1.1***	***1.1***	***1.1***	***1.1***	***1.1***		2.7	***1.1***	2.7
PP	9/25/08	***1.1***	***1.1***	***1.1***	***1.1***	***1.0***	***1.1***	N	***1.1***	***1.1***	***1.1***	***1.1***
PP	10/25/08	N	N	***1.1***	***1.1***	N	N	N	***1.1***	***1.1***	***1.1***	***1.1***

* Value dissregarded in test for outliers see Appendix 1J-1

A.10.1 Dissolved Chromium test for outliers

Outlier Test for Dissolved Chromium							
C061							
Date	**Potential outlying value**	**Range between 25 and 75 quartile**	**Lower extreme boundary**	**Lower Mild Boundary**	**Upper Mild Boundary**	**Upper extreme boundary**	**Result**
	mg/l	**mg/l**	**mg/l**	**mg/l**	**mg/l**	**mg/l**	
4/11/08	34.12	3.4	<LDL	<LDL	9.65	14.78	disregarded
C121							
Date	**Potential outlying value**	**Range between 25 and 75 quartile**	**Lower extreme boundary**	**Lower Mild Boundary**	**Upper Mild Boundary**	**Upper extreme boundary**	**Result**
	mg/l	**mg/l**	**mg/l**	**mg/l**	**mg/l**	**mg/l**	
4/3/08	9.68	2.63	<LDL	<LDL	7.68	11.63	disregarded
7/14/08	9.01	1.16	<LDL	<LDL	4	5.75	disregarded

A.11 Total Dissolved Zinc

Total Dissolved Zinc Detection limit above 4.8ug/l												
		A061	**A121**	**AFF1**	**AFF2**	**C061**	**C121**	**C181**	**CFF1**	**CFF2**	**AVG AFF**	**AVG CFF**
PP	1/10/08	28.4	11.9	61.4	69.6	N	N	N	73.7	65.5	65.5	69.6
PP	2/12/08	N	N	120.0	58.0	N	N	55.0	51.0	23.0	89.0	37.0
PP	3/4/08	25.0	N	10.0	27.0	19.0	N	***2.4***	***2.4***	***2.4***	18.5	***2.4***
PP	3/31/08	N	N	28.0	1491.0	N	N	15.0	N	N	759.5	N
PP	4/3/08	19.0	25.0	2218.0	654.0	N	30.0	N	N	557.0	1436.0	557.0
PP	4/11/08	14.0	N	74.0	94.0	35.0	N	N	241.0	55.0	84.0	148.0
PP	4/26/08	***2.4***	N	107.0	75.0	N	***2.4***	N	90.0	73.0	91.0	81.5
PP	5/27/08	8.0	N	N	22.0	N	N	***2.4***	43.0	21.0	22.0	32.0
PP	5/31/08	39.0	N	51.0	45.0	N	16.0	10.0	33.0	39.0	48.0	36.0
PP	6/27/08	N	N	122.0	121.0	N	66.0	N	221.0	101.0	121.5	161.0
PP	7/14/08	N	N	57.0	24.0	N	26.0	N	N	92.0	40.5	92.0
PP	7/23/08	34.0	40.0	78.0	88.0	***2.4***	***2.4***	25.0	38.0	84.0	83.0	61.0
PP	9/5/08	***2.4***	10.0	252.0	25.0	***2.4***	18.0	N	26.0	54.0	138.5	40.0
PP	9/12/08	18.0	50.0	52.0	42.0	14.0	N	24.0	N	34.0	47.0	34.0
PP	9/25/08	***2.4***	***2.4***	***2.4***	***2.4***	***2.4***	***2.4***	N	***2.4***	***2.4***	***2.4***	***2.4***
PP	10/25/08	N	N	***2.4***	***2.4***	N	N	N	***2.4***	***2.4***	***2.4***	***2.4***

Appendix B

B.1 EXTRACTION METHOD

Purpose

The purpose of this standard operating procedure (SOP) is to demonstrate the extraction procedure to quantify the Polynuclear Aromatic Hydrocarbons (PAHs) in water samples.

Scope

This SOP scope refers to the HP 6890-5973 gas chromatograph (Hewlett Packard, Rolling Meadows, IL) equipped with Mass spectrometer and capillary column (DB-1) 30 m x 0.32 mm x 3 um.

Materials

The following materials are required to perform this method:

- Separatory Funnels, capacity 500 mL
- Laboratory Scale
- Oven, capacity 500 °C
- Vacuum Pump
- Vacuum Volumetric Flask
- Beakers, capacity 500 mL
- Beakers, capacity 50 mL
- EPA 8270 Semivolatile Internal Standard Mix
    - Sigma - Aldrich
- Polynuclear Aromatic Hydrocarbons Standard
    - 16 certified analytes
    - Spex Certi prep catalog #CLPS-B
- 9” Disposable Pasteur Pipettes
- Glass Filter Paper (Whatman 47 mm Grade GF/F particle down to 0.7μm)
- Silica Gel (pore size 60 Å, pore size 0.75 cm3/g pore volume, 70-230 mesh, for column chromatography 1kG)
- 4mm glass beads
- 1 mL SGE Gas-Tight Syringe
- Pyrek disposable cleanup/drying column, capacity 10mL
- Methylene Chloride, GC Reslv Grade
- Hexane, GC Reslv Grade
- Methanol, GC Reslv Grade
- Magnetic Stirrer
- Supelco GC 2mL amber vials with screw tops
- Supelco Screw caps for 12 x 32 Vials with 8 mm Teflon faced silicone septa.

Work Instructions

Prior collecting sample, perform the following

1.0 Cleaning

1.1 Sample Bottle

1.1.1 Wash bottle with detergent
1.1.2 Rinse with 10% acid solution
1.1.3 Rinse with DI water
1.1.4 Bake at 300 °C for at least 1hour
1.1.5 Seal the bottle with aluminum foil

Note: An abrupt change in temperature could result in cracking the glassware

1.2 TFE

1.2.1 Wash the bottle caps with detergent
1.2.2 Rinse with 10% acid solution
1.2.3 Rinse repeatedly with organic free water

1.3 Laboratory Pipettes

1.3.1 Wash pipettes with detergent
1.3.2 Rinse with 10% acid solution and methanol
1.3.3 Rinse with DI water
1.3.4 Bake at 150 °C for at least 1 hour

1.4 Laboratory Separators

1.4.1 Wash separators with detergent
1.4.2 Rinse with 10% acid solution and methanol
1.4.3 Rinse with DI water
1.4.4 Bake at 300 °C for at least 1 hour

1.5 Magnetic Funnels

1.5.1 Wash with detergent
1.5.2 Rinse with methanol

2.0 Filter Preparation

2.1 Insert filter in filtration equipment
2.2 Apply vacuum
2.3 Wash with 3 succession 20 mL portion of reagent-grade water
2.4 Place the filter in the aluminum dish
2.5 Dry in oven at 103 °C to 105 °C for 1hr
2.6 Cool in desicator to balance temperature

3.0 Silica gel

3.1 Weight 3 g per sample in an aluminum dish

3.2 Pre-activate at 450 °C for 2hr
3.3 Store at 100 °C prior use

4.0 Adsorption Column Setup
4.1 Add twenty 4 mm glass beads to the bottom of the column
4.2 When the silica gel section is completed add ten 4mm glass beads to the top

After completion of these steps, collect samples at the designated area and perform the following:

5.0 Sample volume for analysis
5.1 Take 200 mL sample

6.0 To preserve the sample for future analysis;
6.1 Hold at 4 °C with minimal exposure to light and atmosphere. The holding time is 1 week.

7.0 Standard Preparation
7.1 To the 200 mL sample add 5 μL of 2000 mg/L EPA 8270 internal standard solution and mix for 10 min with a magnetic stirrer.
7.2 Take 200 ml of reagent grade water, add 5 μL of 2000 mg/L EPA 8270 Internal Standard, and 5 μL of 2000 mg/L 16 Certified Compound PAH Standard solution

8.0 Filtering (Use if any samples are not filtered in the field i.e. first flush or grab samples)
8.1 Remove the filter with the aluminum dish from the desiccators
8.2 Weight the filter and the aluminum dish
8.3 Remove the filter and place it in the filtration equipment
8.4 Apply vacuum
8.5 Filter the sample
8.6 Rinse the glass beaker, with the magnetic stirrer inside the beaker, with 5 mL methylene chloride and add to the designated separatory funnel. Repeat 1 more time.
8.7 Aqueous Phase
8.7.1 Liquid-Liquid Extraction
8.7.1.1 Prime the separator with solvent to remove any small contaminant
8.7.1.2 Add sample to separators
8.7.1.3 Rinse the glass beaker, with the magnetic stirrer inside the beaker, with 5 mL methylene chloride and add to the designated separatory funnel. Repeat 1 more time
8.7.1.4 Insert 20 mL of the solvent.
8.7.1.5 Shake the sample vigorously for 1 min
8.7.1.6 Wait for both phases to separate, between 5 to 10 min
8.7.1.7 Remove the solvent. Make sure the sample stays behind.

8.7.1.8 Transfer the solution to the adsorption column (silica gel)
8.7.1.9 Repeat 1 more time with 45 mL total solvent
8.7.1.10 Discard the initial sample

8.8 Solid Phase
- 8.8.1 Dry filter to 35 °C
- 8.8.2 Weight the filter
- 8.8.3 Place the filter in the separator flask
- 8.8.4 Rinse the aluminum dish with solvent. Add content to separatory funnel
- 8.8.5 Extraction
  - 8.8.5.1 Add 15 mL of solvent
  - 8.8.5.2 Shake the sample for 2 min.
  - 8.8.5.3 Remove the solvent from the separator
  - 8.8.5.4 Transfer the solution to the adsorption column (silica gel)

9.0 Liquid-Liquid extraction

9.1 Use if samples do not contain unfiltered sediment
- 9.1.1 Prime the separator with solvent to remove any small contaminant
- 9.1.2 Add sample to separators
- 9.1.3 Rinse the glass beaker, with the magnetic stirrer inside the beaker, with 15 mL methylene chloride and add to the designated separatory funnel. Repeat 1 more time
- 9.1.4 Insert 10 mL of the solvent.
- 9.1.5 Shake the sample vigorously for 1 min
- 9.1.6 Wait for both phases to separate, between 5 to 10 min
- 9.1.7 Remove the solvent. Make sure the sample stays behind.
- 9.1.8 Repeat 1 more time with 45 mL total solvent
- 9.1.9 Discard the initial sample
- 9.1.10 Insert 15 mL of solvent into empty separatory funnel.
- 9.1.11 Shake for 2 min
- 9.1.12 Remove solvent from seperator
- 9.1.13 Transfer the solvent solution to the adsorption column (silica gel)

10.0 Water Bath
- 10.1.1 Add 2 L of DI water to the water bath
- 10.1.2 Set the water bath to 45 °C (± 2 °C)P. (Set the dial to number 6)
- 10.1.3 Place the extracted samples in the water bath
- 10.1.4 Concentrate the fractioned solution using N2 flux to 1.9 mL at 2 psi and turn the sample valves at 2 revolution
- 10.1.5 Transfer to GC vial. The vial must be filled with at least 1.9 mL of the concentrated sample.

11.0 Gas Chromatography analysis
- 11.1 Turn on the GC equipment
- 11.2 Turn on the Computer

11.3 Setup the GC System with the following operation parameters

11.3.1 Equipment: HP6890-5973 GC/MS

11.3.2 Column: DB-1 30 m x 0.32 mm x 3 um

11.3.3 Carrier: Helium at 44 cm/sec

11.3.4 Solvent delay time, 10 min

11.3.5 Injection, automatic 2μL

11.3.6 Oven

11.3.6.1 Initial Temperature, 40 °C

11.3.6.2 Hold 4 min

11.3.6.3 Step 1

11.3.6.3.1 Rate, 20°C/min

11.3.6.3.2 Oven temperature, 220 ^{o}C

11.3.6.3.3 Hold, 15 min

11.3.6.4 Step 2

11.3.6.4.1 Rate, 10 ^{o}C/min

11.3.6.4.2 Oven Temperature, 270 ^{o}C

11.3.6.4.3 Hold, 60 min

11.3.6.5 Run Time, 93 min

11.3.6.6 Blank samples of Methylene chloride, every 4th sample analyzed

12.0 Internal standard Calibration

12.1 Should be completed along with any samples extracted

12.2 Follow extraction procedure

12.2.1 Place 5 μL of 2000 mg/l internal standard and PAH standard in 200 mL of reagent grade water

12.2.2 Follow the same extraction procedure as for the unknown samples

12.3 Analyze in GC

12.4 PAH compounds and the corresponding internal standards used to calibrate their concentrations (US EPA 1996).

Napthalene d8	**Acenaphthene d10**	**Phenanthrene d10**	**Chrysene d12**	**Perylene d12**
Napthalene	Acenphthylene	Phenanthrene	Pyrene	Benzo(a)pyrene
	Acenaphthene	Anthracene	Benz(a)anthracene	Benzo(b)fluoranthene
	Fluorene	Fluoranthene	Chrysene	Benzo(k)fluoranthene
				Indeno(1,2,3-d,d)pyrene
				Dibenz(a,h)anthracene
				Benzo(g,h,i)perylene

12.5 Calculate the Response Factor

$$RF = \frac{(A_s)(C_{IS})}{(A_{IS})(C_s)}$$

12.5.1 RF= Response Factor

12.5.2 A_s = Area of PAH compound

12.5.3 C_{is} = Concentration of Internal Standard (50 μg/L)
12.5.4 A_{iS} = Area of internal standard
12.5.5 C_s = Concentration of standard (50 μg/L)

12.6 PAH concentration calculation

$$\text{Concentration } (\mu g/L) = \frac{(A_s)(I_s)}{(A_{is})(RF)(V_0)}$$

12.6.1 I_s = Mass of internal standard extracted (10 μg)
12.6.2 V_o = Volume of water extracted (0.2 L)

12.7 Approximate Method PAH retention times and ions

PAH Standards				
Compound	**EPA 8270 Ret Time (min)**	**Bench Top Method Ret. Time (Min)**	**Primary ion**	**Secondary ions**
Naphthalene	9.8	12.8	128	129,127
acenphthylene	14.6	15.1	152	151,153
Acenaphthene	15.1	15.4	154	153,152
Fluorene	16.7	16.3	166	165,167
Phenanthrene	19.6	18.2	178	179,176
anthracene	19.8	18.3	178	176,179
Fluoranthene	23.3	21.7	202	101,203
Pyrene	24.0	22.7	202	200,203
Benz(a)anthracene	27.8	30.5	228	229,226
chrysene	28.0	30.8	228	226,229
benzo(b)fluoranthene	31.5	44.6	252	253,125
benzo(k)fluoranthene	31.6	45.0	252	253,125
Benzo(a)pyrene	32.8	50.2	252	253,125
Indeno(1,2,3-d,d)pyrene	39.5	78.8	276	138,227
Dibenz(a,h)anthracene	39.8	80.8	278	139,279
benzo(g,h,i)perylene	41.4	88.0	276	138,277

Internal Standards				
Compound	**EPA 8270 Ret Time (min)**	**Bench Top Method Ret. Time (Min)**	**Primary ion**	**Secondary ions**
1,4-Dichlorobenzene-d4	6.4	11.19	152	150, 115
Naphthalene-d8	9.8	12.76	136	68
Acenaphthene-d10	15.1	15.32	164	162, 160
Phenanthrene-d10	19.6	18.14	188	94, 80
Chrysene-d12	27.9	30.57	240	120, 236
Perylene-d12	33.1	51.2	264	260, 265

Historical Summary

Version	1.0
Original	
Version	1.1
Change 6.1 from sulfuric acid to hydrogen chloride and added “using no more than 1.0 mL	
Version	1.2
-Added Material List -In Step 1.5.2 Erased 10% acid -In Step 6.0, erased preservation with HCl acid -In Step 7.0, clarify the use of only one internal standard solution and the mixing time -In step 8.7, added a step to rinse all glass beaker with solvent -In Step 8.8.5, change the multiple repetition of 15 mL to one single repetition with 30 mL -In Step 8.9.4, change the evaporation from almost dry to 1.9 mL. -Erased 8.9.5	
Version	1.3
– Added section 9.5 Operating Parameter for GC	
Version	1.4
– Added section 8.9 Liquid-Liquid extraction for lysmeter samples – Changed section 9 to the procedure for the HP5890 CGMS – Removed section 9.5.5, 9.5.6, 9.5.7, 9.5.8, 9.5.9, 9.5.10, 9.5.11	
Version	1.5
– Changed section 8.9.1.4 from 40 mL to 15 mL – Changed section 8.9.1.8 from 55 mL to 50 mL – Added section 8.9.1.10 through 8.9.1.13	
Version	1.6
– Moved section 8.9 from previous version to 8.10 – Added 8.9 adsorption column procedure – Changed the calibration curve information to reflect the porous pavement study.	
Version	1.7
– Changed GC/MS model from HP5890 to HP6890-5973 – Changed Column from DB-PETRO to DB-1 – Changes volume of solvent to 100 ml total – Removes section 8.10 absorption column vacuum procedure – Added 9.0 GC/MS method – Added 11.0 Internal Standard calibration – Added 12.0 Sample concentration calculation – Added 12.3 ret1ention times and ions	

B.2 PAH full results

Compound	MDL µg/L	Blank µg/L	PVC µg/L	PC1A µg/L	PC1B µg/L	PC2A µg/L	PC2B µg/L
Napthalene	1.0	ND	***0.07***	ND	***0.04***	***0.05***	***0.06***
Acenphthylene	0.9	ND	***0.07***	ND	ND	***0.11***	ND
Acenphthene	0.9	ND	***0.11***	***0.14***	***0.15***	***0.12***	***0.16***
fluorene	0.6	ND	ND	ND	ND	ND	ND
Phenanthrene	0.2	ND	***0.06***	***0.03***	***0.06***	***0.03***	ND
Anthracene	0.3	ND	***0.08***	***0.04***	***0.07***	***0.04***	ND
fluoranthrene	0.4	ND	***0.10***	ND	***0.03***	ND	ND
Pyrene	1.2	ND	***0.11***	ND	***0.02***	ND	ND
Benz(a)anthracene	1.3	ND	ND	***0.01***	ND	ND	ND
Chrysene	1.5	ND	***1.23***	***0.11***	***0.03***	ND	ND
Benzo(b)fluoranthene	4.5	ND	***0.02***	***0.02***	***0.09***	ND	***0.04***
Benzo(k)anthrene	4.7	ND	***0.10***	***0.06***	***0.10***	ND	***0.06***
Benzo(a)pyrene	38.2	ND	ND	***0.05***	ND	***0.82***	ND
Ideno(1,2,3-d,d)pyrene	17.0	ND	***0.20***	ND	ND	***0.78***	ND
Dibenz(a,h)anthracene	18.0	ND	ND	***0.12***	***0.15***	ND	***0.14***
Benzo(g,h,i)perylene	20.0	ND	***0.20***	***0.04***	ND	ND	***0.14***
Total PAH		ND	2.35	0.61	0.74	1.94	0.60

Compound	MDL µg/L	PA1A µg/L	PA1B µg/L	PA2A µg/L	PA2B µg/L
Napthalene	1.0	ND	***0.04***	ND	ND
Acenphthylene	0.9	ND	ND	ND	ND
Acenphthene	0.9	ND	***0.09***	***0.09***	***0.14***
fluorene	0.6	ND	ND	ND	ND
Phenanthrene	0.2	ND	***0.03***	***0.01***	***0.01***
Anthracene	0.3	ND	***0.04***	***0.01***	***0.01***
fluoranthrene	0.4	***0.04***	ND	ND	ND
Pyrene	1.2	ND	ND	***0.05***	***0.02***
Benz(a)anthracene	1.3	ND	0.09	***0.05***	ND
Chrysene	1.5	ND	ND	***0.03***	ND
Benzo(b)fluoranthene	4.5	***0.06***	ND	ND	ND
Benzo(k)anthrene	4.7	ND	***0.05***	***0.05***	ND
Benzo(a)pyrene	38.2	***0.12***	***0.17***	ND	***0.14***
Ideno(1,2,3-d,d)pyrene	17.0	ND	ND	***0.17***	ND
Dibenz(a,h)anthracene	18.0	***0.10***	ND	ND	ND
Benzo(g,h,i)perylene	20.0	ND	ND	ND	***0.23***
Total PAH		0.32	0.50	0.47	0.55

Appendix C

C.1 Average Temperature Results

Date	Air temp (°C)	PA surface (°C)	PC surface (°C)	PA Runoff (°C)	PC Runoff (°C)	AVG. runoff temp (°C)	Bed temp (°C)
3/26/09	8.4	6.5	6.4	7.0	6.8	6.9	8.3
3/28/09	14.4	10.4	10.2	9.7	9.5	9.6	7.0
4/3/09	11.6	14.3	14.2	13.0	12.8	12.9	8.5
4/11/09	9.9	7.9	7.9	9.9	9.7	9.8	9.1
4/13/09	8.5	6.5	6.6	8.6	8.1	8.3	9.1
5/1/09	17.4	16.3	16.2	19.7	20.1	19.9	13.6
5/14/09	21.9	NT	NT	20.6	20.6	20.6	15.3
6/2/09	19.0	NT	NT	19.5	20.2	19.9	18.0
6/9/09	21.1	NT	NT	21.8	22.0	21.9	18.7
7/31/09	26.1	28.1	28.2	27.2	27.0	27.1	24.2
8/2/09	22.2	21.3	21.4	23.4	23.0	23.2	24.1
8/8/09	22.7	24.2	24.2	26.0	25.1	25.6	23.8

C.2 Temperature Range

Date	Air (°C)	PA surface (°C)	PC surface (°C)	PA side Runoff (°C)	PC side Runoff (°C)	Bed Temp. (°C)
3/26/09	3.3	3.5	3.1	1.5	0.7	1.2
3/28/09	14.4	18.0	17.5	6.5	6.5	0.5
4/3/09	7.3	20.5	21.0	2.8	3.5	0.9
4/11/09	1.1	0.5	0.5	2.5	0.8	0.1
4/13/09	3.3	3.5	3.5	6.0	4.8	0.9
5/1/09	7.2	12.5	11.5	8.8	7.8	1.9
5/14/09	15.0	NT	NT	6.5	6.8	1.7
6/2/09	14.4	NT	NT	10.8	10.5	1.6
6/9/09	0.7	NT	NT	3.0	3.0	0.9
7/31/09	1.3	11.0	11.0	2.0	2.5	1.2
8/2/09	1.8	3.0	2.5	7.5	7.0	0.8
8/8/09	2.1	16.5	17.5	10.5	9.3	1.3

C.3 Storm temperature raw data

1

Storm	3/26/09	start time	6:05	duration	14hrs	Rainfall Volume (cm)	1.2
sample name	air temp (^{o}C)	A surface	C surface	A First flush	C first flush	C bed	
Average temp	8.4	6.5	6.4	7.0	6.8	8.3	
max	10.0	8.0	7.6	7.8	7.3	9.1	
min	6.7	4.5	4.5	6.3	6.5	7.8	
range	3.3	3.5	3.1	1.5	0.7	1.2	

2

Storm	3/28/09	start time	21:45	duration	16.7hrs	Rainfall Volume	0.8
sample name	air temp	A surface	C surface	A First flush	C first flush	C bed	
Average temp	14.4	10.4	10.2	9.7	9.5	7.0	
max	23.9	25.0	24.5	14.8	14.8	7.3	
min	9.4	7.0	7.0	8.3	8.3	6.8	
range	14.4	18.0	17.5	6.5	6.5	0.5	

3

Storm	4/3/09	start time	3:25	duration	8.7hrs	Rainfall Volume	3.8
sample name	air temp	A surface	C surface	A First flush	C first flush	C bed	
Average temp	11.6	14.3	14.2	13.0	12.8	8.5	
max	15.7	25.0	26.0	14.8	15.0	9.1	
min	8.4	4.5	5.0	12.0	11.5	8.2	
range	7.3	20.5	21.0	2.8	3.5	0.9	

4

Storm	4/11/09	start time	6:05	duration	8.8hrs	Rainfall Volume	2.3
sample name	air temp	A surface	C surface	A First flush	C first flush	C bed	
Average temp	9.9	7.9	7.9	9.9	9.7	9.1	
max	10.6	8.0	8.5	12.0	11.0	9.4	
min	9.4	7.5	7.5	9.5	9.5	9.0	
range	1.1	0.5	1.0	2.5	1.5	0.4	

5

Storm	4/13/09	start time	3:50	duration	42.3hrs	Rainfall Volume	3.9
sample name	air temp	A surface	C surface	A First flush	C first flush	C bed	
Average temp	8.5	6.5	6.6	8.6	8.1	9.1	
max	10.0	8.5	8.0	13.0	11.3	9.5	
min	6.7	5.0	4.5	7.0	6.5	8.6	
range	3.3	3.5	3.5	6.0	4.8	0.9	

6

Storm	5/1/09	start time	8:01	duration	220.8hrs	Rainfall Volume	11.8
sample name	air temp	A surface	C surface	A First flush	C first flush	C bed	
Average temp	17.4	16.3	16.2	19.7	20.1	13.6	
max	21.7	24.5	23.5	25.5	25.5	14.9	
min	14.4	12.0	12.0	16.8	17.8	13.1	
range	7.2	12.5	11.5	8.8	7.8	1.9	

7

Storm	5/14/09	start time	7:30	duration	73hrs	Rainfall Volume	2.6
sample name	air temp	A surface	C surface	A First flush	C first flush	C bed	
Average temp	21.9	NT	NT	20.6	20.6	15.3	
max	29.4	NT	NT	24.0	24.0	16.0	
min	14.4	NT	NT	17.5	17.3	14.3	
range	15.0	N	N	6.5	6.8	1.7	

8

Storm	6/2/09	start time	15:41	duration	77.5 hrs	Rainfall Volume	5.9
sample name	air temp	A surface	C surface	A First flush	C first flush	C bed	
Average temp	19.0	NT	NT	19.5	20.2	18.0	
max	28.9	NT	NT	25.8	26.0	18.8	
min	14.4	NT	NT	15.0	15.5	17.2	
range	14.4	N	N	10.8	10.5	1.6	

9

Storm	6/9/09	start time	6:41	duration	1.2	Rainfall Volume	0.9
sample name	air temp	A surface	C surface	A First flush	C first flush	C bed	
Average temp	21.1	NT	NT	21.8	22.0	18.7	
max	21.4	NT	NT	23.3	23.5	18.9	
min	20.7	NT	NT	20.3	20.5	18.0	
range	0.7	N	N	3.0	3.0	0.9	

10

Storm	7/31/09	start time	15:00	duration	1.33	Rainfall Volume	3.9
sample name	air temp	A surface	C surface	A First flush	C first flush	C bed	
Average temp	26.1	28.1	28.2	27.2	27.0	24.2	
max	26.8	33.0	33.0	27.5	27.5	24.7	
min	25.4	22.0	22.0	25.5	25.0	23.6	
range	1.3	11.0	11.0	2.0	2.5	1.2	

11

Storm	8/2/09	start time	5:48	duration	6.8	Rainfall Volume	8.3
sample name	air temp	A surface	C surface	A First flush	C first flush	C bed	
Average temp	22.2	21.3	21.4	23.4	23.0	24.1	
max	23.5	22.5	22.5	29.5	28.5	24.7	
min	21.7	19.5	20.0	22.0	21.5	23.8	
range	1.8	3.0	2.5	7.5	7.0	0.8	

12

Storm	8/8/09	start time	23:30	duration	18.7	Rainfall Volume	4.6
sample name	air temp	A surface	C surface	A First flush	C first flush	C bed	
Average temp	22.7	24.2	24.2	26.0	25.1	23.8	
max	23.8	36.5	37.0	33.0	31.3	24.7	
min	21.7	20.0	19.5	22.5	22.0	23.4	
range	2.1	16.5	17.5	10.5	9.3	1.3	